Speech Enhancement and Noise-Robust Automatic Speech Recognition

- Harvesting the Best of Two Worlds

Dennis A. L. Thomsen & Carina E. Andersen
Group: 15gr1071

Signal Processing and Computing
June 3, 2015

Supervisors:
Zheng-Hua Tan & Jesper Jensen

Department of Electronic Systems
Aalborg University
Fredrik Bajers Vej 7B
DK-9220 Aalborg

AALBORG UNIVERSITY

Department of Electronic Systems
Frederik Bajers Vej 7
DK-9220 Aalborg Ø
http://es.aau.dk

Title:

Speech Enhancement and Noise-Robust Automatic Speech Recognition - Harvesting the Best of Two Worlds

Theme:

Signal Processing and Computing

Project period:

September 1st 2014 - June 3rd 2015

Project group:

15gr1071

Members:

Carina Enevold Andersen
Dennis Alexander Lehmann Thomsen

Supervisors:

Zheng-Hua Tan
Jesper Jensen

No. printed Copies: 3

No. of Pages: 130

Total no. of pages: 144

Attached: 1 CD

Synopsis:

This project investigates any potential relationship between the performances of noise reduction algorithms in the context of speech recognition and speech enhancement. General theory related to speech production and hearing is presented together with the basics of the Mel-frequency cepstral coefficients speech feature. The fundamental theory of hidden Markov model speech recognition is stated along with the standard feature-extraction method European telecommunication standards institute (ETSI) advanced frontend (AFE). The performance of the ETSI AFE algorithm and state-of-the-art speech enhancement algorithms are investigated in both fields using speech data from the Aurora-2 database. The aggressiveness of the noise reduction applied has been identified as a major difference between the algorithms from the two fields, and has been adjusted to increase performance in the rivalling field. Using a logistic model, estimators of recognition performance are created for the ETSI AFE using the distortion measures for speech quality and intelligibility. The most accurate estimator of the recognition performance of the ETSI AFE, proved to be the one designed for short-time objective intelligibility measure using a recogniser trained with clean and noisy speech data.

Table Of Contents

Preface

This master thesis presents the final project of the Master of Science in Signal Processing and Computing at Aalborg University. The project has been prepared by project group 15gr1071 at the Institute of Electronic Systems between September 2014 and June 2015. The project has been done in collaboration with Oticon and has been supervised by Jesper Jensen and Zheng-Hua Tan.

The formatting should be interpreted as follows:

- Figures, tables, equations and algorithms are numbered consecutively according to the chapter number.
- Citations are written with indicies in squared brackets, i.e. $[index]$.
- The enclosed CD contains a digital copy of this thesis, Matlab scripts and software used to perform feature extraction and speech recognition.

Aalborg University, June 3, 2015

Carina Enevold Andersen
cean13@student.aau.dk

Dennis Alexander Lehmann Thomsen
dthoms13@student.aau.dk

List of Abbreviations

AFE	Advanced Front-End
ANS	Audible Noise Suppression
AR	Autoregressive
ASR	Automatic Speech Recognition
DCT	Discrete Cosine Transform
DFT	Discrete Fourier Transform
DRT	Diagnostic Rhyme Test
DSR	Distributed Speech Recognition
ESR	Embedded Speech Recognition
ETSI	European Telecommunications Standards Institute
FFT	Fast Fourier Transform
FIR	Finite Impulse Response
GSM	Global System for Mobile Communication
HMM	Hidden Markov Model
HTK	Hidden Markov Model Toolkit
IDCT	Inverse Discrete Cosine Transform
iid	independent and identically distributed
ITU	International Telecommunication Union
IWF	Iterative Wiener Filtering
LTI	Linear Time-Invariant
MAP	Maximum a Posteriori

MFCC	Mel-Frequency Cepstral Coefficients
MIRS	Motorola Integrated Radio System
ML	Maximum Likelihood
MMSE	Minimum Mean-Square Error
MSE	Mean-Square Error
NSR	Network Speech Recognition
PESQ	Perceptual Evaluation of Speech Quality
PSD	Power Spectral Density
RMSE	Root Mean Square Error
SDR	Signal-to-Distortion Ratio
SE	Speech Enhancement
SNR	Signal-to-Noise Ratio
SSE	Sum of Squares Error
STFT	Short-Time Fourier Transform
STOI	Short-Time Objective Intelligibility
STSA	Short-Time Spectral Amplitude
SWP	SNR-dependent Waveform Processing
TF	Time-Frequency
VAD	Voice Activity Detection
WE	Weighted Euclidean
WF	Wiener Filter

List of Notations

Symbol	Description
$f(a)$	The variable a is continuous
$f[a]$	The variable a is discrete
$f[a,b)$	The variable a is discrete, b is continuous
$\mathbb{Z}_+$	The set of all positive integers, $Z_+ = \{1,2,\ldots\}$
$\mathbf{a}$	Column vector, $\mathbf{a} = [a_0,\ldots,a_{K-1}]^{\mathrm{T}}$ where $K \in \mathbb{Z}_+$
$\mathbf{a}^{\mathrm{T}}$	Row vector, $\mathbf{a}^{\mathrm{T}} = [a_0,...,a_{K-1}]$ where $K \in \mathbb{Z}_+$
$(\mathbf{a})_k$	Element number k in the vector $\mathbf{a}$, $(\mathbf{a})_k = a_k = \mathbf{a}[k]$

Introduction 1

In many speech communication environments the presence of background noise causes the quality and intelligibility of speech signals to degrade. Acoustical noise sources in the environment where interpersonal communication takes places can also be introduced by encoding, decoding and transmission over noisy channels[3, 11]. Today, mobile speech processing applications are expected to work anywhere and at any time. This places high demands on the robustness of these devices to operate well in acoustical challenging conditions.

Speech enhancement (SE) for human listeners can be used to process the noisy speech signal to reduce the impact of disturbances and improve the quality and intelligibility of the degraded speech signal at the receiving end. In speech recognition systems, the speech recognition performance can be significantly degraded when using speech signals that have been transmitted over mobile channels compared to the unmodified signals. Noise- and channel-robust automatic speech recognition (ASR) techniques are suitable for recognition of noisy speech signals using a parameterized representation of the speech (called feature vector). The advanced front-end (AFE) defined by the the European Telecommunications Standards Institute (ETSI) is a powerful algorithm for extracting these ASR features from noisy speech signals [7]. Beside feature extraction, ETSI AFE includes extra processing stages that are designed to help achieving acceptable recognition accuracy when processing noisy speech signals. Feature vectors can be corrupted by acoustic noise and cause large reduction in recognition accuracy, if noise reduction is not applied before the feature extraction process. Therefore the ETSI AFE algorithm contains pre-processing stages that perform noise reduction on the noisy speech signals [33].

The primary difference between the research areas of SE for humans listeners and the noise-robust ASR, is the intended recipient of the processed speech signals: while ASR is aimed at machine receivers, the SE algorithms for human listeners are intended for humans obviously. While the research areas do have overlapping technical problems in retrieving a target signal from a noisy observation, the development in the field of SE for human listeners is, however, usually not inspired by research in noise-robust ASR.

In [14] it has been found that a significantly better ASR performance is obtained using the ETSI AFE feature extraction algorithm compared to feature extraction methods inspired by selected SE algorithms for human receivers. This raises the question regarding the performance of the ETSI AFE as a SE algorithm for humans compared to selected state-of-the-art SE algorithms. The observations in [14] have been made for a limited number of SE algorithms for human listeners. Thus in this thesis the validity of the observations in [14] is checked for the state-of-the-art SE algorithms considered (in this thesis), and which properties influence the ASR performance are investigated. This inspire an investigation into the relationship and dependence between the ASR and SE performance measures for selected noise reduction algorithms.

1.1 Problem Statement

The purpose of this project is to:

- Analyse and compare the SE performance of the pre-processing stages of the ETSI AFE algorithm to state-of-the-art SE methods in terms of human auditory perception, i.e. speech intelligibility and quality.
- Analyse the ASR performance of feature extraction methods utilizing SE algorithms designed for human receivers and compare to the ASR performance of the ETSI AFE.
- Analyse the differences and dependencies between SE and ASR performance for selected algorithms. Identify techniques that can be used to improve performance of an algorithm in the rivalling field.
- Design and validate an estimator of recognition performance using the SE performance of speech signals denoised by the feature preprocessing algorithm.

1.2 Project Scope

This section provides an overview of the procedure followed to successfully resolve the question proposed in the problem statement. All the speech data used in this thesis originate from the Aurora-2 database [26], which is a common framework for evaluating ASR. SE performance is evaluated by the use of objective estimators of speech quality and intelligibility. ASR performance is evaluated by comparing transcriptions of the speech signals produced by the ASR machine to reference transcriptions.

In order to evaluate the impact on performance of the pre-processing that occur before feature extraction in the ETSI AFE algorithm, internal time-domain speech signals are extracted. It has been chosen to use the following SE algorithms for comparison: Audible noise suppression

(ANS) [16], the iterative Wiener filter (IWF) [16] and the short-time spectral amplitude (STSA) estimator based on the weighted euclidean (WE) distortion measure [16]. These have been selected as they represent different SE approaches. The IWF algorithm and the ANS exploit assumptions about speech production and human auditory perception, respectively. Unlike IWF and ANS, the STSA WE is a Bayesian estimator that do not make strong assumptions about target or receiver of the signal.

The analysis of ASR performance is carried out by using the ETSI AFE algorithm and feature extraction methods applying noise reduction utilizing the same SE methods as previously mentioned. Additional feature extraction methods are considered based on the internal speech signals extracted from within the ETSI AFE algorithm.

In order to identify and explain the differences in performance, spectrogram analysis is performed using speech signals processed by selected algorithms. Furthermore the influence of the noise-only regions on the ASR performance is investigated for the algorithms. Correlation measures and scatter plots are used to study the dependence between ASR and SE performance measures. Regression analysis is then used to fit an estimator to a subset of speech data of the Aurora-2 database. The remaining subset of the database is used to validate the estimator.

1.3 Delimitations

Speech enhancement methods in general vary depending on the context of the problem: The application, the characteristics of the noise source or interference, the relationship (if any) of the noise to the clean signal, and the number of microphones or sensors available are all important aspects to consider. The interference could be noiselike, e.g. fan noise, but it could also be speech, such as in a restaurant environment with competing speakers. Acoustic noise could be additive to the clean signal or convolutive in the form of reverberation. Additionally, the noise may be statistically correlated or uncorrelated with the clean speech signal. Furthermore, the performance of SE systems typically improves the more microphones available [16].
As there are several parameters influencing the problem of SE, it is necessary to limit the project by a number of assumptions:

- The speaker and listeners in this set-up have normal speech production and auditory systems.
- Only the noisy signal, containing both the clean speech and additive noise, is available from a single microphone, when performing SE or ASR. In other words, there is no access to an additional microphone e.g. picking up the noise signal.

- The speech signal is degraded by statistically independent additive noise. However, the clean speech signal is available when testing algorithms for SE performance.
- For SE algorithms to be relevant in some practical devices e.g. hearing aids, it must execute in real-time with a latency of a few milliseconds. Some hearing aid users can hear both the sound which has been amplified through the hearing aid and the sound that enters the ear canal directly. When there is too great a latency between direct and processed sound, then perceptible artifacts starts to occur [22]. However, in the context considered in this thesis, SE performance is considered of higher priority than latency.
- Another important issue to consider in relation to SE devices is the computational complexity of the SE algorithm. When limited in size of hardware, as in the case of hearing aid devices, computational and memory complexities are limited as well in order not to introduce to much computation time. However, as previously mentioned the SE performance has more focus in this thesis, therefore the computational and memory complexities are considered the lower priority.

Introduction to Speech Fundamentals 2

In this chapter theory of speech fundamentals is presented, as in the development of noise robust ASR systems and speech enhancement (SE) algorithms for human listeners, concepts from fundamental speech theories are utilized. The characteristics of speech signals are defined from the speech generation process, which are then utilized in the assumptions made for noise robust ASR and SE algorithms. Speech production and auditory masking effects are considered, which are exploited in SE algorithms to be used in this thesis. Furthermore, the theory of human hearing is presented, which provides an understanding of how the operation of the cochlear of the inner ear can be interpreted as overlapping bandpass filters. This is exploited in the feature extraction method presented in this chapter called Mel-frequency cepstral coefficients (MFCC), which makes use of the Mel-frequency scale that mimic the process of the human ear.

2.1 Speech Communication

Speech is the primary form of communication between humans. In order for the communication to take place, a speaker must produce a speech signal in the form of a sound pressure wave, which travels from the mouth of the speaker to the ears of the listener. The pathway of communication from speaker to listener begins by an idea that is created in the mind of the speaker. This idea is transformed into words and sentences of a language. When the speaker uses his/her speech production system to initiate a sound wave it propagates through space, subsequently, results in pressure changes at the ear canal and thus vibrations of the ear drum of the listener. The brain of the listener then performs speech recognition and understanding. This activity between the speaker and the listener can be thought of as the "transmitter" and "receiver", respectively, in the speech communication pathway. But there exist other functionalities besides basic communication. In the transmitter there is feedback through the ear which allows correction of one's own speech. The receiver performs speech recognition and is robust to noise and other interferences [28].

2.2 Characteristics and Production of Speech

In this section the characteristics and the production of speech is presented, which is relevant to consider in order to analyze and model speech. This is fundamental for the development of SE and noise-robust ASR algorithms. The speech waveform is a pressure wave which is generated by movements of anatomical structures that make up the human speech production system. In Figure 2.1, a cross-sectional view of the anatomy of speech production is shown. The speech organs can be divided into three main groups: the lungs, the larynx and the vocal tract [28].

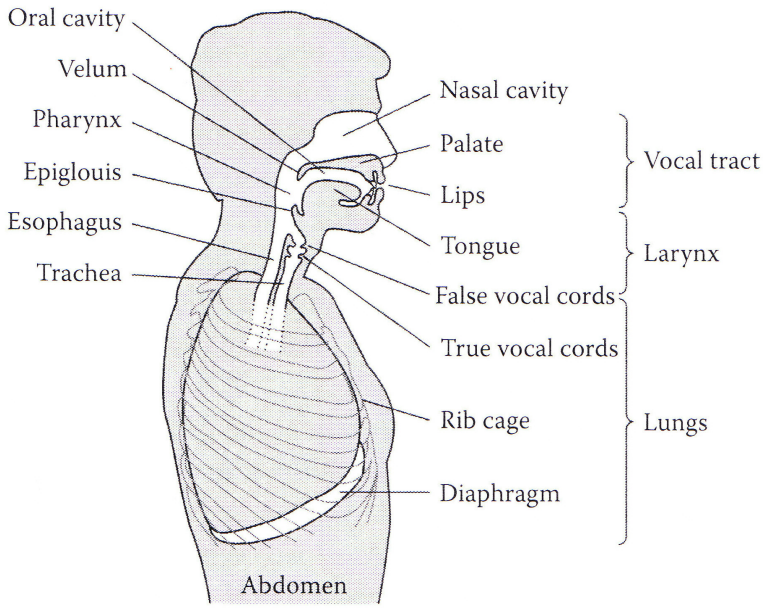

Figure 2.1: The anatomy of speech production [28].

The purpose of lungs is the inhalation and exhalation of air. When inhaling air, the chest cavity is enlarged, where the air pressure in the lungs is lowered. This causes the air to rush through the vocal tract, down the trachea and into the lungs. When exhaling air, the volume of the chest cavity is reduced, which increases air pressure within the lung. The increase in pressure causes air to flow through the trachea into the larynx. The lungs then act as a "power supply" and provide airflow to the larynx stage of the speech production process [16, 28].

The larynx is the organ responsible of voice production. It controls the vocal folds (or vocal cords), which are two masses of ligament and muscle stretching between the front and back of the larynx as shown in Figure 2.2. The glottis is the opening between the two folds.

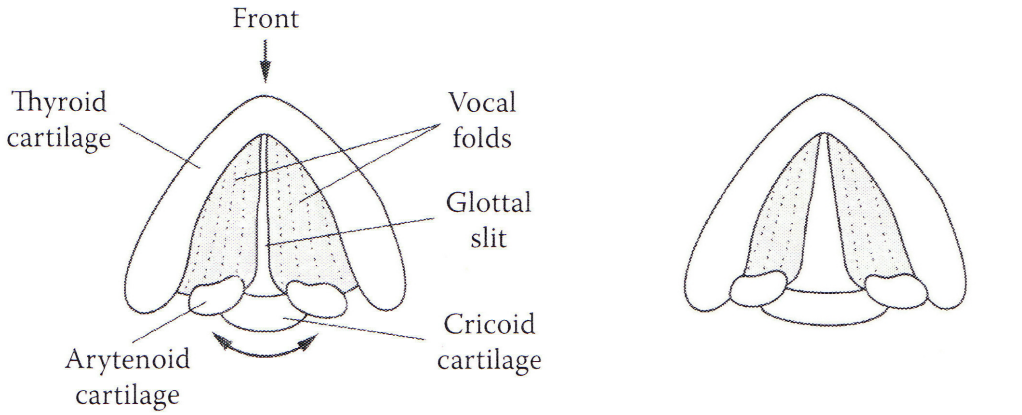

(a) Larynx in the voicing state.

(b) Larynx in the breathing state.

Figure 2.2: Sketches of the human larynx from a downward-looking view [28].

The vocal folds can assume three states: breathing, voiced and unvoiced. In the breathing state, the glottis is wide open as shown in Figure 2.2b. The air from the lungs flows freely through the glottis with no notable resistance from the vocal folds. In the voicing state, as the production of a vowel (e.g. /aa/), the arytenoid cartilages move toward each other as shown in Figure 2.2a. The tension of the folds increases and decreases, while the pressure at the glottis increases and decreases, which makes the folds open and close periodically. The time duration of one glottal cycle, which is the time between successive vocal openings, is known as the pitch period and the reciprocal of the pitch period is known as the fundamental frequency. Thus the periodically vibration of the vocal folds is responsible for "voiced" speech sounds. Unvoiced sounds is generated when the vocal folds are in the unvoicing state. The state is similar to the breathing state in that the vocal folds do not vibrate. The folds, however, are tenser and come closer together, thus allowing the air stream to become turbulent as it flows through the glottis. This air turbulence is called aspiration. Aspiration occurs in normal speech when producing sounds like /h/ as in "house" or when whispering. Unvoiced sound include the majority of consonants [16].

The vocal tract consists of the oral cavity and the nasal cavity. The input to the vocal tract is the air flow wave coming via the vocal folds. The vocal tract acts a physical linear filter that spectrally shapes the input wave to produce distinctly different sounds. The characteristics of the filter (e.g. frequency response) change depending on the position of the articulators, i.e. the shape of the oral cavity [16].

Characteristic of the speech signal can be defined from the speech generation process [16, 28, 37]:

- Speech signals are changing continuously and gradually, not abruptly. They are time

variant.

- The frequency content of a speech signal is changing across time. But the speech signal can be divided into sound segments which have some common acoustic properties for a short time interval. Therefore speech signals are referred to as being quasi-stationary.
- When producing voiced speech, air is exhaled out of the lungs through the trachea and is interrupted periodically by the vibrating vocal cords. This means that voiced speech is periodic in nature, where the frequency of the excitation provided by the vocal cords is known as the fundamental frequency.
- At unvoiced regions, the speech signal has a stochastic spectral characteristic, where the vocal cords do not vibrate and the excitation is provided by turbulent airflow through a constriction in the vocal tract. This gives the time-domain representation of phonemes (sound classes) a noisy characteristic.
- When producing speech and communicating to a listener, phrases or sentences are constructed by choosing from a collection of finite mutually exclusive sounds. The basic lingustic unit of speech is called phoneme. Many different factors, including for example, gender, accents and coarticulatory effects, cause acoustic variations in the production of a given "phoneme". Phonemes represents the way we understand sounds produced in speech. Therefore, the phoneme represents a class of sound that has the same meaning. These have to be distinguished from the actual sounds produced in speaking called phones.

2.3 Speech Production Model

The vocal tract can be modelled as a linear filter that spectrally shapes the input wave to produce different sounds, as described in Section 2.2. The characteristics of the vocal tract have led to the development of an engineering model of speech production, as shown in Figure 2.3 [16]. This speech production model is considered, as it is utilized in the SE algorithm called iterative Wiener filtering (IWF) [16] presented in Section 4.1.

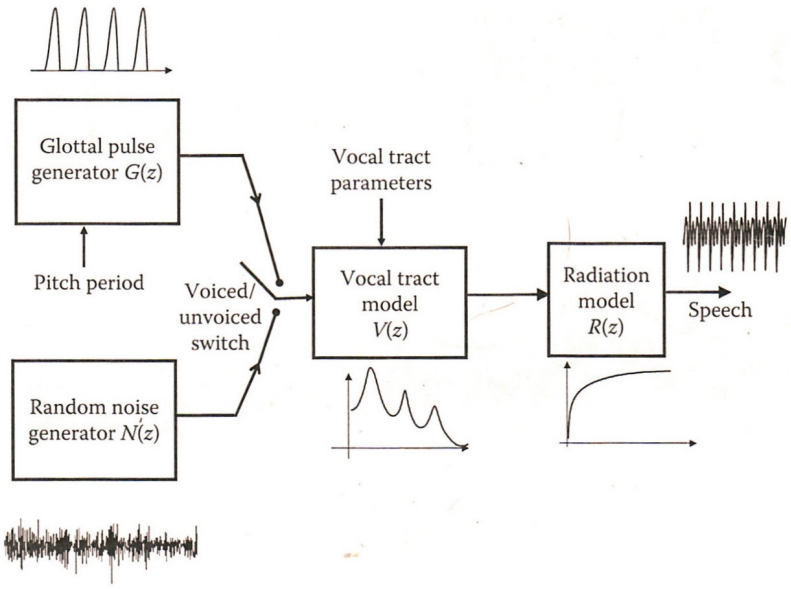

Figure 2.3: Engineering model of speech production[16].

This model assumes that the source of sound, i.e. the excitation signal from the lungs, and the filter that shapes that sound, i.e. the vocal tract system, are independent. This independence makes it possible to measure the source separately from the filter. The vocal folds can assume one of two states: voices and unvoiced speech, where the breathing state is ignored. This is modelled by a switch.

For the production of voiced speech, air flows from the lungs through the vocal folds that make the vocal folds vibrate periodically. Therefore when the input is a periodic glottal airflow sequence, the z-transform at the output of the lips can be written as the product of three transfer functions modelling the glottal source ($G(z)$), the vocal tract ($V(z)$) and the lip radiation ($R(z)$):

$$X(z) = G(z)V(z)R(z). \tag{2.1}$$

For the production of unvoiced speech, the vocal folds become tenser and do not vibrate. The excitation of the vocal tract has a characteristics like noise. Therefore the input sequence may be modelled as random noise with a flat spectrum, i.e. white noise and the output of the lips can be written as:

$$X(z) = N(z)V(z)R(z), \tag{2.2}$$

where $N(z)$ is the z-transform of the noise sequence [16].

The vocal tract is modelled by a linear time-invariant filter. The vocal tract system has the following all-pole form in the z-domain:

$$V(z) = \frac{g}{A(z)} = \frac{g}{1 - \sum_{k=1}^{p} a_k z^{-k}}, \tag{2.3}$$

where g is the gain of the system, $\{a_k\}$ are the all-pole coefficients and p is the number of coefficients. The output of the vocal tract filter is fed to the sound radiation filter, that model the effect of sound radiation at the lips. A filter of the following form is typically used as the sound radiation filter:

$$R(z) = 1 - z^{-1}. \tag{2.4}$$

This sound radiation block introduces about a 6 dB/octave high-pass boost. The output of the model is the speech signal, which is generally observable [16].

2.4 Hearing

In this section the human hearing system is introduced and along with how the inner ear is capable of performing frequency analysis of incoming sound signals. This leads to a description of how the operation of the cochlear of the inner ear can be interpreted as overlapping bandpass filters, which is utilized in specific ASR algorithms. There are three main components of the human ear: The outer ear, the middle ear and the inner ear, which are illustrated in Figure 2.4. They form the pathway along which the incoming sound signal travel to the point where the signal is carried by nerve fibres from the ear to the brain [13].

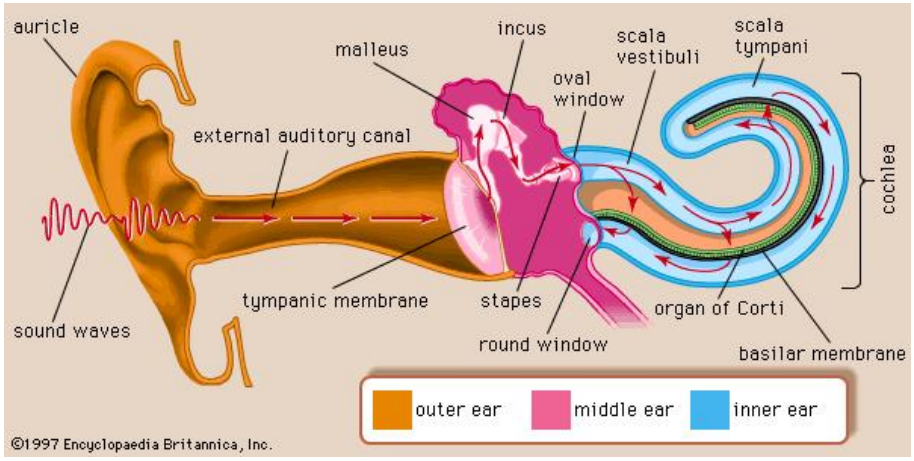

Figure 2.4: The outer, middle and inner ear [4].

The sound is collected by the pinna (the external flap of the ear) and focused through the ear canal toward the ear drum (tympanic membrane). The ear drum is a membrane and it converts the acoustic pressure variations from the outside world into mechanical vibrations in the middle ear. The mechanical movements of the ear drum are transmitted through three small bones known as ossicles, comprising the malleus, incus and stapes, to the oval window of the cochlea, which are illustrated in Figure 2.5 [13].

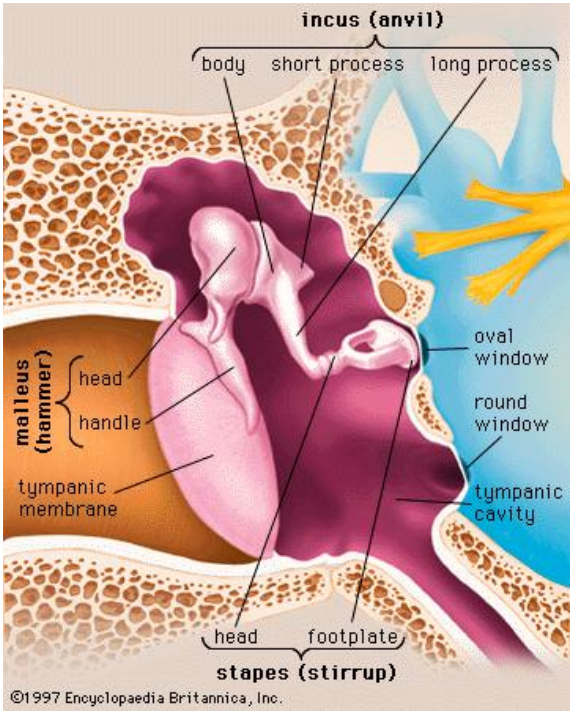

Figure 2.5: The auditory ossicles of the middle ear [4].

One end of the stapes, the stapes footplate, is attached to the oval window. The oval window is an opening which leads from the middle ear to the inner ear, which is covered by a membrane. The effective pressure acting on the oval window is greater than that acting on the ear drum. The reason for this is that there is a higher resistance to the movement of the cochlea, since it is filled by fluid. Resistance to movement can be thought of as 'impedance' to movement and the impedance of fluid to movement is high compared to that of air. The ossicles then act as a mechanical 'impedance converter'. Thus the acoustic vibrations are transmitted via the ear drum and ossicles as mechanical movements to the cochlea of the inner ear [13].

The inner ear consists of a curled tube known as the cochlea, which is illustrated in Figure 2.4. The function of the cochlea is to convert mechanical vibrations into neural impulses to be processed by the brain. The cochlea has three fluid-filled canals, the scala vestibuli, the scala tympani and the scala media (cochlear duct). A cross-section through the cochlea tube is shown in Figure 2.6.

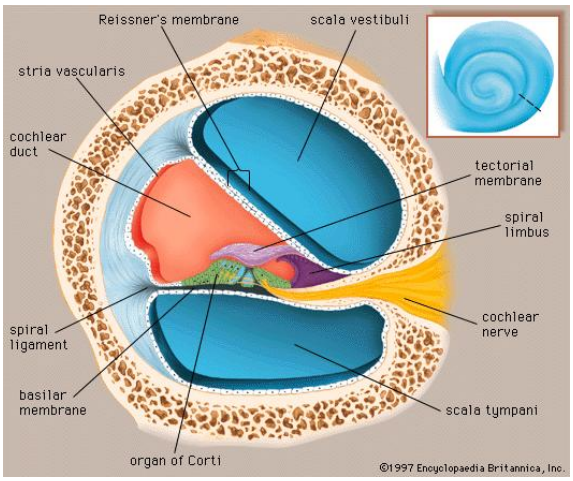

Figure 2.6: A cross-section of the cochlea [4].

The scala media (cochlear duct), located in the middle of the cochlea, is separated from the scala vestibuli by Reissner's membrane and from the scala tympani by the basilar membrane as seen in Figure 2.6. Besides the oval window, there is another opening into the inner ear called the round window as shown in Figure 2.4, but it is closed off from the middle ear by a membrane. The end of the cochlea at the round and oval windows is the 'base' and the other end is the 'apex' [13].

A sound signal results in a piston-like movement of the stapes footplate at the oval window, which moves the fluid within the cochlea. The membrane covering the round window moves to compensate for oval window movements, since the fluid within the cochlea is incompressible. The round window membrane vibrates with opposite phase to the vibrations entering the inner ear through the oval window. This causes travelling waves to be created in the scala vestibuli, which displaces both Reissner's membrane and the basilar membrane [13].

The basilar membrane carries out a frequency analysis of the input sound signal. The shape of the basilar membrane for a cochlea is shown in Figure 2.7, where it can be seen that the basilar membrane is both narrow and thin at the base end of the cochlea, but becomes wider and thicker along its length to the apex. Vibrations of the basilar membrane occur in response to stimulation by signals in the audio frequency range [13].

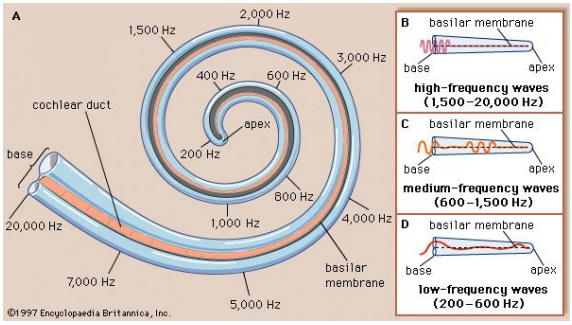

Figure 2.7: Basilar membrane motions of the cochlear at different frequencies [4].

As shown in Figure 2.7, the basilar membrane responds best to high frequencies where it is narrow and thin (at the base) and to low frequencies where it is wide and thick (at the apex). Since its thickness and width changes gradually along its length, inputting pure tones at different frequencies produce a maximum basilar membrane movement at different positions along its length. It has also been shown that the linear distance measured from the apex to the point of maximum basilar membrane displacement is approximately proportional to the logarithm of the input frequency [13].

The basilar membrane separates sound according to their frequency and the organ of Corti located along the basilar membrane as shown in Figure 2.4, hosts a number of hair cells that transform the vibrations of the basilar membrane into nerve signals, which are transmitted by the cochlear nerve and ultimately ends up in the brain [21].

The ability of the hearing system to discriminate between the individual frequency components of an input sound provide the basis for understanding the frequency resolution of the hearing system. The cochlea behaves as if it consists of overlapping bandpass filters as illustrated in Figure 2.9, where the passband of each filter is known as the critical band. Each filter has an asymmetric shape, as shown in Figure 2.8 [13].

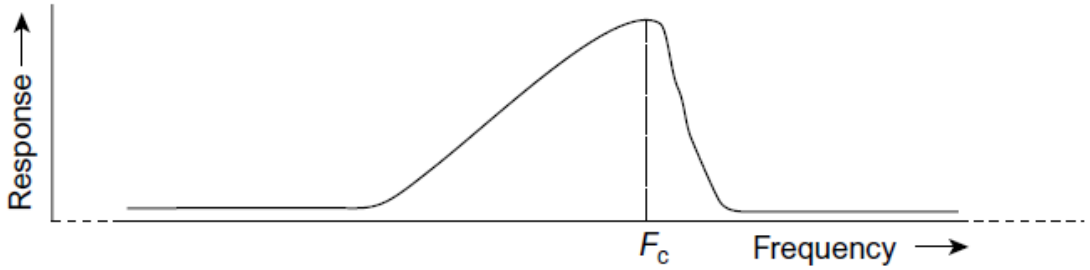

Figure 2.8: Idealised response of an auditory filter for the bank of overlapping bandpass filters estimating the action of the basilar membrane with center frequency F_c Hz, which is asymmetric in shape [13].

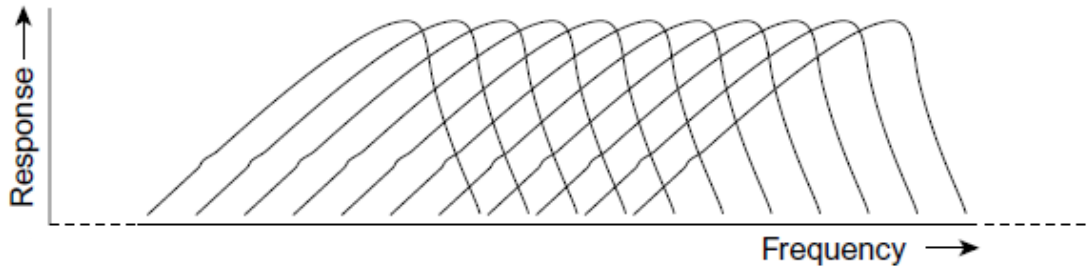

Figure 2.9: Idealised bank of overlapping bandpass filters, which model the frequency analysis capability of the basilar membrane [13].

Each frequency component of an input sound results in a displacement of the basilar membrane at a particular place. Whether or not two frequency components that are of similar amplitude and close in frequency can be discriminated depends on how clearly separated the components are. If the frequency difference between the two frequency components is within the critical bandwidth, the ear is roughly speaking, not able to distinguish the two frequencies and they then interact in a specific way, like beating or auditory roughness. For majority of listeners beats are heard when the frequency difference between two tones is less than about 12.5 Hz and auditory roughness is sensed when the frequency difference is increased above approximately 15 Hz. A further increase in the frequency difference results in separation of the tones but a roughness can still be sensed and a further increase of frequency difference is needed for a rough sensation to become smooth. Therefore the critical bandwidth can be defined as the frequency separation required between two pure tones for beats and roughness to disappear and for the resulting tones to sound clearly apart, which is illustrated in Figure 2.10 [13].

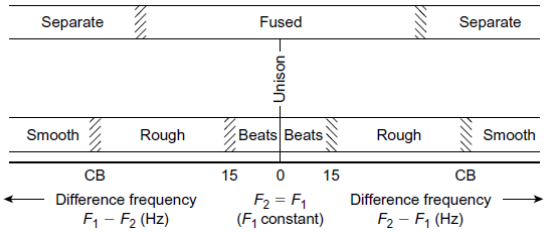

Figure 2.10: Perceptual changes occuring when hearing a pure tone at a fixed frequency F_1 combined with a variable pure tone of variable frequency F_2. The frequency difference between the pure tones at the point where the perception of a listener changes from rough and separate to smooth and separate is known as the critical bandwidth and is marked as CB [13].

2.5 Auditory Masking

The scenario where one sound is made inaudible in the presence of other sounds is referred to as masking. Auditory masking is considered as it is utilized in the SE algorithms considered in this thesis called audible noise suppression (ANS) [16] and the short-time spectral amplitude (STSA) estimator based on the weighted euclidean (WE) distortion measure [16], which are presented in Section 4.2 and Subsection 4.3.1, respectively. The sound source which causes the masking is known as the masker and the sound source which is masked is known as the maskee. There are two types of masking principles:

- Simultaneous masking: When two sound events, masker and maskee, occur at the same time.
- Non-simultaneous masking: A situation where the masker and maskee is out of synchrony and do not occur at the same time.

Only simultaneous masking is relevant in this thesis, where speech signals with additive noise is considered. The unmasked threshold is the smallest level of the maskee which can be perceived without a masking signal is present. The masked threshold is the lowest level of the maskee necessary to be just audible in the presence of a masker. The amount of masking is the difference in dB between the masked and the unmasked threshold [8, 13].

In Figure 2.11 an example of a masking pattern is shown, where the amount of masking produced by a given masker is shown. The masker consists of narrowband noise centred at 410 Hz presented at different intensities from 20 dB to 80 dB with an interval of 10 dB. The maskee is a pure-tone signal. For every fixed intensity of the masker, a corresponding curve of the masked threshold is shown. At the lower intensity levels of the masker, the masking effect tends to be similar for frequencies above and below the masking frequency at 410 Hz. As the intensity of the masker is raised, the masking level curve becomes increasingly asymmetric. The amount of masking grows non-linearly on the high-frequency side, which is called the upward spread of masking. This means that the masking effect is highly dependent on the amplitude of the masker. In Figure 2.11 it can also be seen that as the maskee frequency is shifted away from the masking frequency at 410 Hz, the less an effect the masker have in overwhelming the maskee sound source. But when the maskee frequency is equal to the masking frequency at 410 Hz, the most noticeable masking effect takes place [23].

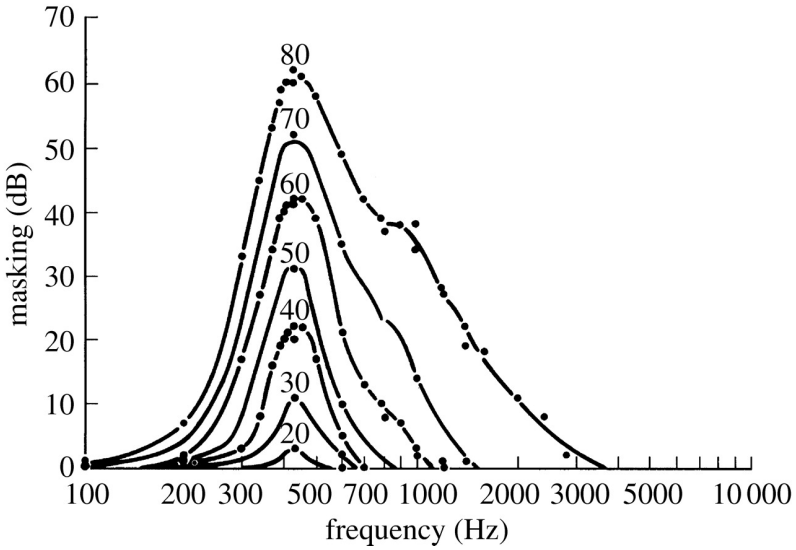

Figure 2.11: Masking pattern for a masker of narrowband noise centered at 410 Hz. Each curve represents the threshold of a pure-tone signal as a function of signal frequency. The intensity level of the masker for each curve is indicated above each curve, respectively. [23]

2.6 Mel-frequency Cepstral Coefficients (MFCCs)

In this section the Mel-frequency cepstral coefficients (MFCCs) are explained, which is the feature extraction algorithm used for ASR in this thesis. Although, other features for speech recognition exist, the MFCCs are used because the ETSI AFE standard, used in this thesis see Section 3.1, specify its features as MFCCs.

The purpose of feature extraction is to transform speech signals into dimension reduced features while preserving critical information. This is particular important as the information required tends to depend on the application, and the information can not be recovered once discarded. Feature extraction is also commonly known as acoustic preprocessing or frontend processing.

MFCC calculations are often preceded by a pre-emphasis operation, which filters a speech signal with the following transfer function[27]:

$$P(z) = 1 - \mu z^{-1}, \tag{2.5}$$

where $\mu \leq 1$ is a real value. The speech signals are processed by the high-pass filter $P(z)$ to achieve a more spectrally balanced speech signal, as the spectrum of speech signals tend to lie at the low frequencies. Furthermore it also helps ensure any DC components are removed [33][27].

First basic concepts of Mel-frequency scale and short-time frequency analysis utilized in the calculation of MFCCs are explained in the following subsections. Then the characteristics of the cepstral features are explored.

2.6.1 Mel-frequency Scale

Due to effectiveness of the human auditory system in perceiving and recognizing human speech, feature extraction techniques based on the characteristics of the human auditory system have been shown to provide excellent performance for ASR [38].

The Mel-frequency scale models the human ear in regard to the non-linear properties of pitch perception. The scale was proposed in 1937 by Stevens, Volkmann and Newman [31], based on experiments where test subjects were asked to adjust the frequency of a tone until they judged it to be half of a fixed tone. The name is meant to symbolise that the scale is based on pitch comparisons, as Mel is a abbreviation of melody. The Mel frequency can be approximated by [25]:

$$f_{\text{mel}}(f\,[\text{Hz}]) = 1127.01048 \ln\left(1 + \frac{f}{700}\right) = 2595 \log_{10}\left(1 + \frac{f}{700}\right). \tag{2.6}$$

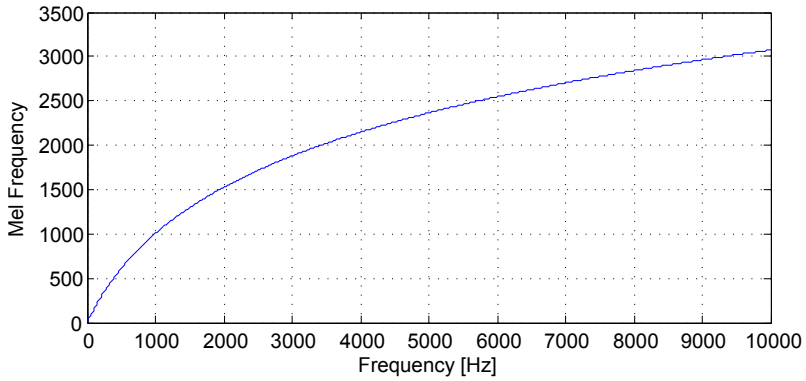

Figure 2.12: The Mel frequency scale as a function of frequency.

The Mel scale is approximately linear up to 1000 Hz, although it is logarithmic, see Figure 2.12 [25]. Nonlinear scales such as the Mel scale, are widely used in ASR. Nonlinear filter banks or bilinear transforms can be used to apply the Mel scale, though the bilinear transform only provides an approximation[38]. As mentioned in Section 2.4 the frequency filtering behaviour of the cochlea can be approximated as overlapping bandpass filters, consequently it is common in ASR to model the operation with filter banks [38]. The spectral energy around the centre frequencies are average by the M triangular filters ($m = 1, 2, \ldots, M$), which constitute the non-linear filter bank, that simulate the critical bands of the cochlea. These filters may be designed

by[38]:

$$H_m[k] = \begin{cases} 0, & k < f[m-1] \\ \frac{2(k-f[m-1])}{(f[m+1]-f[m-1])(f[m]-f[m-1])}, & f[m-1] \leq k \leq f[m] \\ \frac{2(f[m+1]-k)}{(f[m+1]-f[m-1])(f[m+1]-f[m])}, & f[m] \leq k \leq f[m+1] \\ 0, & k > f[m+1] \end{cases}, \tag{2.7}$$

where f is defined as:

$$f[m] = \frac{N}{f_{\text{sampling}}} f_{\text{mel}}^{-1}(f_{\text{lowest}} + m\frac{f_{\text{lowest}} - f_{\text{highest}}}{M+1}). \tag{2.8}$$

f_{lowest} and f_{highest} are the lowest and highest frequencies of the filter bank, respectively, and N are the number of bins in the linear frequency domain. The triangular filters are designed such that the half way point between center frequencies is the 3 dB point, i.e. the point where its half of the maximum spectral power [38]. Additionally, at higher frequencies the width of the filters increase. Figure 2.13 shows a Mel filter bank which uses same amplitude for all filters, however, some implementations weight the filters such that the maximum amplitude of the filters decrease at higher frequencies, in order to maintain an equal energy level in each filter [30].

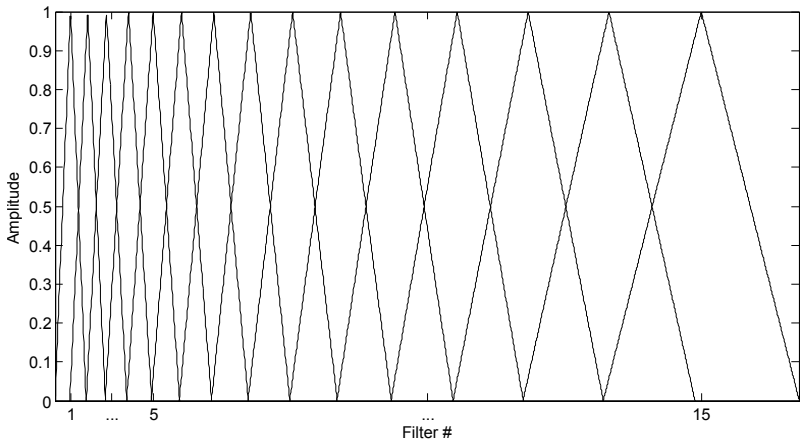

Figure 2.13: A Mel filter bank that uses same amplitude for all filters.

2.6.2 Short-time Frequency Analysis

Short-time frequency analysis have long since been considered the fundamental approach in speech processing. As mentioned in Section 2.2 speech signals are quasi-stationary signals, therefore the signal to be recognised are often separated into short time-domain windows, where the signal can be thought of as stationary. Separating signals into frames, require balancing the pros and cons associated with different frame lengths.

Short window segments increase the time resolution while long segments increases the frequency resolution of the power spectrum. In order to obtain insensitivity to the glottal

cycle relative to the position of the frame, an adequate an frame length is necessary[38]. Both the degree of smoothing of the temporal variations during unvoiced speech and the degree of blurring for rapid event (e.g. release of stop consonants) are determined by the frame length. Consequently the frame length should ideally depend on the speed with which the vocal tract changes shape. The values assigned to frame length and the frame shift ensures the frame overlap each other, with typical values being between 16-32ms and 5-15ms, respectively [38].

The speech signal is segmented into frames via a windowing function. The shape of the window function influences the characteristics of the frequency domain of the frame, where the frequency resolution is in particular affected by this. It is desired to avoid abrupt edges in the windows, which leads to large sidelobes in the frequency domain [38], as the spectrum of the frame is convolved together with the Fourier transform of the window function. Therefore there arises a leakage of the energy from a given frequency into adjacent regions. This is what is normally referred to as spectral leakage, the size of which is proportional to the magnitude of the sidelobes [38]. It is known that window functions without abrupt edges have smaller sidelobes, therefore in speech processing the Hamming window is often applied, see Figure 2.14. The Hamming window is defined as[38]:

$$w[n] = \begin{cases} 0.54 - 0.46\cos(\frac{2\pi n}{N_w}), & 0 \leq n \leq N_w \\ 0, & \text{otherwise} \end{cases} . \tag{2.9}$$

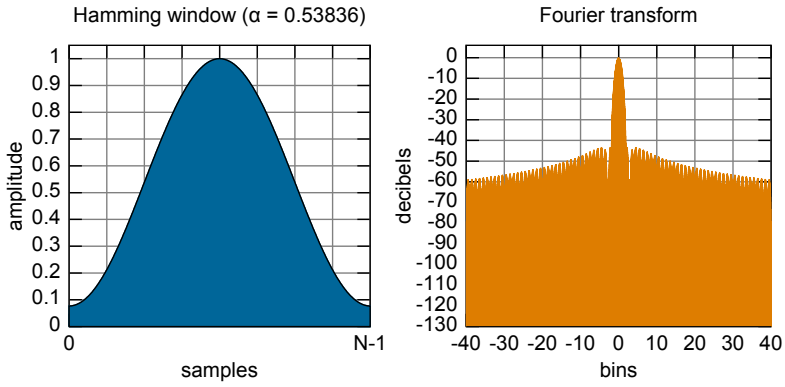

Figure 2.14: A Hamming window and its Fourier transform.

2.6.2.1 Spectrogram

The analysis of phonemes and their transitions is enabled by the energy density as a function of angular frequency w and discrete time frame k. The graphical representation of the energy density is called the spectrogram and defined as follows[38]:

$$\text{Spectrogram}_k(e^{j\omega}) \triangleq |X[k, e^{j\omega})|^2. \tag{2.10}$$

$X[k, e^{j\omega})$ is the short-time Fourier transform (STFT) given by:

$$X[k, e^{j\omega}) \triangleq \sum_{m=-\infty}^{\infty} x[n+m]\, w[m] e^{-j\omega m}, \tag{2.11}$$

where k is discrete and ω is continuous, $w[m]$ is a window function e.g. a Hamming or Gaussian window function, which is used to break the signal into frames. Each frame is then Fourier transformed. In speech applications spectrograms tends to utilize the logarithmic frequency scale because human speech has a large dynamic range[38]:

$$\text{Logarithmic Spectrogram}_k(e^{j\omega}) = 20\log_{10}|X[k, e^{j\omega})|. \tag{2.12}$$

Depending on whether the duration of the window used, is short (less than one pitch period) or long (≥ two pitch periods), the utilized spectrogram is differentiated between wide-band or narrow-band, respectively [38]. The use of wide-band spectrogram results in good time resolution, but the harmonic structure is smeared. In comparison, the narrow-band spectrogram provides better frequency resolution but poorer time resolution. In addition, during segments containing voiced speech the harmonics of the pitch can be observed as horizontal striations due to the increased frequency resolution [38].

2.6.3 Definition and Characteristics of Cepstral Sequences

Although originally intended for differentiation of underground echoes [38], cepstral features have been used in ASR for more than 30 years and is today widely used in a range for of different speech applications. The names stem from the inventors who realized that the operations they utilize in the transform domain, are typical exclusively used in the time domain. Hence, the name cepstrum was chosen by reversing the first letters in spectrum[38]. The complex cepstrum z-transform is defined as:

$$\hat{X}(z) \triangleq \log X(z), \tag{2.13}$$

where $X(z)$ is the z-transform of a stable sequence $x(n)$ (n is the discrete time index), $\hat{X}(z)$ is the z-transform of the complex cepstrum and $\log(\cdot)$ is a complex-valued logarithm, hence the name complex cepstrum. This leads to the following definition for the complex cepstrum[38]:

$$\hat{x}[n] = \frac{1}{2\pi}\int_{-\pi}^{\pi} \log X(e^{j\omega}) e^{j\omega n} d\omega, \tag{2.14}$$

which is the inverse Fourier transform of $\log X(e^{j\omega})$, the real cepstrum is then defined as:

$$c_x[n] \triangleq \frac{1}{2\pi}\int_{-\pi}^{\pi} \log|X(e^{j\omega})| e^{j\omega n} d\omega. \tag{2.15}$$

The real cepstrum $c_x[n]$ is the inverse transform of the real part of $X(e^{j\omega})$. Characteristics of the cepstral sequence is investigated using the time-series cepstral representation $\hat{h}[n]$ of a transfer system of a linear time-invariant system [38]:

$$\hat{h}[n] = \begin{cases} \log|K|, & n = 0 \\ -\sum_{m=1}^{M_i} \frac{c_m^n}{n} + \sum_{m=1}^{N_i} \frac{d_m^n}{n}, & n > 0 \\ -\sum_{m=1}^{M_o} \frac{a_m^{-n}}{n} - \sum_{m=1}^{N_o} \frac{b_m^{-n}}{n}, & n < 0 \end{cases}, \tag{2.16}$$

where $|a_m|$, $|b_m|$,$|c_m|$,$|d_m| < 1$, M_i and N_i are the number of zeroes and poles inside the unit circle, respectively. M_o and N_o are the number of zeroes and poles outside the unit circle, and K is a real constant.

It can be shown that the cepstrals coefficients are a casual sequence of the system if it is a minimum phase system (i.e. both the transfer function of the system and its inverse are stable and casual), meaning that $\hat{h}[n] = 0 \ \ \forall \ n < 0$. In addition the cepstral coefficient $\hat{h}(n)$ decay at a rate of at least $^1/_n$ meaning most information about the spectral shape of the transfer system is contained with the lower order coefficients. It is possible to derive a second cepstral sequence $\hat{x}_{\min}[n]$ for the minimum phase system, where the cepstra of $\hat{x}_{\min}[n]$ and $\hat{x}[n]$ have the different phase but the same magnitude. An expression for $x_{min}[0]$ can then be derived as[38]:

$$\hat{x}_{\min}[n] = \begin{cases} 0, & n < 0 \\ \hat{x}[0], & n = 0 \\ 2\hat{x}[n], & n > 0 \end{cases} . \tag{2.17}$$

Especially $x_{min}[0]$ and $x_{min}[1]$ of the lower order cepstral coefficient can be given intuitive meaning. The average power of the input signal can be observed in $x_{min}[0]$, though for ASR purposes more reliable power measures are typical utilized. $x_{min}[1]$ is on the other hand a measure of how the spectral energy is distributed between high and low frequencies [38]. The sign of $x_{min}[1]$ provides information about where the spectral energy is concentrated, positive and negative values indicate energy concentration at low and high frequencies, respectively [38].
Increasing levels of spectral details can be found in the higher order cepstral coefficients. It can be shown that an infinite number of cepstral coefficients is produced by an finite input sequence, however, to archive accurately ASR results a finite number of coefficients is sufficient[38]. Depending on the sampling rate, only the first 12-20 coefficients are typically used. This occurs because lower order coefficients contribute more than higher orders to class separation [38].

Discarding the higher orders of the cepstral coefficients provide an additional benefit due to another characteristic of the cepstral sequence. By removing the higher order coefficients from a sequence of cepstral coefficients it is possible to remove the periodic excitation $p[n]$ occurring due to the vocal cords. If it is assumed that the sequence $x[n]$ is given by convolution:

$$x[n] = h[n] * p[n], \tag{2.18}$$

where $h[n]$ is the impulse response of a linear time-invariant system and $p[n]$ is the periodic excitation with an period T_0 of the system. Removing $p[n]$ from the speech signal $x[n]$ is advantageous as the goal is to extract a representation of $h[n]$ from $x[n]$. From this the

following expression for the complex cepstrum can then be derived [38]:

$$\hat{x}[n] = \hat{h}[n] + \hat{p}[n], \tag{2.19}$$

meaning that if two sequences are convolved in the time domain, then their complex cepstra are simply added together. Combining this with Equation 2.17, the cepstral sequence for minimum phase system can then be expressed as:

$$\hat{x}_{\min}[n] = \hat{h}_{\min}[n] + \hat{p}_{\min}[n]. \tag{2.20}$$

It has been proven [38] that when $p[n]$ is an periodic excitation with a period T_0, then $\hat{p}[0] = 0$ and $\hat{p}[n]$ is periodic with period of $N_0 = T_0/T_s$ samples [38], where T_s is an sampling interval. Consequently, $\hat{p}[n]$ is only nonzero at $\hat{p}[kN_0]$. Meaning that the liftering (the name comes from reversing the first four letters of filtering) operation can be utilized to recover $\hat{h}_{\min}[n]$ [38]:

$$\hat{h}_{\min}[n] \approx \hat{x}_{\min}[n]\omega[n], \tag{2.21}$$

where

$$\omega[n] = \begin{cases} 1, & \forall 0 \leq n < N_0, \\ 0, & \text{otherwise.} \end{cases} \tag{2.22}$$

If $h[n]$ then is the impulse response of the vocal tract of a speaker and $p[n]$ the periodic excitation produced by the vocal cords during voiced speech, Equation 2.21 shows how the cepstral domain can remove the periodic excitation resulting from the vocal cords, by simply removing higher order cepstral coefficients, so that spectral envelope made by the shape of the vocal tract can be found [38].

2.6.4 Calculating Cepstral Coefficients

In ASR acoustic features are typical produced from the minimum phase equivalent $\hat{x}_{min}[n]$ of the cepstral sequence. These features can be found by calculating an intermediate value $c_x[n]$ (2.15) using the inverse discrete Fourier transform (DFT), which can be used to find $\hat{x}_{min}[n]$[38]:

$$\hat{x}_{\min}[n] = \begin{cases} 0, & n < 0 \\ c_x[0], & n = 0 \\ 2c_x[n], & n > 0 \end{cases}. \tag{2.23}$$

Another option is to use the type 2 discrete cosine transform (DCT), to apply the inverse DCT to log-power spectral density $\log|X(e^{j\omega})|$:

$$\hat{x}_{\min}[n] = \sum_{m=0}^{M-1} \log|X(e^{j\omega_m})| T^{(2)}_{n,m}, \tag{2.24}$$

where $T^{(2)}_{n,m}$ is a component of the type 2 DCT. The calculation of the MPCCs is summarized in Figure 2.15. First the pre-emphasis spectrally balance the signal using a high-pass filter.

Then the Hamming window is used to separate the speech signal into frames. In order to reveal more of the structure these frame are then transformed into the power spectrum using the DFT. Using Mel-filterbanks the spectrum is mapped to reflect the human hearing, which is non-linear in frequency. Next the dynamic range of human hearing, which is also non-linear, is modelled by taking the logarithm. The periodic excitation from the vocal cords are then removed, by taking the DCT and discarding the higher-order coefficients, so the spectral envelope produced by the vocal tract remains [33].

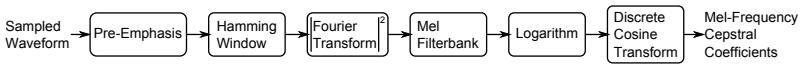

Figure 2.15: Mel-frequency cepstral coefficients

The MFCC is one of the most popular feature extraction schemes used for ASR. It is, however, dependent on the application of the automatic speech recognizer, where the feature extraction scheme provides the superior results [38]. MFCC is known to provide superior results under clean conditions.

2.6.5 Feature Augmentation

Concerning categorization and discrimination of human phonetic, it has been shown that time segments of 100ms or less produce poor ASR results[38]. This perhaps somewhat surprising as the analysis window utilized in ASR is typically no more than 32 ms. Consequently the information from a single window of short-time spectral analysis that make up the feature vector have to have its observation content extended. It is possible to extend the observation content by augmenting the speech frame using either static or dynamic features. It has been proven however, that the dynamic features are more resilient than the static features to the effects of additive noise[38]. In addition the dynamic features are also immune to the constant offset in the logarithmic spectrum or cepstrum domain resulting from short-time convolutional distortion[38]. Perhaps the simplest way to obtain the dynamic features are by taking the difference between consecutive frames, to estimate the differential. Dynamic features are estimated over multiple frames, typically five to seven frames, so as to produce more reliable estimates, by minimizing the effect of any random variation between frames which could be harmful[38].

The dynamic features can be further extended by including acceleration features, however, a longer time is required to accurately estimate the second-order dynamics. The first-order derivation can be estimated by[38]:

$$s[k] \approx \sum_{m=-M}^{M} ms[k+m]. \tag{2.25}$$

Higher order derivations can be found by reapplying the linear phase filter in Equation 2.25 consecutively to output from the previous order. The first and second order derivations is referred to as the Delta and Delta-Delta coefficients, respectively.

Automatic Speech Recognition 3

This chapter presents the feature extraction method and the machine learning algorithm, which are used to generate the ASR results within this thesis. The speech database to be used for training acoustic models and for recognition experiments is described along with the performance evaluation measures.

The general principle of speech recognition is shown in Figure 3.1. Speech recognition is performed by first separating the speech signals into overlapping speech frames, which are then transformed into dimension reduced features, e.g. MFFCs presented in Section 2.6. The duration of these speech frames is kept short so that the speech waveform can be approximated as stationary [41]. These feature vectors, as they are called, are used to limit the number of variables required in the analysis of the speech signals, which reduce the amount of memory and computational power needed, both of which can be major issues when dealing with large data sets. The feature extraction process also helps eliminating any irrelevant information from the input signal, while retaining only what is considered critical information [33]. Recognition is performed by the use of acoustic models, which are trained using sequences of feature vectors to represent words [41].

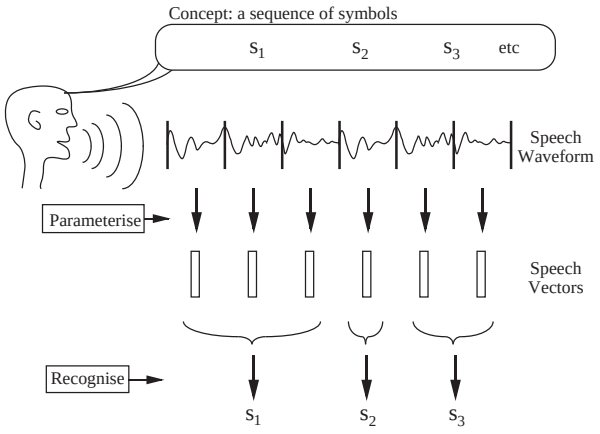

Figure 3.1: General principle of the speech recognition process [41].

In this thesis the ASR results are produced by the use of the advanced frontend (AFE) feature extraction algorithm applied on the Aurora-2 database. In addition the Hidden Markov Model Toolkit (HTK) is used to model speech and recognize speech. It has been chosen to use these methods, as they have been used in [14] which raises the issue of applying an algorithm from one field to the other. Furthermore, [12] intended to establish a baseline, using these methods, to ease comparison of ASR performance. This make these methods suitable choices for this thesis.

3.1 ETSI Advanced Front-End

The advanced frontend (AFE) is one of four standards developed by the European Telecommunications Standards Institute (ETSI) that specify feature extraction and compression algorithms for distributed speech recognition (DSR) [7]. DSR is one of three architectures used in ASR on mobile devices, where the two other architectures are network speech recognition (NSR) and embedded speech recognition (ESR)[33].

The ESR architechture is characterised by doing all the processing on the terminal site. The NSR architecture is, however, characterised by transmitting an encoded speech signal from the terminal to a server which decodes the speech signal and then performs feature extraction and recognition. In DSR, feature extraction is performed by the terminal device, the features are then transmitted to the server [27].

Figure 3.2 shows the block diagram of the terminal AFE processing chain, which consists of a *feature extraction* block, a *feature compression* block and bit-stream formatting algorithms.

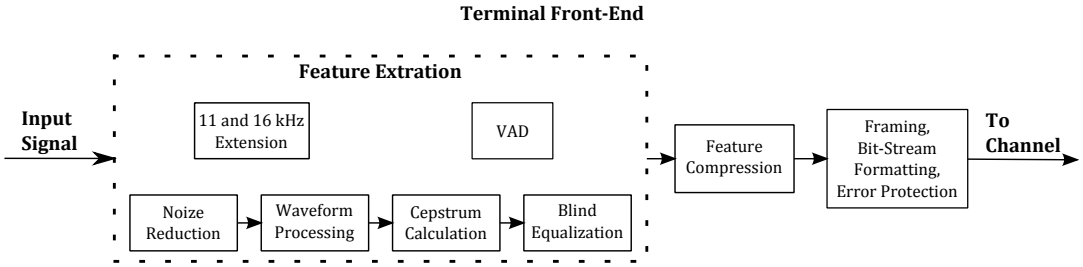

Figure 3.2: Block diagram of the terminal side advanced frontend [7].

The focus in this thesis is on the *feature extraction* block and the steps within. The actual transform of the MFCCs occurs within the *cepstrum calculation* block. In order to ensure noise robustness, the speech signal is first processed by a *noise reduction* block, where a 2-stage Wiener filter is employed [27].

3.1.1 Feature Extraction

In order to enable classification it is necessary to transform the input data into a suitable form of MFCCs feature vectors. In addition to *cepstrum calculation* the *feature extraction* block includes a number of sub-blocks, that perform preprocessing and postprocessing. The input to the *feature extraction* block is fed to the *noise reduction* block, which uses Wiener filter techniques. This is followed by *waveform processing* which attempts to maximise the signal-to-noise ratio (SNR) using a time-domain approach, as opposed to the frequency-domain approach used by the Wiener filters. The final stage after *cepstrum calculation* is the *blind equalization* block which equalizes the cepstral coefficients according to a least mean square filtering approach.

As standard the *feature extraction* block requires the speech signal to have a sampling rate of 8 kHz, which stems from the speech database used. Although, there are extensions available allowing for 11 kHz and 16 kHz sampling rates. In this section the functionality of the each block is presented.

3.1.1.1 Noise Reduction

In the first block of the AFE, noise reduction is applied to the speech signals. It utilizes a two-stage mel-warped Wiener filter as shown in figure Figure 3.3. This filtering is the main source of noise reduction for the AFE. In each stage of the *noise reduction* block, the noisy signal is denoted $y[k]$, where it is considered that the original clean signal $x[k]$ has been corrupted by additive noise $n[k]$, i.e. $y[k] = x[k] + n[k]$, which is obviously different in each stage. k is the discrete time index.

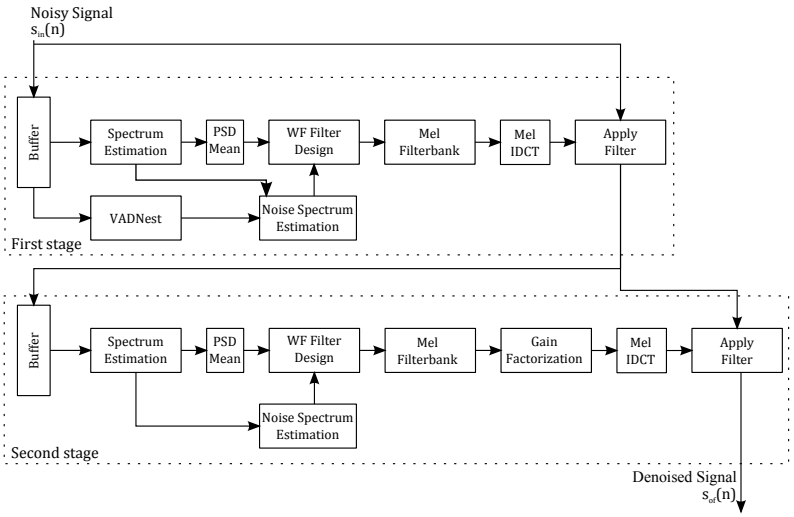

Figure 3.3: Block diagram of the *noise reduction* block of the AFE.

Noise reduction is performed on a frame-by-frame basis, where one frame is defined as 80

samples [7]. Each of the two stages operates with a 4 frame buffer. The first stage performs the initial denoising of the signal, which is further processed in the second stage using dynamic noise reduction depending on signal-to-noise ratio (SNR) of the output from the first stage [7]. It is because of the inaccurate spectrum estimates used during the first stage that the second stage is necessary. The purpose of the *spectrum estimation* block is to find an estimation of the linear spectrum for each frame. The *PSD mean* block then smooths out this spectrum estimate along the time dimension. The *noise spectrum estimation* block uses the silent segments where only the noise signal $n[k]$ is present (located using Voice Activity Detection (VAD) for noise estimation (VADNest)) to find an estimate of the noise spectrum. Then the frequency domain Wiener filter coefficients are found in the *WF Filter design* block using both the spectrum and noise spectrum estimates for the current frame. The *Mel filterbank* block smooth the linear Wiener filter coefficients along the frequency domain using a Mel filterbank, to obtain a Mel-warped frequency domain Wiener filter. The *gain factorization* block in the second stage adjusts the aggressiveness of the noise reduction on a frame-by-frame basis depending on whether it is a speech or silent frame. From the Mel-warped Wiener filter, the corresponding impulse response is found by applying the *Mel IDCT* (Mel-warped Inverse Discrete Cosine Transform). The *Apply Filter* block then filter the input signal at each stage [27]. In the following the operation of each block in the *noise reduction* block is expanded upon.

Spectrum Estimation and PSD Mean

Each stage of the Wiener Filtering (WF) uses a buffer with a fixed frame length of $25ms$, and a frame shift of $10ms$. For speech signals sampled at sampling frequency $F_s = 8000$ Hz this translates to a frame length of $N_{\text{in}} = 200$ samples and a shift of $M = 80$ samples.

In order to obtain the power spectrum of the input signal, each frame is applied a Hanning window followed by a FFT using $N_{\text{FFT}} = 256$. The spectrum for each frame is then smoothed in frequency. Time smoothing is then performed in *PSD Mean* block[27]. The frequency smoothing perform by the *spectrum estimation* block is given by:

$$\begin{aligned} |\tilde{Y}_t[i]|^2 &= \frac{|Y_t[2i]|^2 - |Y_t[2i+1]|^2}{2}, \quad 0 \le i \le \frac{N_{\text{FFT}}}{4} \\ |\tilde{Y}_t[N_{\text{FFT}}/4]|^2 &= |\tilde{Y}_t[N_{\text{FFT}}/2]|^2, \end{aligned} \tag{3.1}$$

where $|Y_t[i]|^2$ is the spectrum for frame t where $i = 0, \ldots, N_{\text{FFT}} - 1$. The time smoothing performed by the *PSD mean* is given by:

$$\overline{|Y_t[i]|}^2 = \frac{\tilde{Y}_t[i] - \tilde{Y}_{t-1}[i]}{2} \quad 0 \le i < N_{\text{SPEC}} = \frac{N_{\text{FFT}}}{4} + 1. \tag{3.2}$$

Noise Spectrum Estimation

The VADNest detector finds and marks the silent frames by tracking significant changes in the speech signal with a full-band-energy VAD. Those frames marked as silence by the VADNest detector are then used to compute the noise spectrum. The log-energy is found for each frame

using the average background noise log-energy and the frame is then classified as speech or silence based on the difference between the log-energy of the noisy signal and the log energy of the background noise [27]. This decision is based on a fixed threshold. During silent frames the *noise spectrum estimation* block finds estimates of the noise $\hat{N}_t[f]$ using a recursive smoothing filter [27]:

$$|\hat{N}_t[f]| = \lambda_t|\hat{N}_{t-1}[f]| + (1-\lambda_t)\overline{|Y_t[f]|}, \tag{3.3}$$

where λ_t is a forgetting factor that depend on the frame number t and $0 \leq f \leq F_s/2$. For the first 100 frames it is $(1-1/t)$ and for the subsequent frames it is 0.99. During speech frames the noise is estimated by $|\hat{N}_t[f]| = |\hat{N}_{t-1}[f]|$. The noise spectrum estimation is performed differently in the second stage, for the first 10 frames, otherwise it is executed in the same way as in the first stage (see Equation 3.3). All subsequent frames, regardless of classification are found using [27]:

$$|\hat{N}_t[f]|^2 = \gamma|\hat{N}_{t-1}[f]|^2 + (1-\gamma)|\tilde{N}_t[f]|^2, \tag{3.4}$$

where $\gamma = 0.9$, and $|\tilde{N}_t[f]|^2$ is the initial estimate of noise spectrum at time t.

Wiener Filter Design

The WF design is carried out in two iterations(for each stage in the *noise reduction* block). In the first iteration the WF filter $|H_{1,t}[f]|$ is found and then used to find the first estimate of the clean spectrum $|\hat{X}_{2,t}[f]|$, which in turn is used to calculate the final WF filter $|H_{2,t}[f]|$ [27]. Filtering $|\hat{X}_{2,t}[f]|$ with this final filter, the final estimate $|\hat{X}_{3,t}[f]|$. The WF in each iteration is found by:

$$H_{i,t}[f] = \frac{|\hat{X}_{i,t}[f]|}{|\hat{X}_{i,t}[f]| + |\hat{N}_t[f]|} = \frac{\sqrt{\xi_{i,t}[f]}}{1+\sqrt{\xi_{i,t}[f]}}, \tag{3.5}$$

where $|\hat{N}_t[f]|$ is the noise spectrum estimate at time t and $\xi_{i,t}[f] = |\hat{X}_{i,t}[f]|^2/|\hat{N}_t[f]|^2$ is an estimate of *a priori* SNR and i indicates the iteration number. The initial estimate of the clean spectrum can be found using spectral subtraction:

$$|\hat{X}_{1,t}[f]| = \beta|\hat{X}_{3,t-1}[f]| + (1-\beta)\max(\overline{|Y_t[f]|} - |\hat{N}_t[f]|, 0), \tag{3.6}$$

where $\beta = 0.98$. The first true clean speech estimate is then found by $|\hat{X}_{2,t}[f]| = \hat{H}_{1,t}[f]\overline{|Y_t[f]|}$. Substituting $|\hat{X}_{2,t}[f]|$ as the estimate for clean speech, the transfer function $|H_{2,t}[f]|$ of the second iteration can then be found using Equation 3.5. The final step is then to find $|\hat{X}_{3,t}[f]| = H_{2,t}[f]|\tilde{Y}_t[f]|$, which is needed to compute $|\hat{X}_{1,t}[f]|$ in the next frame (see Equation 3.6). Traditional Wiener filters uses the Power Spectra, while Equation 3.5 uses the magnitude spectra. This means that the Wiener filter used can be interpreted as a magnitude spectral subtraction technique, since normal Wiener filters can be interpreted as spectral subtraction [27].

Mel Filterbank

A Mel-scaled triangular filter-bank is applied to the frequency response $\hat{H}_{2,t}[f]$, where the filter-bank uses $K_{\text{FB}} = 23$ frequencies bands including the marginal frequencies 0 and $F_s/2$, which brings the total to 25 filters [27]. This is done as adding perception qualities, which emulate the characteristics of the human auditory system, tends to improve recognition systems as mentioned in Subsection 2.6.1. The filters in the bank are weighted by the following expression:

$$H_{2,t}^{(\text{mel})}[f_k] = \frac{\sum_f w(f_k, f) H_{2,t}[f]}{\sum_f w(f_k, f)}, \tag{3.7}$$

where $w(f_k, f)$ represents the kth filterbank channel (see Figure 2.13). f_k and f are the central frequency and N_{SPEC} frequency values in the linear-frequency domain, respectively ($N_{\text{SPEC}} = \frac{N_{\text{FFT}}}{4} + 1$) [27].

Gain Factorization (Exclusive To Second Stage)

The purpose of the *gain factorization* block is to adjust the level of the noise reduction performed such that silent frames are treated more aggressively than speech frames. As previously mentioned, the implemented WF can be interpreted as magnitude spectral subtraction, thus the corresponding transfer function is:

$$H[f)] \approx \frac{|\hat{X}[f]|}{|\hat{X}[f]| + |\hat{N}[f]|}. \tag{3.8}$$

This requires an initial estimate of the clean speech spectrum $|\hat{X}[f]|$:

$$|\hat{X}[f]| = |Y[f]| - \alpha|\hat{N}[f]|. \tag{3.9}$$

where the level of aggressiveness is adjusted by controlling the amount of subtracted noise using a factor α. The WF can then be expressed as:

$$H^{(\text{GB})}[f] = (1-\alpha) + \alpha\left(\frac{|\hat{N}[f]|}{|Y[f]|}\right) = (1-\alpha) + \alpha H[f]. \tag{3.10}$$

In the AFE, the level of aggression applied to each frame varies depending on the SNR of frame. The range of the α factor span from 0.1 to 0.8 for speech frames and silent frames, respectively. The α factor is controlled by two different SNR measures, SNR_{aver}, a smoothed SNR over the last 3 frames, and $SNR_{\text{low\_track}}$, which is the lowest value of SNR_{aver} recorded during the previous frames [27].

Mel-IDCT

In the *Mel-IDCT* block the time domain impulse response of the WFs are found. Given a filter frequency response $H(f)$ is real and even, its impulse response is obtained by:

$$h_{\text{WF}}[n] = \sum_{k=0}^{K_{\text{FB}}+1} H_{2_{WF}}[f_k] \cdot IDCT_{mel}(f_k, n), \quad 0 \le n \le K_{\text{FB}} + 1, \tag{3.11}$$

where $H_{2_{WF}}[f_k]$ are the Mel Wiener filter coefficients, and f_k are the central frequencies of the Mel-filterbank. In the ETSI AFE standard [7], this expression is referred to as the Mel-IDCT. The f_k are found by taking a weighted average of each band:

$$f_k = \frac{\sum_f w(f_k, f) f}{\sum_f w(f_k, f)} \quad 0 \leq k \leq L = K_{\text{FB}} + 1. \tag{3.12}$$

where $w(f_k, f)$ represents the kth filterbank channel [27].

Apply Filter

The filter is applied using convolution in the time domain, where the input signal is convolved with the WF impulse response. In order to obtain a smooth frequency response the filter coefficients are truncated using a Hanning window of length $FL = 17$ samples centered around $n = 0$ [27]. The frames of the denoised signal $\hat{x}[n]$ are calculated by convolving the final filter $\tilde{h}[n]$ with the first $M = 80$ samples (for 8 kHz speech signals) of the input signal $y[n]$ in the buffer, in order to avoid overlapping samples [27]:

$$\hat{x}[n] = \sum_{(\text{FL}-1)/2}^{i=-(\text{FL}-1)/2} \tilde{h}[i]\, y[n-i], \quad 0 \leq n \leq M-1. \tag{3.13}$$

3.1.1.2 Waveform Processing

SNR-dependent waveform processing (SWP) is applied in the time-domain, in order to increase SNR. It utilizes the fact that during voiced speech segments the signal energy varies even within one pitch period. When the glottis is closed the signal energy is at its peak and afterwards it rapidly declines. However, during a pitch period the energy of the noise is assumed constant and therefore the SNR varies within the interval [27]. Consequently, the SNR of the signal can be increased by increasing or decreasing the energy depending on if the energy in the periods is high or low, respectively. The first step is to find the smoothed energy contour using the discrete version of the Teager operator where the instantaneous signal energy can be found by [27]:

$$E_{Teag}[n)] = |s_{of}^2[n] - s_{of}[n-1]\, s_{of}[n+1]|. \tag{3.14}$$

The instantaneous energy is found for each frame consisting of $N_{in} = 200$ samples. The samples $s_{of}[0]$ and $s_{of}[N_{in}-1]$ are repeated for previous and future samples in order to enable calculation of the Teager operator at the boundaries of the frames. The mean over the interval $[n-4, n+4]$ is then defined as the smoothed energy contour $E_{Teag_Smooth}[n]$ [27]. The next step in SWP is then to locate consecutive energy peaks, which is done using a strategy of peak-picking that finds the frames N_{MAX} maxima. The expectation of [27] is that a maxima occur every 25 to 80 samples. A weighting function $w[n]$ (sequence of rectangular unit windows) is utilized to locate high-energy portions of the frame, low-energy portions are found using

$1-w[n]$. Amplification and attenuation of the high- and low-energy portion in $s_{of}[n]$ are done by:

$$s_{swp}[n] = \gamma\omega[n]s_{of}[n] + \epsilon(1-\omega[n])s_{of}[n], \tag{3.15}$$

where $\gamma = 1.2$ and $\epsilon = 0.8$. It should be noted that these values mean that energy in the frame is not preserved [27].

3.1.1.3 Cepstrum Calculation

The purpose of the *cepstrum calculation* block is to extract 13 cepstral coefficients MFCC(0−12) and a logarithmic energy coefficient per frame (MFCC(0) and log-energy are later combined to a single coefficient representing the energy of the frame) [27]. The AFE uses a frame size of $N_{in} = 200$ with a shift of $M = 80$ samples, the value of these are for a fixed sampling frequency of $f_s = 8$kHz. The log-energy is calculated by:

$$\log E = \log \sum_{n=0}^{N_{in}} s_{pre}[n]^2. \tag{3.16}$$

The AFE pre-emphasise the output signal $s_{swp}[n]$ from the *waveform processing* block which is then denoted by $s_{pre}[n]$ when calculating the MFCCs, with a factor $\mu = 0.9$ (see Equation 2.5). The Mel-filterbank centre frequencies lie within the range from 64Hz to $F_s/2$ [27]. See Section 2.6 for detail of how MFFC are calculated.

3.1.1.4 Blind Equalization

The purpose of equalization is to achieve a system where the accuracy of ASR is robust against channel variations such as the use of different microphones [27]. In the ETSI standard the last stage of *feature extraction* is the *blind equalization* where the cepstrum coefficients are equalized according to a least mean square filtering, which operates with a reference cepstrum corresponding to the cepstrum of a flat spectrum. An additive operation is used to perform equalization in the cepstral domain:

$$c_{eq}(n) = c[n] + c_h[n], \tag{3.17}$$

where $c[n](n = 0, 1, \ldots, 12)$ are the MFCC coefficients found in the previous step. $c_{eq}[n]$ and $c_h[n]$ are the equalized cepstrum and the cepstrum of the equalization filter, respectively. The equalization filter is found by minimizing the MSE function:

$$MSE[n] = E\left[\left(c_{ref}[n] - c_{eq}(n)\right)^2\right], \tag{3.18}$$

where $c_{ref}[n]$ is the reference cepstrum (corresponding to a flat spectrum) and $c_{eq}[n]$ tries to compensate for the bias between $c[n]$ and $c_{ref}[n]$. $c_h[n]$ can then be found by the following Least Mean Square (LMS) solution:

$$c_h[n;t+1] = c_h[n;t] + \mu\left(c_{ref}[n;t] - [c_h[n;t] + c[n;t)]\right), \tag{3.19}$$

where t is the frame number and $\mu = 0.008789u$ $(0 \leq u \leq 1)$ is the step-size, which [7] makes dependent on the frame energy u. Low- and high-energy frames are denoted by $u = 0$ and $u = 1$, respectively.

3.2 HMM Based Speech Recognition System

In this section the evaluation of the noise robust ASR system based on AFE feature extraction is presented. The evaluation is defined by the experiment called the ETSI Aurora-2 task [26], which contains distorted versions of spoken digits. The basic concepts of HMMs are presented and their use in speech recognition, where HTK (Hidden Markov Model Toolkit) [41] is a software toolkit used to build the HMMs and recognizing speech.

3.2.1 ETSI Aurora-2 Task

ETSI has defined a set of speech recognition experiments called the Aurora-2 task [26], which is publicly available to be used by the speech community. The purpose of the experiment is to provide a common framework for evaluating noise-robust speech recognition systems. Therefore the ASR results presented in this thesis are provided as defined by this experiment.

Aurora-2 provides a clean speech database, which is based on a downsampled version of the TIDigit database. It consists of speech signals recordings of male and female American people, where connected digits are spoken in sequences of up to 7 digits, which constitutes a sentence [26].

In order to consider realistic frequency characteristics of terminals and equipment within the telecommunication area, two "standard" filters have been defined by the International Telecommunication Union (ITU). They are denoted by G.712 and MIRS. The difference between the filters are that G.712 has a flat frequency characteristics in the range between 300 Hz and 3400 Hz, whereas the MIRS has a rising characteristics in this range with slightly more attenuation of the lower frequencies. MIRS can be seen as a filter that simulates the behaviour of a telecommunication terminal, that meets the official requirements for the terminal input frequency response as specified e.g. for Globel System for Mobile Communications (GSM) [26].

A noise database is also provided by Aurora-2 consisting of eight background noises considered often to take place in real life, where the conditions recorded are:

- Suburban train (subway)
- Crowd of people (babble)
- Car
- Exhibition hall (exhibition)

- Restaurant
- Street
- Airport
- Train station

The noise is added to the clean speech data at various SNR levels (20, 15, 10, 5, 0, -5 dB). Additionally a clean case is considered, where no noise is added to the clean speech data. In this context the SNR is defined as the ratio of the signal to noise energy after filtering both signals with the G.712 filter. The speech and noise energy is determined by the ITU recommendation P.56 [26].

The software package HTK (Hidden Markov Model Toolkit) [41] is applied to perform speech recognition. It is a software toolkit, available in C source form, for modelling speech with HMMs and recognizing speech by Viterbi decoding. HTK is used to do whole word HMMs for all digits [41]. The HMMs are defined by the following parameters:

- 16 states per word
- Simple left-to-right models without skipping over states
- 3 Gaussian mixtures per state
- The covariance matrices are diagonal, so only the variances of all acoustic coefficients are provided.

There are two modes for training the HMMs:

- *Clean* training mode: Training with clean speech only
- *Multi-conditioned* training mode: Training with clean and noisy speech. The noises added in *multi-condition* training are subway, babble, car and exhibition.

In the *clean* training mode, the speech signals are filtered with the G.712 standard frequency characteristic. When training on clean data only, the models are not robust to noisy data. The highest performance that can be obtained with this type of training is when testing on clean data only.

In the *multi-conditioned* training mode both the speech and noise signals are filtered with the G.712 characteristic before adding. This *multi-conditioned* training is performed both with clean and noisy speech data, which makes it more robust to noise. It usually leads to highest recognition performance when training and testing are done in the same noise conditions.

When testing, there exists three test sets known as A, B and C. Test set A and B each consists of 4004 speech signals, which are divided into 4 subsets of 1001 speech signals. Four different types of noise are added to each subset at SNR levels (20, 15, 10, 5, 0, -5 dB) and including the clean case with no additional noise, it gives total gives 28 subsets for test set A and B, respectively. Again speech and noise are filtered with the G.712 characteristic before adding.

Test set C only contains two subset of 1001 speech signals and two noise types are added at the seven SNR levels, which gives a total of 14 subsets. But this time the speech and noise are filtered with the MIRS characteristic before adding.

In test set A the noise types added to each speech signal are subway, babble, car and exhibition, which are the same noise types used in the *multi-conditioned* training. Therefore test set A evaluates the system in matched conditions. In test set B, the noise types used are restaurant, street, airport and train station. Since these noise types are not used for the *multi-conditioned* training, test set B evaluates the system in mismatched conditions (mismatched noise).

In test set C the two noise types subway and street are used for the two subsets of speech signal. So test set C evaluates the system in mismatched conditions (mismatched frequency characteristics), since the speech and noise of this test set are filtered with the MIRS filter characteristic and not the G.712 filter used for the training data [26].

3.2.2 Hidden Markov Model (HMM)

In the field of machine learning, predictions are made based on models of observed data. A simplified model can be made by assuming that the observations are independent and identically distributed (iid). But when considering sequential data, as in sequences of spoken words, treating the observations as iid would not exploit the dependencies between observations close in the sequence such as correlation. Therefore the iid assumption needs to be relaxed and a model is required which exploits the sequential pattern in the data [1].

A Markov process is used to model sequential data, which is described by N states $\{s_1, s_2, ..., s_N\}$. Each state in the Markov process represents a certain observation and at each time interval the system changes from one state to another (transition). The state at time t is denoted by o_t. Markov processes are characterized by the fact that the current state depend on all previous states. This means that the process has memory. But it is impractical to consider a model for sequential data in which future predictions depend on all the previous observations, because it results in a complexity that would grow without limit as the number of observations increases. Therefore a first order Markov chain model is considered in which it is assumed that future predictions are independent of all previous observations, except from the most recent one. The transition probabilities from one state to another in such a process are described by:

$$a_{ij} = P(o_t = s_j | o_{t-1} = s_i). \tag{3.20}$$

The probability of observing a sequence of T observation $\mathbf{O} = \{o_1, o_2, ..., o_T\}$, when modelling the observations by the use of a first order Markov chain model, is computed by:

$$p(o_1, ..., o_T) = p(o_1) \prod_{n=2}^{T} p(o_t | o_{t-1}). \tag{3.21}$$

When introducing a hidden state x_t at time t corresponding to each observation o_t and assuming that the hidden states form a Markov chain, a Hidden Markov Model (HMM) is generated. The hidden states in a HMM are discrete, while the observations may be discrete or continuous. A discrete HMM is characterized by the following elements:

- A set $\mathbf{S}$ of N states $\mathbf{S} = \{s_1, s_2, ..., s_N\}$ interconnected by arcs, where the model is in a certain state at each time t, which is denoted by x_t.
- A set $\mathbf{V}$ with M observations $\mathbf{V} = \{v_1, v_2, ..., v_M\}$. At each time t, the model generates one symbol which is denoted by o_t.
- A transition matrix $\mathbf{A} = \{a_{ij}\}$ consisting of the transition probabilities of moving from state s_i to state s_j. The transition probabilities are defined by:

  $$a_{ij} = P(x_{t+1} = s_j | x_t = s_i) \quad i, j = 1, ..., N. \tag{3.22}$$

  These probabilities must verify:

  $$\sum_{j=1}^{N} a_{ij} = 1 \quad i = 1, ..., N. \tag{3.23}$$

- An observation probability matrix $\mathbf{B} = \{b_i(v_k)\}$, where each element represents the probability of generating a certain symbol in a certain state:

  $$b_i(v_k) = P(o_t = v_k | x_t = s_i) \quad i = 1, ..., N; k = 1, ..., M. \tag{3.24}$$

  These probabilities must verify:

  $$\sum_{k=1}^{M} b_i(v_k) = 1 \quad i = 1, ..., N. \tag{3.25}$$

- A matrix Π of initial states, where each element represents the probability of having a certain state as the initial state:

  $$\mathbf{\Pi} = \{\pi_i\} \quad \text{with} \quad \pi_i = P(x_1 = s_i) \quad i = 1, ..., N. \tag{3.26}$$

  These probabilities must verify:

  $$\sum_{i=1}^{N} \pi_i = 1 \quad i = 1, ..., N. \tag{3.27}$$

The HMM is then defined by the parameters $\boldsymbol{\lambda} = (\mathbf{A}, \mathbf{B}, \boldsymbol{\Pi})$.

A six state HMM is shown in Figure 3.4 and the left-to-right topology shown is the one used when applying HMM to the ASR system considered in this thesis. In ASR systems, the speech signals are represented by a sequence of equally spaced discrete speech vectors $\mathbf{o}_t$, where it is assumed that the observed speech vectors are generated by a HMM. Only the observation sequence is known and the underlying state sequence is hidden. In Figure 3.4 the HMM moves through the state sequence $\mathbf{s} = \{s_1, s_2, s_3, s_4, s_5, s_6\}$ in order to generate the sequence of speech vectors $\mathbf{o}_1$ to $\mathbf{o}_6$. In this model the entry and exit states, s_1 and s_6, are non-emitting, meaning they do not generate any observation vectors or take up any time units. This means that the need for initial state probabilities π_i is avoided, which is useful for concatenating HMMs in ASR systems, this is elaborated on in Subsection 3.2.4. The HMMs of this ASR system is then defined by the parameters $\boldsymbol{\lambda} = (\mathbf{A}, \mathbf{B})$. In this thesis HMM-based speech recognition is

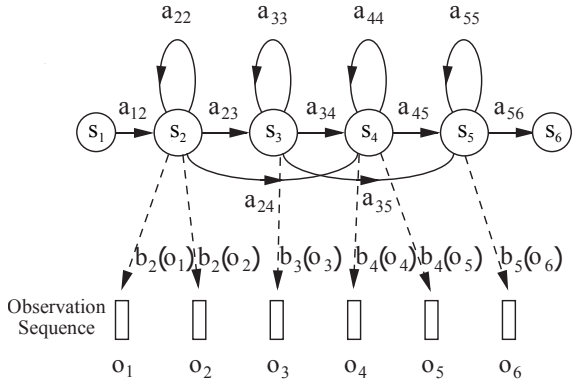

Figure 3.4: A six state HMM, where a hidden state sequence generates the observation sequence of speech vectors $\mathbf{o}_1$ to $\mathbf{o}_6$.

performed with digit sequences from the Aurora-2 database using the HTK tool. Whole word HMMs are modelled for all digits rather than phonemes, this is referred to as connected digit speech recognition. The digits are modelled as whole word HMMs, consisting of 16 states using a mixture of 3 Gaussians per state. The HTK tool provides a non-emitting state at the beginning and at the end of the HMM, giving a total of 18 states. There are two pause models defined. The first one is called 'sil' and consists of 3 states with a mixture of 6 Gaussians per state, which model pauses before and after the speech signal. The second pause model is called 'sp' and is used to model pauses between words. This consists of a single state, which is a state that is shared with the middle state of the 'sil' pause model [26]. It means that the state output distributions of the HMMs are represented as a mixture of Gaussians:

$$b_j(\mathbf{o}_t) = \sum_{k=1}^{K} c_{jk} \mathcal{N}\left(\mathbf{o}_t; \boldsymbol{\mu}_{jk}, \boldsymbol{\Sigma}_{jk}\right) \quad 1 \leq j \leq N, \tag{3.28}$$

where K is the number of mixture components and c_{jk} is the mixture weight with $c_{jk} \geq 0$ and $\sum_{k=1}^{K} c_{jk} = 1$. $\boldsymbol{\mu}_{jk}$ is the mean vector and $\boldsymbol{\Sigma}_{jk}$ is the covariance matrix associated with state j

and mixture k [41]. It should be noted that the mixture components can be considered to be a special form of sub-state in which the transition probabilities are the mixture weights as shown in Figure 3.5. It means that the essential problem is to estimate the means and covariances of a

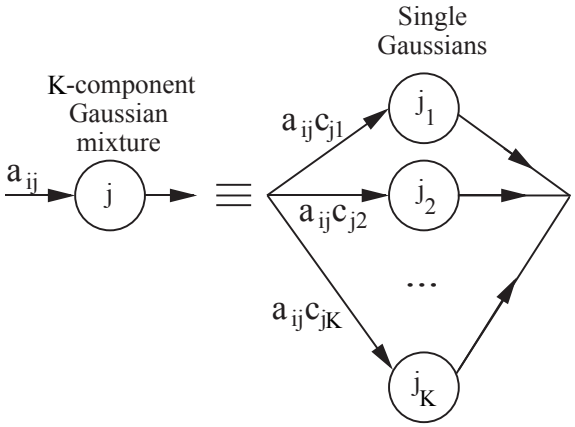

Figure 3.5: An K-component Gaussian mixture of a state output can equivalently be written as K states of single Gaussian distributions in which the mixture weights determines the transition probabilities.

HMM for single component Gaussians as given by Equation 3.29 and the associated transition probabilities in the HMM.

$$b_j(\mathbf{o}_t) = \frac{1}{\sqrt{(2\pi)^n |\mathbf{\Sigma}_j|}} e^{-\frac{1}{2}(\mathbf{o}_t - \boldsymbol{\mu}_j)^T \mathbf{\Sigma}_j^{-1} (\mathbf{o}_t - \boldsymbol{\mu}_j)}. \tag{3.29}$$

3.2.3 Training

This subsection covers the training procedure involved when performing HMM-based speech recognition of digit sequences from the Aurora-2 database. Given a set of training data, the parameters $\boldsymbol{\lambda} = (\mathbf{A}, \mathbf{B})$ of the different models must be estimated. The parameters of the models are determined automatically by a re-estimation procedure carried out by the HTK tool [41]. There is no efficient algorithm for global optimization and therefore an effective iterative algorithm for local optimization is used, which is known as the Baum-Welch re-estimation procedure. The Baum-Welch algorithm uses the forward-backward algorithm to find the maximum likelihood estimate of the parameters $\boldsymbol{\lambda} = (\mathbf{A}, \mathbf{B})$ of a HMM given a set of training sequences [41].

First the parameters of the HMMs needs to be initialized by the use of the training data, several approaches exists for doing this. The initialization of the state output distribution $\mathbf{B}$ of the HMMs for the corresponding ASR results presented in this thesis are carried out by the HTK tool, which compute the global mean and covariance of the training data. Then all the means and covariances are set equal to the global data mean and covariance, so all models are initially given the same parameters. Furthermore, a floor of the variance is specified in order to prevent variances being badly underestimated. The transition probabilities $\mathbf{A}$ are also predefined by

the HTK tool, where the allowable transitions between states should be indicated with non-zero values in the transition matrix and zero elsewhere. The rows of the transition matrix must sum to one except from the final row, where all the elements should be zero [41].

Then the Baum-Welch re-estimation procedure is used, this applies the maximum likelihood (ML) estimation criterion:

$$\hat{\boldsymbol{\lambda}} = \arg\max_{\boldsymbol{\lambda}} P(\mathbf{O}|\boldsymbol{\lambda}). \tag{3.30}$$

This means that it is desired to obtain the parameter set $\boldsymbol{\lambda}$ that fits a given training sequence $\mathbf{O}$. This is based on the fact that $P(\mathbf{O}|\boldsymbol{\lambda})$ can be expressed as

$$P(\mathbf{O}|\boldsymbol{\lambda}) = \sum_{i=1}^{N} \alpha_t(i)\beta_t(i). \tag{3.31}$$

It requires the use of the forward-backward algorithm to compute the forward-backward probabilities, $\alpha_t(i)$ and $\beta_t(j)$ for $i, j = 1, ..., N$. These are used to compute the following probabilities:

$$\xi_t(i,j) = P(x_t = s_i, x_{t+1} = s_j|\mathbf{O}, \boldsymbol{\lambda}) = \frac{\alpha_t(i)a_{ij}b_j(\mathbf{o}_{t+1})\beta_{t+1}(j)}{P(\mathbf{O}|\boldsymbol{\lambda})}, \tag{3.32}$$

$$\gamma_t(i) = P(x_t = s_i|\mathbf{O}, \boldsymbol{\lambda}) = \sum_{j=1}^{N} \xi_t(i,j) = \frac{\alpha_t(i)\beta_t(i)}{P(\mathbf{O}|\boldsymbol{\lambda})}. \tag{3.33}$$

Considering that $\sum_{t=1}^{T} \xi_t(i,j)$ is the expected number of transitions from state s_i to state s_j and that $\sum_{t=1}^{T} \gamma_t(i)$, then the following re-estimation equations can be obtained:

$$\bar{a}_{ij} = \frac{\sum_{t=1}^{T-1} \xi_t(i,j)}{\sum_{t=1}^{T-1} \gamma_t(i)}, \tag{3.34}$$

$$\hat{\boldsymbol{\mu}}_j = \frac{\sum_{t=1}^{T} \gamma_t(j)\mathbf{o}_t}{\sum_{t=1}^{T} \gamma_t(j)}, \tag{3.35}$$

$$\hat{\boldsymbol{\Sigma}}_j = \frac{\sum_{t=1}^{T} \gamma_t(j)(\mathbf{o}_t - \hat{\boldsymbol{\mu}}_j)(\mathbf{o}_t - \hat{\boldsymbol{\mu}}_j)^T}{\sum_{t=1}^{T} \gamma_t(j)}. \tag{3.36}$$

It can be shown that applying Equation 3.34-3.36 iteratively, the probability $P(\mathbf{O}|\boldsymbol{\lambda})$ is increased at each step, at least leading to a local maximum of $P(\mathbf{O}|\boldsymbol{\lambda})$ [27]. The forward probability is defined as

$$\alpha_t(i) = P(\mathbf{o}_1\mathbf{o}_2...\mathbf{o}_t, x_t = s_i|\boldsymbol{\lambda}), \tag{3.37}$$

which is, the probability that the generated sequence up to time t is $\mathbf{o}_1\mathbf{o}_2...\mathbf{o}_t$ and the state at that time is s_i, given the model $\boldsymbol{\lambda}$.

The procedure of computing the forward probability efficiently is shown in Algorithm 3.1.

Algorithm 3.1: Forward probability

Initialization: $\alpha_1(1) = 1; \alpha_1(j) = a_{1j} b_j(\boldsymbol{o}_1) \quad for \quad j = 2, ..., N-1$

for $j = 1, ..., N;\ t = 2, ..., T-1$ **do**

$\alpha_{t+1}(j) = \left[\sum_{i=1}^{N} \alpha_t(i) a_{ij}\right] b_j(\mathbf{o}_{t+1})$

end

Output: $P(\boldsymbol{O}|\boldsymbol{\lambda}) = \alpha_T(N) = \sum_{i=1}^{N} \alpha_T(i)$

The backward probability is defined as

$$\beta_t(i) = P(\mathbf{o}_{t+1}\mathbf{o}_{t+2}...\mathbf{o}_T | x_t = s_i, \boldsymbol{\lambda}), \tag{3.38}$$

which is, the probability of having sequence **O** from time $t+1$, with current state s_i for model $\boldsymbol{\lambda}$. The procedure of computing the backward probability efficiently is shown in Algorithm 3.2.

Algorithm 3.2: Backward probability

Initialization: $\beta_T(i) = a_{iN} \quad for \quad i = 1, ..., N$

for $j = 1, ..., N;\ t = T-1, T-2, ..., 1$ **do**

$\alpha_{t+1}(j) = \left[\sum_{i=1}^{N} \alpha_t(i) a_{ij}\right] b_j(\mathbf{o}_{t+1})$

end

Output: $P(\boldsymbol{O}|\boldsymbol{\lambda})$

It should be noticed that the computation of the forward and backward probabilities involves taking the product of a large number of probabilities. This means that the numbers involved in practice becomes very small. In order to avoid numerical problems, the forward backward computation is computed using logarithmic computations in the HTK tool [41].

3.2.4 Recognition

This subsection covers the HMM-based speech recognition procedure of digit sequences from the Aurora-2 database. As described in Subsection 3.2.1, Aurora-2 provides 3 different test sets (A,B and C) to be used for the recognition task. The HTK tool is used to carry out the recognition task on this test data, but requires additional input elements:

- Dictionary
- Word network
- Trained HMMs

The dictionary defines the required words and the word network defines the allowable sequences of words. The dictionary to be used with Aurora-2 is defined by:

{`one,two,three,four,five,six,seven,eight,nine,zero,oh,sp,sil`}.

Beside digit words, this dictionary also includes the pauses 'sp' and 'sil'. 'sp' represents pauses between words and 'sil' represents pauses before and after speech signals. A simplified version of the word network for this dictionary is shown in Figure 3.6. In this word network the digits are shown as one node, since they share the same connections. Furthermore, an empty node is included in order to reduce the number of arcs from the digit nodes to the 'sp', 'sil' and 'exit' nodes. It is possible to set up probabilities for the different sequences of words in a word

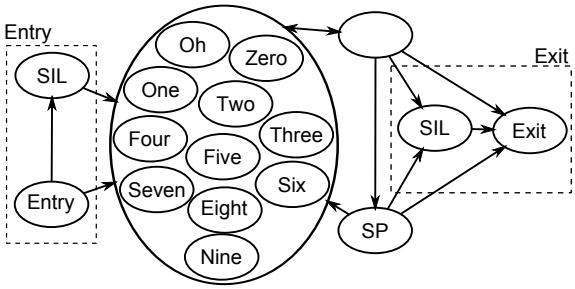

Figure 3.6: Word network representing the allowable sequences of digit words, when using the speech data of the Aurora-2 database.

network, but in this case of digit word sequences, equal probability is given to all sequences of words. When the HMMs have been trained, they are attached to the word network. HMMs have been trained both for both *clean* and *multi-conditioned* training data, which means speech recognition is performed for the three test sets (A,B and C) with two different sets of HMMs.

The objective of HMM-based speech recognition is to find the most probable word sequence for a series of observation vectors, which means finding the most likely sequence of hidden states for a given HMM. This is carried out by the use of the Viterbi decoding algorithm, which is a recursive procedure for finding the maximum likelihood state sequence.

As shown in Figure 3.7, the Viterbi decoding algorithm can be visualized as finding the best path through a matrix where the vertical dimension represents the states of the HMM and the horizontal dimension represents the frames of speech (i.e. time). Each large dot represent the log probability of observing that frame at that time and each arc between the dots corresponds to a log transition probability. Given a HMM with parameters $\boldsymbol{\lambda} = \{\mathbf{A}, \mathbf{B}\}$, the optimal path is recursively computed as shown in Algorithm 3.3.

Algorithm 3.3: Viterbi Algorithm

Initialization: $\delta_1(1) = 1,\ \delta_j(1) = a_{1j} b_j(\boldsymbol{o}_1),\ \psi_1(j) = 0 \quad j = 2, ..., N-1$

for $j = 1, ..., N;\ t = 2, ..., T$ **do**

$$\delta_t(j) = \max_{i=1,...,N} \left[\delta_{t-1}(i) a_{ij}\right] b_j(\mathbf{o}_t)$$

$$\psi_t(j) = \arg \max_{i=1,...,N} \left[\delta_{t-1}(i) a_{ij}\right]$$

end

End: $\hat{x}_T = \arg \max_{i=1,...,N} [\delta_T(i)]$

Backtracking: $\hat{x}_t = \psi_{t+1}(\hat{x}_{t+1}) \quad t = T-1, T-2, ..., 1$

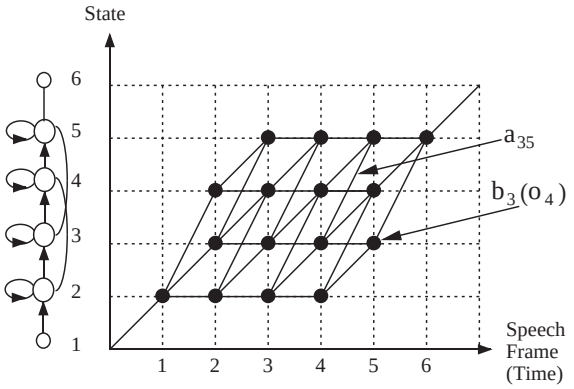

Figure 3.7: Visualization of using the Viterbi algorithm for HMM-based speech recognition, where a large dot represents the log probability of observing that frame at that time and an arc represents the log transition probability.

In the Viterbi algorithm shown in Algorithm 3.3, the maximum likelihood of observing speech vectors $\mathbf{o}_1$ to $\mathbf{o}_t$ and being in state j at time t is denoted as $\delta_t(j)$. The algorithm uses the function $\psi_t(j)$ to recover the optimal path when the recursion finishes. So by using the Viterbi algorithm, the probability of moving through all the many paths in the HMM are computed and the path which have the highest probability is selected. Again it should be noticed that the computations involved in Algorithm 3.3 is computed using logarithmic computations in order to avoid numerical problems.

3.3 Performance Evaluation Methods

The measures used for evaluating ASR system are relative simple measures that only require reference transcriptions of the speech signals are available. The simplest way to measure the performance of ASR systems would be the error rate this is, however, not used as there exists different types of errors in speech recognition systems when using continuous speech recognition i.e. utterances are entire sentences with no guarantee of pauses between words [27]. These are defined as:

- Substitutions: A word appears substituted by a different word in the recognized sentence compared to the reference sentence
- Deletions: A word is missing in the recognized sentence compared to the reference sentence
- Insertions: A new word is included in the recognized sentence between two words of the reference sentence

The performance measures percent correct (PC), the word error rate (WER) and the word accuracy, which account for these errors, are some of the most commonly used in ASR, and

are given by[27, 41]:

$$PC = 100 \cdot \frac{C-I}{N} = \frac{N-D-S}{N}, \tag{3.39}$$

$$WER = 100 \cdot \frac{S+D+I}{N}, \tag{3.40}$$

$$\text{WordAccuracy} = 100 \cdot \frac{N-(S+D+I)}{N}, \tag{3.41}$$

where

- C: Number of words correctly recognized
- I: Total number of insertions
- N: Total number of evaluated words
- S: Total number of substitutions
- D: Total number of deletions

PC is often used to measure the performance of a recogniser over both words and sentences referred to as word correct and sentence correct, respectively [41]. The sentence correct is more sensitive to errors than the other measures, as sentences tends to contain multiple words all of which have to be correct. Word accuracy and WER are measures of the same types of errors, therefore only the word accuracy, word correct and sentence correct measures are used in this thesis.

Speech Enhancement 4

This chapter presents the speech enhancement (SE) techniques designed for human listeners, which are used to generate the SE results within in this thesis. Furthermore the objective performance measures used to evaluate SE of the denoised speech signals are provided.

SE aims at improving the intelligibility and/or quality of a degraded speech signal by the use signal processing techniques [11]. The following additive signal model is considered to represent the noisy signal in this chapter:

$$y(n) = x(n) + d(n), \tag{4.1}$$

where $y(n)$ is the observed noisy signal, $x(n)$ is the unknown target signal, $d(n)$ is the noise signal and n is the discrete-time index [11]. Furthermore the SE methods presented in this chapter are based on the assumptions provided in Section 1.3, where it stated that the additive noise and the clean speech signal are statistical independent.

In this thesis it has been chosen to consider SE algorithms differentiating in their approach in order for them to be representative of this field. The algorithms considered are: The iterative Wiener filtering (IWF) algorithm [16], the audible noise suppression (ANS) algorithm [16] and the short-time spectral amplitude (STSA) estimator based on the weighted euclidean (WE) distortion measure [16]. The IWF algorithm exploits *a priori* assumptions of the target sound, which is based on a speech production model. The ANS algorithm, on the other hand, exploits assumptions on the receiver of the sound, which is based on human auditory perception and auditory masking. The STSA WE algorithm, however, does not make any strong assumptions about either the target signal or the receiver.

MATLAB implementations of the SE algorithms considered in this section have been provided by [17]. These have been used for the generation of the simulation results presented in this thesis. An overview of the MATLAB implementations are given by Appendix B.

4.1 Iterative Wiener Filtering

In this section a SE approach based on iterative Wiener filtering (IWF) is presented. Performing SE by the use of a Wiener filtering approach consists of deriving an enhanced signal by optimizing an error criterion, the mean-square error (MSE) between the original clean signal and the estimated enhanced signal. In should be noted that the IWF approach assumes stationarity overa short time interval and therefore the algorithm is applied frame-by-frame. A block diagram of the statistical filtering problem considered is shown in Figure 4.1. The purpose is to design a linear time-invariant (LTI) system with the noisy input speech signal $y(n) = x(n) + d(n)$ such that the output signal $\hat{x}(n)$, is as close to the clean speech signal $x(n)$ as possible in a MSE sense. This is carried out by computing the estimation error $e(n)$ and making it as small as possible. The optimal filter that minimizes the estimation error is called the Wiener filter [16]. The filter is linear and often a finite impulse response (FIR) filter is used because they are stable and the resulting solution is computationally easy to evaluate. When assuming a FIR filter is used, then $\hat{x}(n)$ is given by:

$$\hat{x}(n) = \sum_{k=0}^{M-1} h_k y(n-k) \quad n = 0, 1, 2, ..., N, \tag{4.2}$$

where $\{h_k\}$ are the filter coefficients, M is the number of filter coefficients and N is the number of samples within a frame of the input speech signal. It is desired to compute the filter coefficients $\{h_k\}$ such that the estimation error $e(n) = x(n) - \hat{x}(n)$ is minimized. The mean square of the estimation error is commonly used as criterion for minimization:

$$J = E[e^2(n)]. \tag{4.3}$$

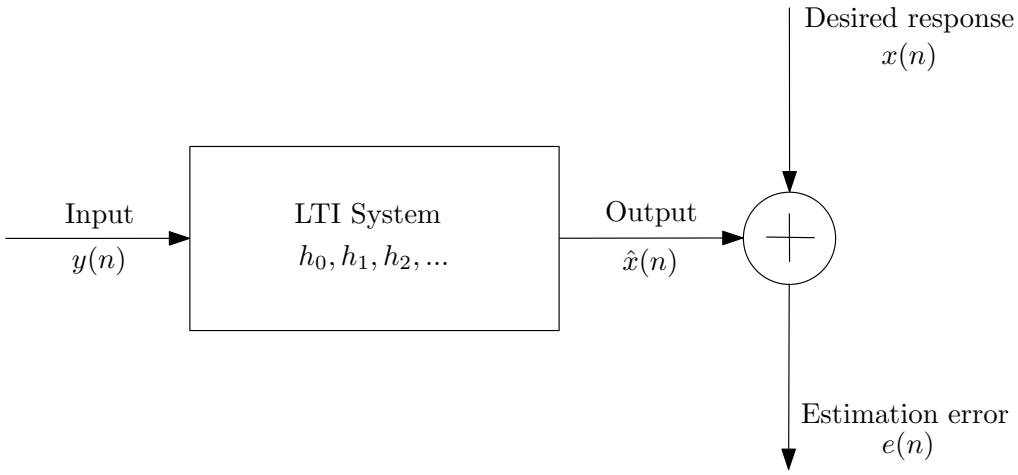

Figure 4.1: Block diagram of the statistical filtering problem.

The iterative Wiener filtering approach make use of frequency domain filtering. The Fourier transform of the input signal $y(n)$ is given by:

$$Y(\omega_k) = X(\omega_k) + D(\omega_k). \tag{4.4}$$

The frequency domain estimation error is defined by:

$$E(\omega_k) = X(\omega_k) - \hat{X}(\omega_k) = X(\omega_k) - H(\omega_k)Y(\omega_k). \tag{4.5}$$

The optimal frequency domain filter $H(\omega_k)$ is found by computing the complex derivative of the mean-square error $J_2 = E[|E(\omega_k)|^2]$ with respect to $H(\omega_k)$ and setting it equal to zero:

$$\frac{\partial J_2}{\partial H(\omega_k)} = 0. \tag{4.6}$$

When solving Equation 4.6 for $H(\omega_k)$ the following frequency domain Wiener filter is obtained:

$$H(\omega_k) = \frac{P_{xx}(\omega_k)}{P_{xx}(\omega_k) + P_{dd}(\omega_k)} = \frac{\xi_k}{\xi_k + 1}, \tag{4.7}$$

where $P_{xx}(\omega_k) = E[X(\omega_k)X^*(\omega_k)]$ is the power spectrum of the clean signal $x(n)$, $P_{dd}(\omega_k) = E[D(\omega_k)D^*(\omega_k)]$ is the power spectrum of the noise signal $d(n)$ and $\xi_k = \frac{P_{xx}(\omega_k)}{P_{dd}(\omega_k)}$ is the *a priori* SNR at frequency ω_k. $H(\omega_k)$ is real, nonnegative and even, because $P_{xx}(\omega_k) \geq 0$, $P_{dd}(\omega_k) \geq 0$ and $P_{xx}(\omega_k)$ and $P_{dd}(\omega_k)$ have even symmetry. As $H(\omega_k)$ is even and real, it means that the impulse response h_k must be even as well. Therefore h_k is not causal and the Wiener filter is not realizable. Furthermore it requires knowledge about the power spectrum of the clean signal, which is not available [16]. Therefore the Wiener filter must be estimated from the noisy signal. The iterative Wiener filtering approach estimate the Wiener filter in an iterative procedure. An iterative procedure is considered, where in the $(i+1)$ iteration the enhanced signal spectrum is estimated by:

$$\hat{X}_{i+1}(\omega_k) = H_i(\omega_k)Y(\omega_k), \tag{4.8}$$

where $H_i(\omega_k)$ is the Wiener filter obtained in the i^{th} iteration. The resulting speech signal is then assumed to be generated by an AR process where the task is to estimate the clean AR parameters. As described in Section 2.3, the vocal tract can be modelled by a linear time-invariant filter. The vocal tract transfer function V(z) has the following all-pole form:

$$V(z) = \frac{g}{A(z)} = \frac{g}{1 - \sum_{k=1}^{p} a_k z^{-k}}, \tag{4.9}$$

where g is the gain of the system, $\{a_k\}$ are the all-pole coefficients and p is the number of coefficients. The speech waveform $x(n)$ is assumed to satisfy the following difference equation:

$$x(n) = \sum_{k=1}^{p} a_k x(n-k) + g \cdot w(n) \quad n = 0, 1, ..., N-1, \tag{4.10}$$

where g is the gain factor and $w(n)$ is the input excitation to the system which is assumed to be white Gaussian noise with zero mean and unit variance. In vector notation, Equation 4.10 is given by:

$$x(n) = \mathbf{a}^{\mathrm{T}}\mathbf{x}_p + g \cdot w(n), \tag{4.11}$$

where $\mathbf{a} = [a_1, a_2, ..., a_p]^{\mathrm{T}}$ and $\mathbf{x}_p = [x(n-1), x(n-2), ..., x(n-p)]^{\mathrm{T}}$. But Equation 4.11 requires initial conditions for $n < p$ and these are denoted by $\mathbf{x}_I = [x(-1), x(-2), ..., x(-p)]^{\mathrm{T}}$. The noisy speech signal is then given by:

$$y(n) = x(n) + d(n) \tag{4.12}$$

$$= \mathbf{a}^{\mathrm{T}}\mathbf{x}_p + g \cdot w(n) + d(n), \tag{4.13}$$

where $d(n)$ is a noise signal assumed to be white Gaussian noise with zero mean and variance σ_d^2. The clean speech signal $x(n)$ depends on $2p+1$ parameters: $\mathbf{a}$, $\mathbf{x}_I$ and g. So instead of estimating the clean signal $x(n)$ itself, estimation of the parameters assumed to have been used to generate the signal is made. The iterative Wiener filtering approach performs maximum *a posteriori* (MAP) estimation of the clean signal $x(n)$ given the noisy observations $y(n)$ and the coefficients $\mathbf{a}$, i.e. maximizing the conditional density $p(\mathbf{x}|\mathbf{a},\mathbf{y})$. The gain term g and the initial conditions $\mathbf{x}_I$ are assumed to be known. The following iterative concept has been proposed [16]:

1. Step 1: Estimate $\mathbf{x}$ by maximizing $p(\mathbf{x}|\mathbf{a}_0,\mathbf{y})$ based on an initial estimate of $\mathbf{a}$: $\mathbf{a}_0$. Denote the first estimate of $\mathbf{x}$ by $\mathbf{x}_1$.

2. Step 2: Use $\mathbf{x}_1$ to make a new estimate of $\mathbf{a}$ denoted by $\mathbf{a}_1$ by the use of a linear prediction technique. Go to step 1 and use $\mathbf{a}_1$ in place of $\mathbf{a}_0$.

This iterative procedure has been proved to converge to a local maximum of the joint probability density $p(\mathbf{a},\mathbf{x}|\mathbf{y})$ [16]. Implementing step 1 in the iterative algorithm, $p(\mathbf{x}|\mathbf{a}_i,\mathbf{y})$ needs to be maximized over all $x(n)$. Using Bayes' rule, $p(\mathbf{x}|\mathbf{a}_i,\mathbf{y})$ can be written as

$$p(\mathbf{x}|\mathbf{a}_i,\mathbf{y}) = \frac{p(\mathbf{y}|\mathbf{a}_i,\mathbf{x})\,p(\mathbf{x}|\mathbf{a}_i)}{p(\mathbf{y}|\mathbf{a}_i)}, \tag{4.14}$$

where $\mathbf{a}_i$ are the coefficients obtained at the i^{th} iteration. The denominator can be ignored as it is not a function of $x(n)$. It is assumed that the gain g and the initial conditions $\mathbf{x}_I$ are known and therefore the MAP estimate of step 1 is given by

$$\mathbf{x}_{MAP} = \max_x p(\mathbf{x}|\mathbf{a}_i,\mathbf{y}) = \max_x p(\mathbf{y}|\mathbf{a}_i,\mathbf{x})\,p(\mathbf{x}|\mathbf{a}_i). \tag{4.15}$$

The conditional density $p(\mathbf{y}|\mathbf{a}_i,\mathbf{x})$ is assumed to be Gaussian with mean $x(n)$ and variance σ_d^2:

$$p(\mathbf{y}|a_i,\mathbf{x}) = \frac{1}{\left(2\pi\sigma_d^2\right)^{N/2}} \exp\left(-\frac{1}{2\sigma_d^2}\sum_{n=0}^{N-1}\left(y(n)-x(n)\right)^2\right). \tag{4.16}$$

The conditional density $p(\mathbf{x}|\mathbf{a}_i)$ is also assumed Gaussian with mean $\mathbf{a}^{\mathrm{T}}\mathbf{x}_p$ and variance g^2, i.e. it is given by:

$$p(\mathbf{x}|\mathbf{a}_i) = \frac{1}{(2\pi g^2)^{N/2}} \exp\left(-\frac{1}{2g^2}\sum_{n=0}^{N-1}(x(n)-\mathbf{a}^{\mathrm{T}}\mathbf{x}_p)^2\right). \tag{4.17}$$

By substituting Equation 4.16 and 4.17 into Equation 4.14, an expression is obtained for the conditional density $p(\mathbf{x}|\mathbf{a}_i, \mathbf{y})$:

$$p(\mathbf{x}|\mathbf{a}_i, \mathbf{y}) = C\frac{1}{\left(4\pi^2 g^2 \sigma_d^2\right)^{N/2}} \exp\left(-\frac{1}{2\Delta_p}\right), \tag{4.18}$$

where C is a constant and Δ_p is given by:

$$\Delta_p = \frac{1}{g^2}\sum_{n=0}^{N-1}\left(x(n) - \mathbf{a}^{\mathrm{T}}\mathbf{x}_p\right)^2 + \frac{1}{\sigma_d^2}\sum_{n=0}^{N-1}\left(y(n) - x(n)\right)^2. \tag{4.19}$$

Maximizing $p(\mathbf{x}|\mathbf{a}_i, \mathbf{y})$ with respect to $x(n)$ is equivalent to minimizing Δ_p, as the exponent in Equation 4.18 is negative. $x(n)$ is estimated by minimizing Δ_p, which is carried out by taking the derivative of Δ_p with respect to $\mathbf{x}$ and set it equal to zero:

$$\frac{\partial \Delta_p}{\partial x(n)} = 0, \quad n = 0, 1, ..., N-1. \tag{4.20}$$

It can be shown that the conditional density $p(\mathbf{x}|\mathbf{a}_i, \mathbf{y})$ is jointly Gaussian and therefore the MAP estimate of $\mathbf{x}$ is equivalent to the minimum mean-square error (MMSE) estimate of $\mathbf{x}$ [16] [10]. As N increases, the procedure to obtain the MMSE estimate of $\mathbf{x}$ given by Equation 4.20 approaches a noncausal Wiener filter. This means that the MAP estimate of $\mathbf{x}$ can be obtained by filtering the noisy signal $y(n)$ through the Wiener filter:

$$H(\omega_k) = \frac{P_{xx}(\omega_k)}{P_{xx}(\omega_k) + P_{dd}(\omega_k)} = \frac{P_{xx}(\omega_k)}{P_{xx}(\omega_k) + \sigma_d^2}, \tag{4.21}$$

where $P_{xx}(\omega)$ is the power spectrum of $x(n)$ given $\mathbf{a}_i$ and g:

$$P_{xx}(\omega) = \frac{g^2}{|1 - \sum_{k=1}^{p} a_k e^{-jk\omega}|^2}. \tag{4.22}$$

The gain g in Equation 4.22 is estimated by requiring that the variance of the noisy speech signal, $y(n)$, is equal to the sum of the variances of the clean signal and the noise, because $x(n)$ and $d(n)$ are uncorrelated and have a mean of zero:

$$\sigma_y^2 = \sigma_x^2 + \sigma_d^2, \tag{4.23}$$

where σ_y^2 is the variance of $y(n)$ and σ_x^2 is the variance of the estimated signal $x(n)$. The signal variance σ_x^2 can be computed using Parseval's theorem:

$$\begin{aligned}\sigma_x^2 &= \sum_{n=0}^{N-1} x^2(n) = \frac{1}{2\pi}\int_{-\pi}^{\pi} P_{xx}(\omega)\, d\omega \\ &= \frac{1}{2\pi}\int_{-\pi}^{\pi} \frac{g^2}{|1 - \sum_{k=1}^{p} a_k e^{-jk\omega}|^2}\, d\omega.\end{aligned} \tag{4.24}$$

Substituting Equation 4.24 into Equation 4.23 and solving for g^2 yields:

$$g^2 = \frac{\frac{2\pi}{N}\sum_{n=0}^{N-1} y^2(n) - 2\pi\sigma_d^2}{\int_{-\pi}^{\pi} \frac{1}{|1 - \sum_{k=1}^{p} a_k e^{-jk\omega}|^2}\, d\omega}. \tag{4.25}$$

This is used to compute the power spectrum of the clean given by Equation 4.22. The iterative Wiener filtering algorithm is summarized in Algorithm 4.1. Again, it should be noted that the IWF algorithm is applied frame-by-frame.

Algorithm 4.1: Iterative Wiener Filtering Algorithm [16]

Initialization: $\boldsymbol{x}_0 = \boldsymbol{y}$

for $i = 0, 1, 2, \ldots$ **do**

(I) Given the estimated signal $\mathbf{x}_i$, compute the all-pole coefficients $\mathbf{a}_i$ using the linear prediction tecchnique.

(II) Using $\mathbf{a}_i$, estimate the gain term g^2 according to Equation 4.25.

(III) Compute the short-term power spectrum of the signal $\mathbf{x}_i$:

$$P_{x_i x_i}(\omega) = \frac{g^2}{|1 - \sum_{k=1}^{p} a_i(k) e^{-jk\omega}|^2}, \tag{4.26}$$

where $\{a_i(k)\}$ are the coefficients estimated in (I).

(IV) Compute the Wiener filter:

$$H_i(\omega) = \frac{P_{x_i x_i}(\omega)}{P_{x_i x_i}(\omega) + \sigma_d^2}. \tag{4.27}$$

(V) Estimate the spectrum of the enhanced signal:

$$X_{i+1}(\omega) = H_i(\omega) Y(\omega), \tag{4.28}$$

where $Y(\omega)$ is the spectrum of the noisy speech signal, $y(n)$. Compute the inverse Fourier transform of $X_{i+1}(\omega)$ to get the enhanced signal $\mathbf{x}_{i+1}$ in the time domain.

(VI) Go to (I) using $\mathbf{x}_{i+1}$ for the estimate signal and repeat until a converge criterion is met or repeat for a specified number of iterations.

end

In principle, Algorithm 4.1 is run until a convergence criterion is met, but in practice the algorithm is run for a fixed number of iterations. But determining when to terminate the algorithm is non-trivial. It has been observed that the optimal number of iterations differ for different types of sounds [16]. There has not been found any solution that provides the optimal number of iterations. An example of estimated spectra for a voiced speech segment using the IWF algorithm is shown in Figure 4.2, when running 8 iterations. It can be observed that it is not necessarily beneficial to allow more iterations, as e.g. the two peaks at the lower frequencies are split into two additional peaks for iteration 8 compared to iteration 3 and 4 [16].

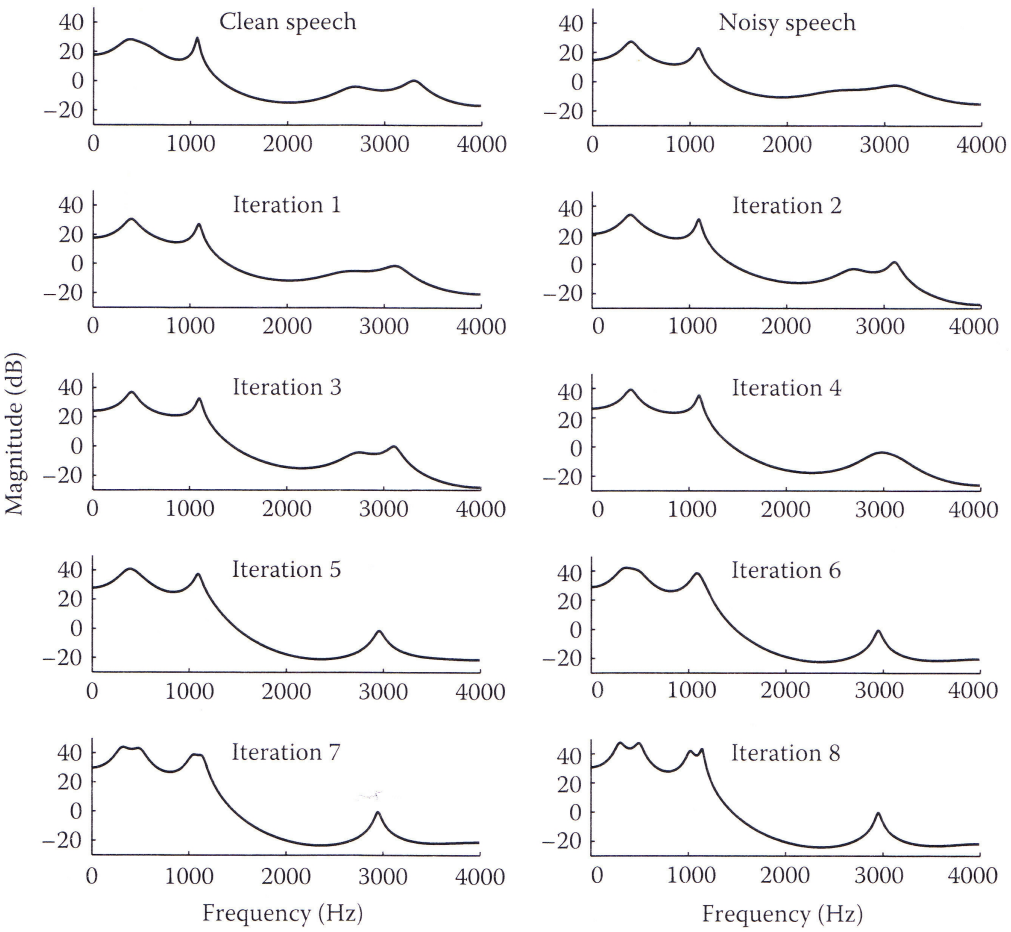

Figure 4.2: Estimated spectra at each iteration of the IWF algorithm for a voiced speech segment [16].

In this thesis it has been chosen to run 2 iterations of the IWF, as this has provided desirable results in [15].

4.2 Audible Noise Suppression

The SE algorithm, Audible Noise Suppression (ANS), presented in this section uses a Wiener-type function to do spectral magnitude modifications based a derived quantity called the audible noise spectrum. The purpose of the audible noise suppression algorithm is to identify and suppress the audible residual noise of the enhanced noisy speech signals, but leave the inaudible components untouched. Audible spectral components are mathematically derived from the masking threshold level. Generally, spectral components above the masking threshold are audible. These are located by taking the maximum between the power spectrum of the speech signal and the corresponding masking threshold for each frequency component (See Equations 4.29 and 4.30) [16]. The audible spectrum of the noisy and the clean speech

signals are denoted by $A_y(\omega_k)$ and $A_x(\omega_k)$, respectively.

$$A_y(\omega_k) = \max\{P_{yy}(\omega_k), T(\omega_k)\}, \tag{4.29}$$

$$A_x(\omega_k) = \max\{P_{xx}(\omega_k), T(\omega_k)\}, \tag{4.30}$$

As in the previous section, the power spectra of the clean and noise signal is denoted $P_{xx}(\omega_k)$ and $P_{dd}(\omega_k)$, respectively. The power spectrum of noisy speech signal is denoted $P_{yy}(\omega_k)$. $T(\omega_k)$ is the masking threshold for frequency bin k. The audible spectrum of the additive noise is obtained by taking the difference between the audible spectrum of the noisy speech signal and the audible spectrum of the clean speech signal [16]:

$$A_d(\omega_k) = A_y(\omega_k) - A_x(\omega_k). \tag{4.31}$$

$A_d(\omega_k)$ is referred to as the audible spectrum of additive noise and the noise spectral components lying above the masking threshold level will be audible and they need to be eliminated or reduced [16]. In Figure 4.3 an example of the difference spectra $P_{yy}(\omega_k) - P_{xx}(\omega_k)$, is shown (Top) along with the audible noise spectrum $A_d(\omega_k)$ (Bottom), from Equation 4.31. Comparing the two it can be seen how the audible spectrum $A_d(\omega_k)$ plotted in the (Bottom) is the spectral components from (Top) above the shown masking threshold.

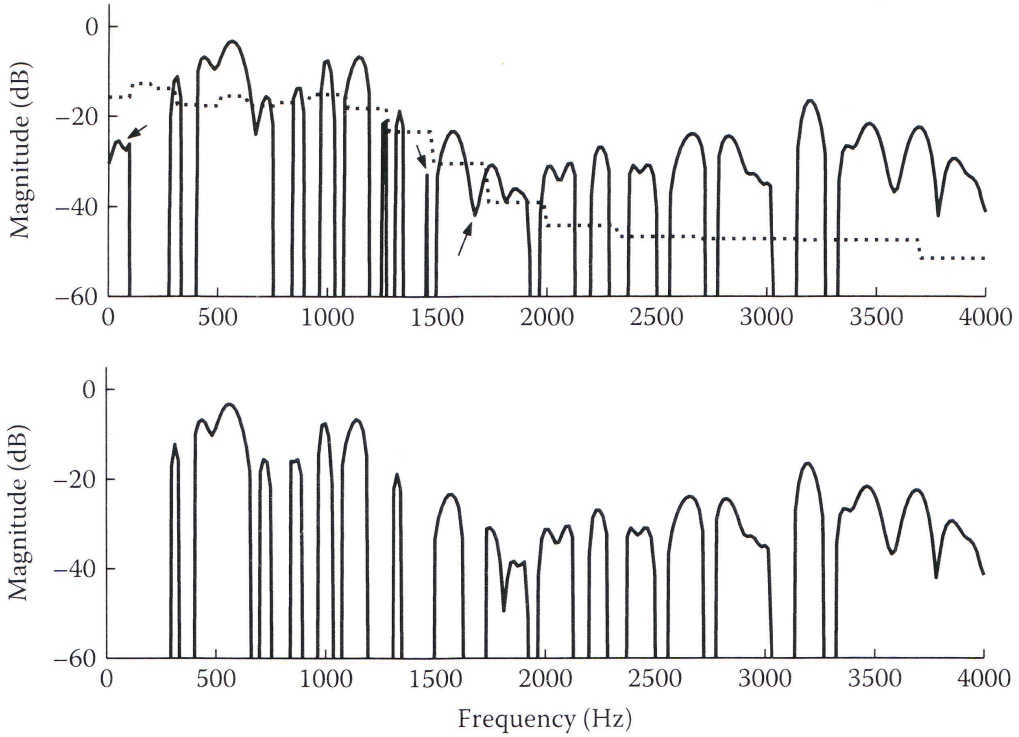

Figure 4.3: (Top) Plot of the difference spectra $(P_{yy}(\omega_k) - P_{xx}(\omega_k))$, with the corresponding masking threshold levels. (Bottom) Plots of the audible noise spectrum $A_d(\omega_k)$. In both plots only the positive values are shown. [16].

The expression for $A_d(\omega_k)$ can be expanded to be more comprehensibly, which is given by:

$$A_d(\omega_k) = \begin{cases} P_{yy}(\omega_k) - P_{xx}(\omega_k) & \text{if } P_{yy}(\omega_k) \geq T(\omega_k) \text{ and } P_{xx}(\omega_k) \geq T(\omega_k) \quad \text{(I)} \\ P_{yy}(\omega_k) - T(\omega_k) & \text{if } P_{yy}(\omega_k) \geq T(\omega_k) \text{ and } P_{xx}(\omega_k) < T(\omega_k) \quad \text{(II)} \\ T(\omega_k) - P_{xx}(\omega_k) & \text{if } P_{yy}(\omega_k) < T(\omega_k) \text{ and } P_{xx}(\omega_k) \geq T(\omega_k) \quad \text{(III)} \\ 0 & \text{if } P_{yy}(\omega_k) < T(\omega_k) \text{ and } P_{xx}(\omega_k) < T(\omega_k) \quad \text{(IV)} \end{cases}. \tag{4.32}$$

From Equation 4.32 it can be seen that it is only in cases I and II that the noise is audible, as the audible noise would either be zero or negative for case III and IV [16]. Consequently, the focus of the algorithm is to reduce the audible noise spectrum $A_d(\omega_k)$ to negative or zero by modifying the noisy speech spectrum $P_{yy}(\omega_k)$, thus making the residual noise inaudible. The enhanced speech spectrum resulting from the modified $P_{yy}(\omega_k)$ is denoted $\hat{P}_{xx}(\omega_k)$. In order for the noise to be inaudible the modified audible noise spectrum $\hat{A}_d(\omega_k)$ must obey:

$$\hat{A}_d(\omega_k) \leq 0, \quad 0 \leq k \leq N-1, \tag{4.33}$$

where N is the size of the FFT. The noisy speech spectrum is modified by a parameric Wiener-type equation:

$$\hat{P}_{xx}(\omega_k) = \frac{P_{yy}^{\nu(k)}(\omega_k)}{\alpha^{\nu(k)}(\omega_k) + P_{yy}^{\nu(k)}(\omega_k)} P_{yy}(\omega_k). \tag{4.34}$$

$\alpha(\omega_k)$ and $\nu(k)$ are time-frequency depending parameters, which are assumed to be positive. By adjusting $\alpha(\omega_k)$ and $\nu(k)$ in Equation 4.34 the suppression of individual spectral components can be varied. The main difference between Equation 4.34 and the Wiener filter can be found at low SNRs, where the Wiener filter provides progressively heavier attenuation as the SNR drops, while Equation 4.34 provides a relative constant attenuation [16]. If the parameters $\alpha(\omega_k)$ and $\nu(k)$ are adjusted to cases I and II in Equation 4.32 then the spectral modification of the noisy speech spectrum can achieve an optimum. By inserting Equation 4.34 into Equation 4.32 an expression for $\alpha(\omega_k)$ and $\nu(k)$ can be found that obey the constraints of case I and II:

$$\frac{P_{yy}^{\nu(k)}(\omega_k)}{\alpha^{\nu(k)}(\omega_k) + P_{yy}^{\nu(k)}(\omega_k)} P_{yy}(\omega_k) - P_{xx}(\omega_k) \leq 0, \quad \text{if } P_{xx}(\omega_k) \geq T(\omega_k) \quad \text{(I)}, \tag{4.35}$$

$$\frac{P_{yy}^{\nu(k)}(\omega_k)}{\alpha^{\nu(k)}(\omega_k) + P_{yy}^{\nu(k)}(\omega_k)} P_{yy}(\omega_k) - T(\omega_k) \leq 0, \quad \text{if } P_{xx}(\omega_k) < T(\omega_k) \quad \text{(II)}. \tag{4.36}$$

The value of $\nu(k)$ is fixed in order to simplify the process, so that only the value of $\alpha(\omega_k)$ is adaptable. If an estimation of the critical-band speech spectrum is used to find the optimal $\alpha(\omega_k)$ instead of relying on an estimation of the whole clean speech spectrum, a dimensional reduction from N frequency components to B critical-band components is achieved [16]. For the ANS algorithm there exist two proposed solutions of how to estimate the parameter $\alpha(\omega_k)$. The first seeks to estimate the spectral minima within each critical band. The second method

estimates the auditory masking threshold. This method is applied in the implementation of the ANS algorithm [17] used in this thesis, which uses the following equation [16]:

$$\alpha_T(i) = (D_b(i) + T(i)) \left[\frac{D_b(i)}{T(i)} \right]^{1/\nu(i)}, \quad 1 \leq i \leq B, \tag{4.37}$$

where B is the number of critical bands, $D_b(i)$ and $T(i)$ is the noise spectrum estimation and the masking threshold estimation in the ith critical band, respectively. $\nu(i)$ is a function of the critical band, which is assumed to be constant within a band. Any audible noise components are suppressed as it can be proven that Equation 4.37 obey the constraint specified in Equation 4.33 if inserted into Equation 4.35 [16]. The estimate of $T(i)$ is obtained using a iterative process similar to the iterative Wiener filter described in Section 4.1, where the noisy speech signal is passed through the suppression function expressed in Equation 4.34 multiple times with $\nu(i) = 1$ [16]. Each iteration produces a better estimate of the clean speech signal thus the resulting estimation of $T(i)$ should also be more accurate. The iterative procedure for the jth iteration is expressed as:

$$\hat{P}_{xx}^{(j)}(i) = \frac{\hat{P}_{xx}^{(j-1)}(i)}{\alpha^{(j)}(i) + \hat{P}_{xx}^{(j-1)}(i)} \hat{P}_{xx}^{(j-1)}(i), \tag{4.38}$$

where $\alpha^{(j)}(i)$ is defined as:

$$\alpha^{(j)}(i) = D^{(j-1)}(i) + \frac{(D^{(j-1)}(i))^2}{T^{(j)}(i)}. \tag{4.39}$$

The noise power estimation for ith band at iteration j is denoted $D^{(j)}(i)$. It is initialized using $\hat{P}_{xx}^{(0)}(i) = P_{yy}(i)$. Power spectrum subtraction is used to process the noisy speech signal into an estimate of the clean spectrum which is used as initial $T^{(1)}(i)$ in Equation 4.39 [16]. The algorithm based on Equation 4.37 is outlined in Algorithm 4.2.

Algorithm 4.2: Audio Noise Algorithm [16]

for *all speech frames* **do**

(I) Use FFT to find the noisy speech signal power spectrum $P_{yy}(\omega_k)$. Retain the phase of the noisy speech spectrum.

(II) Estimate the clean power spectrum $\hat{P}_{xx}(\omega_k)$ using power spectrum subtraction.

(III) Estimate the masking threshold $T(i)$ iteratively using Equations 4.38 and 4.39. Set the initial masking threshold $T^{(1)}(i)$ for Equation 4.39 using $\hat{P}_{yy}(\omega_k)$ from (II) to estimate the masking thresholds.

(IV) In Equation 4.34 set $\nu(i) = 1$. Then use the masking threshold from (III) to adapt $P_{yy}(\omega_k)$ to the constraints given by Equations 4.34 and 4.37.

(V) Use the noisy speech phase spectrum from I to calculate the inverse FFT of the magnitude spectrum estimation from IV.

end

Objective measurements as well as subjective intelligibility measurements have been calculated for simulations run on the threshold parameters estimator. Both objective and the subjective intelligibility measures showed significant improvement for ANS algorithm [16]. The

Diagnostic Rhyme Test [1] (DRT) was used to score the subjective intelligibility in both English and Greek. Particular large intelligibility improvements occur at −5dB SNR [16]. The DRT for English and Greek showed that intelligibility experienced an approximately 30% and 13% increase, respectively [16].

In this thesis it has been chosen to run ANS with 2 iterations, as it has be found that no more than 3 iteration are necessary for sufficient noise suppression [16].

4.3 Statistical Model Based Methods

In this section a statistical model based SE method is presented, which perform nonlinear estimation of the magnitude spectrum of the clean signal using various statistical models and optimization criteria. Initially, statistical model based SE methods are presented in general. The parameters of interest are the DFT coefficients of the clean signal (i.e., the clean signal spectrum). Given the DFT coefficients of the noisy signal (i.e., noisy spectrum) it is desired to find a nonlinear estimator of the DFT coefficients of the noisy signal. There are various techniques for deriving these nonlinear estimators including the maximum-likelihood (ML) estimators and the Bayesian estimators [16].

Maximum-likelihood estimators and Bayesian estimators differ in the assumptions made about the parameter of interest and the form of optimization criteria used. Bayesian estimators assume that the parameter of interest is a random variable unlike ML estimators, which assume that the parameter of interest is deterministic. Therefore a realization of the random variable needs to be estimated , this approach is called Bayesian approach because its implementation is based on Bayes' theorem. Bayesian estimators typically perform better than the ML estimators, as they make use of prior knowledge [16]. Therefore it has been chosen to use a Bayesian estimator in this thesis.

General Bayesian estimators can be derived using the concept of Bayesian risk function. Consider the sampled noisy speech signal:

$$y(n) = x(n) + d(n), \tag{4.40}$$

which consists of the clean signal $x(n)$ and the noise signal $d(n)$. The noisy signal is transformed to the time-frequency domain using the short-time Fourier transform (STFT), which is given by:

$$Y(n,k) = \sum_{m=0}^{N-1} y(nL+m)\, w(m) e^{-j\frac{2\pi}{N}km} = X(n,k) + D(n,k), \tag{4.41}$$

[1] The DRT uses consonant-vowel-consonant sound sequence to construct monosyllabic words. These words are then arranged into rhyming pairs where only initial consonants differ. The DRT uses a total of ninety-six rhyming pairs, which is arranged together in a number of groups based on distinctive speech features. Listeners have a word presented to them by the talker and is then asked to identify which word it is out of a word pair [16].

where $k = 0, 1, ..., N-1$ and m denotes the frequency bin and frame index, respectively. L is the frame shift in samples, $w(m)$ is the analysis window and N denotes the STFT order. Expressing Equation 4.41 in polar form

$$Y_{n,k}e^{j\theta_y(n,k)} = X_{n,k}e^{j\theta_x(n,k)} + D_{n,k}e^{j\theta_e(n,k)}, \tag{4.42}$$

where $\{Y_{n,k}, X_{n,k}, D_{n,k}\}$ denote the magnitudes and $\{\theta_y(n,k), \theta_x(n,k), \theta_d(n,k)\}$ denote the phases at the k^{th} frequency bin and at time n of the noisy speech, clean speech and noise respectively. The purpose is to estimate the magnitude spectrum $X_{n,k}$ of the clean speech from the noisy complex speech spectrum $Y(n,k)$. Letting $\epsilon = X_{n,k} - \hat{X}_{n,k}$ denote the error in estimating the magnitude spectrum $X_{n,k}$ at the k^{th} frequency bin and at time n and letting $d(\epsilon) \triangleq d(X_{n,k}, \hat{X}_{n,k})$ denote a nonnegative function of ϵ, then the Bayes risk $\mathfrak{R}_B$ is given by

$$\mathfrak{R}_B = E\left[d(X_{n,k}, \hat{X}_{n,k})\right] \tag{4.43}$$

$$= \int\int d(X_{n,k}, \hat{X}_{n,k}) p(X_{n,k}, Y(n,k)) dX_{n,k} dY(n,k). \tag{4.44}$$

Bayes risk $\mathfrak{R}_B$ is minimized with respect to $\hat{X}_{n,k}$ and various Bayesian estimators can be obtained depending on the choice of the cost function. If the following squared error cost function is used in Equation 4.44:

$$d(X_{n,k}, \hat{X}_{n,k}) = (X_{n,k} - \hat{X}_{n,k})^2, \tag{4.45}$$

then the traditional MMSE estimator $E[X_{n,k}|Y(n,k)]$ is obtained when minimizing with respect to $\hat{X}_{n,k}$ while holding $Y(n,k)$ fixed. If the following cost function is used:

$$d(X_{n,k}, \hat{X}_{n,k}) = \begin{cases} 0 & |X_{n,k} - \hat{X}_{n,k}| < \delta \\ 1 & |X_{n,k} - \hat{X}_{n,k}| > \delta \end{cases}. \tag{4.46}$$

then no cost is assigned for small errors (smaller than δ) and a cost of 1 is assigned for errors larger than δ. This estimator is known as the maximum *a posteriori* (MAP) estimator [16].

The advantage of the risk functions is that psychoacoustic models can be integrated in the spectral magnitude estimation. Next the Bayesian estimator considered in this thesis is presented, which estimate the short-time spectral amplitude (STSA) of speech based on the weighted euclidean (WE) distortion measure. This estimator is based on a replacement of the squared error cost function with a distortion measure, which has been shown to be subjectively more meaningful [18].

4.3.1 Bayesian Estimator Based on Weighted Euclidean Distortion Measure

In this subsection a Bayesian estimator is presented, which estimates the STSA of speech based on a perceptually motivated cost function. This cost function is referred to as a distortion measure [18]. A distortion measure between two vectors $\mathbf{u} \in \mathbb{R}^M$ and $\mathbf{v} \in \mathbb{R}^M$ is denoted by $d(\mathbf{u}, \mathbf{v})$. Most distortion measures satisfy three properties:

- Positivity: $d(\mathbf{u},\mathbf{v})$ is a real number that is greater than or equal to zero.
- Symmetry: $d(\mathbf{u},\mathbf{v}) = d(\mathbf{v},\mathbf{u})$.
- Triangular inequality: $d(\mathbf{u},\mathbf{z}) \leq d(\mathbf{u},\mathbf{v}) + d(\mathbf{v},\mathbf{z})$, when $\mathbf{z} \in \mathbb{R}^M$.

However, only the property of positivity needs to be satisfied [19]. The weighted euclidean (WE) distortion measure is considered, since it is one of the distortion measures which shows the best performance for reducing noise and producing better speech quality [18]. The WE distortion measure is given by

$$d_{WE}(X_{n,k}, \hat{X}_{n,k}) = X_{n,k}^{p}(X_{n,k} - \hat{X}_{n,k})^2. \tag{4.47}$$

This distortion measure emphasizes spectral peaks when $p > 0$, but emphasizes spectral valleys when $p < 0$. This is illustrated in Figure 4.4, where the magnitude spectrum X_k of the female utterance of the digits 521Z9 from TEST A of the Aurora-2 database is shown along with the spectra X_k^2, $\frac{1}{X_k}$ and $\frac{1}{X_k^2}$.

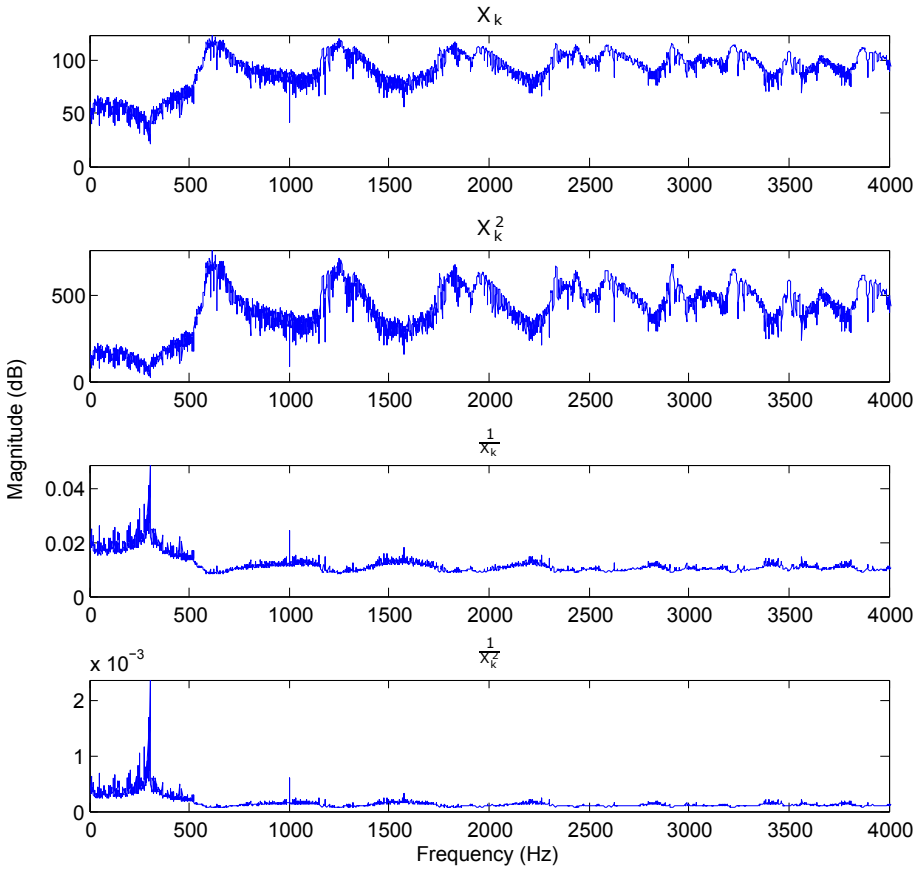

Figure 4.4: Magnitude spectrum X_k of the female utterance of the digits 521Z9 from TEST A of the Aurora-2 database and the spectra X_k^2, $\frac{1}{X_k}$ and $\frac{1}{X_k^2}$.

This distortion measure then exploits the masking properties of the human auditory system, where the frequency spectrum is shaped so less emphasis is placed near the formant peaks and

more emphasis is placed on the spectral valleys, where the amount of noise present is audible [18]. The distortion measure considered is called weighted Euclidean distortion measure, since it is based on the weighted Euclidean distance measure defined by:

$$\text{weighted Euclidean distance} = \sqrt{\sum_{j=1}^{M} w_j(u_j - v_j)}, \tag{4.48}$$

where w_j are non-negative weights and $\mathbf{u} = [u_1, u_2, ..., u_M]^{\mathrm{T}}$ and $\mathbf{v} = [v_1, v_2, ..., v_M]^{\mathrm{T}}$ are two points in M-dimensional space [9]. The weighted Euclidean distortion measure can be written in the form of the squared weighted Euclidean distance:

$$d_{WE}(X_{n,k}, \hat{X}_{n,k}) = (X_{n,k} - \hat{X}_{n,k})^{\mathrm{T}} W (X_{n,k} - \hat{X}_{n,k}), \tag{4.49}$$

where W is a diagonal matrix with the k$^{\text{th}}$ diagonal element $[W]_{kk} = X_{n,k}^{p}$. Using Equation 4.47, the following risk is then minimized:

$$\mathfrak{R} = \int_0^{\infty} X_{n,k}^{p} (X_{n,k} - \hat{X}_{n,k})^2 p(X_{n,k}|Y(n,k)) dX_{n,k}. \tag{4.50}$$

The derivative of $\mathfrak{R}$ with respect to $\hat{X}_{n,k}$ is set to zero:

$$\frac{\partial \mathfrak{R}}{\partial \hat{X}_{n,k}} = \int_0^{\infty} -2X_{n,k}^{p} (X_{n,k} - \hat{X}_{n,k}) p(X_{n,k}|Y(\omega_{n,k})) dX_{n,k} = 0. \tag{4.51}$$

Solving for $\hat{X}_{n,k}$ and using the Gaussian statistical model, it can be shown that $\hat{X}_{n,k}$ evaluates to [16]:

$$\hat{X}_{n,k} = \frac{\sqrt{v_{n,k}}}{\gamma_{n,k}} \frac{\Gamma\left(\frac{p+1}{2}+1\right) \Phi\left(-\frac{p+1}{2}, 1; -v_{n,k}\right)}{\Gamma\left(\frac{p}{2}+1\right) \Phi\left(-\frac{p}{2}, 1; -v_{n,k}\right)} Y_{n,k} = G_p(\xi_{n,k}, \gamma_{n,k}) Y_{n,k}, \quad p > -2. \tag{4.52}$$

Equation 4.52 consists of a nonlinear gain function $G_p(\xi_{n,k}, \gamma_{n,k}) = \frac{\hat{X}_{n,k}}{Y_{n,k}}$, which is a function of *a priori* SNR $\xi_{n,k}$ and *a posteriori* SNR $\gamma_{n,k}$. $\Phi(\cdot)$ and $\Gamma(\cdot)$ denotes the confluent hypergeometric function and the gamma function which are given by Equation 4.53 and 4.54, respectively [16].

$$\Phi(a, b; z) = \sum_{n=0}^{\infty} \frac{a^{(n)} z^n}{b^{(n)} n!}, \tag{4.53}$$

$$\Gamma(n) = (n-1)!\,. \tag{4.54}$$

$a^{(n)}$ denotes the rising factorial as follows:

$$a^{(0)} = 1, \tag{4.55}$$

$$a^{(n)} = a(a+1)(a+2)\cdots(a+n-1). \tag{4.56}$$

The *a priori* SNR $\xi_{n,k}$ can be considered the true SNR of the k^{th} spectral bin at time n and is given by the ratio of the power of the clean signal and of the noise power:

$$\xi_{n,k} = \frac{E\left[X_{n,k}^2\right]}{E\left[D_{n,k}^2\right]}. \tag{4.57}$$

The *a posteriori* SNR $\gamma_{n,k}$ can be considered the observed and measured SNR of the k^{th} spectral bin at time n after noise is added which is given by the ratio of the squared magnitude of the observed noisy signal and the noise power:

$$\gamma_{n,k} = \frac{Y_{n,k}^2}{E\left[D_{n,k}^2\right]}. \tag{4.58}$$

Furthermore $\upsilon_{n,k}$ is given by:

$$\upsilon_{n,k} = \frac{\xi_{n,k}}{1+\xi_{n,k}}\gamma_{n,k}. \tag{4.59}$$

Since the clean speech signal is not available, the *a priori* SNR $\xi_{n,k}$ is approximated by the use of the decision-directed approach. The decision-directed *a priori* estimator is defined by the following recursive equation [16]:

$$\hat{\xi}_{n,k}(m) = a\frac{\hat{X}_{n,k}^2(m-1)}{E[D_{n,k}(m-1)^2]} + (1-a)\max\left[\gamma_{n,k}(m)-1,0\right], \tag{4.60}$$

where $0 < a < 1$ is the weighting factor, where it has been chosen to use $a = 0.98$ as recommended by [16]. $X_{n,k}^2(m-1)$ is the amplitude estimator obtained in the previous frame. The max$(\cdot)$ operator is used to ensure positiveness of the estimator, as $\hat{\xi}_{n,k}(m)$ needs to be non-negative. Therefore the estimator of the *a priori* SNR $\xi_{n,k}$ given by Equation 4.60 is a weighted average of the past *a priori* SNR (given by the first term) and a present *a priori* SNR estimate (given by the second term). Because of this, Equation 4.60 is called a decision-directed estimator, since $\hat{\xi}_{n,k}(m)$ is updated using information from the previous amplitude estimate. The following initial condition for the first frame (i.e. for $m = 0$) in Equation 4.60 has been recommended by [5]:

$$\hat{\xi}_{n,k}(0) = a + (1-a)\max\left[\gamma_{n,k}(0)-1,0\right]. \tag{4.61}$$

In Figure 4.5 the gain function $G_p(\xi_{n,k},\gamma_{n,k})$ is shown as a function of the instantaneous SNR $(\gamma_{n,k}-1)$ for a fixed value of $\xi_{n,k}$ ($\xi_{n,k} = -5$dB) for several values of the power exponent p. It is seen that the amount of attenuation is dependent on the value of the power exponent p. Large and positive values of p provide small attenuation, whereas large and negative values of p provide larger attenuation [18]. In this it has been chosen to a power exponent p with a value of $p = -1$, which has been shown to provide a good compromise between speech distortion and residual noise [18].

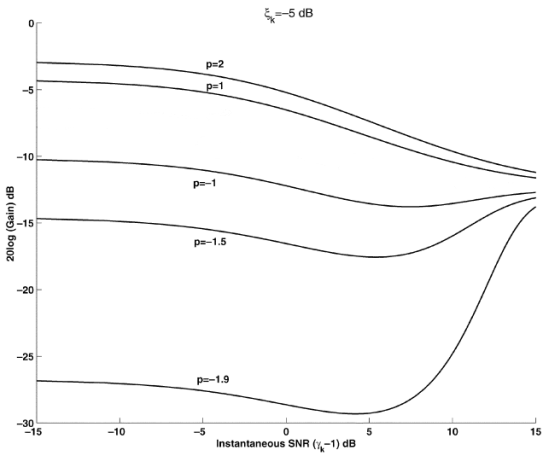

Figure 4.5: Gain function of the WE distance estimator as a function of the instantaneous SNR ($\gamma_{n,k}-1$) and for several values of the power exponent p for $\xi_{n,k}=-5$ dB.

4.4 Noise Power Spectrum Estimation

In this section the estimation procedures of the noise power spectrum are presented for the MATLAB implementations of the SE algorithms presented in the previous sections of this chapter.

The only signal available is the observed noisy signal. Therefore the noise power must be estimated during the absence of the clean signal. The ANS algorithm and the STSA WE algorithm use voice activity detection (VAD) approach to estimate the noise power spectrum. The following VAD decision rule is used:

$$\frac{1}{N}\sum_{k=1}^{N-1}\log\Lambda_k \underset{H_0}{\overset{H_1}{\gtrless}} \delta, \tag{4.62}$$

where

$$\Lambda_k = \frac{1}{1+\xi_k}\exp\left\{\frac{\gamma_k\xi_k}{1+\xi_k}\right\}, \tag{4.63}$$

where ξ_k and γ_k are the *a priori* and *a posteriori* SNRs, which are given by Equation 4.57 and 4.58, respectively. N is the size of the FFT, H_1 denotes the hypothesis of speech presence, H_0 denotes the hypothesis of speech absence and δ is a fixed threshold, which is set to $\delta=0.15$ as given by [16]. When speech absence is detected, the noise power spectrum is updated as follows:

$$D_{n,k}(i) = (1-\beta)\cdot Y^2_{n,k}(i) + \beta D_{n,k}(i-1), \tag{4.64}$$

where $\beta=0.98$, $D_{n,k}(i)$ is the noise power spectrum in frame i, for frequency bin k and $Y^2_{n,k}(i)$ is the noise speech power spectrum. Initially the noise power is estimated by assuming that the first 6 frames of the noisy signal is noise or silence and then the noise power is estimated by averaging the noise power spectrum over the first 6 frames [16].

However, the MATLAB implementations of IWF algorithm only provides the initial estimate of the noise power by averaging the noise power spectrum over the first 6 frames, which is fixed for all the speech frames of the speech signal.

4.5 Performance Evaluation Methods

In this section the measures used to evaluate the performance of SE algorithms are presented. It is not uncommon for SE algorithms to strive for improved signal quality, while simply trying to avoid too much degradation of the speech intelligibility [16]. Therefore it is desired to compare the effect of SE algorithms designed for human and machine receivers on both signal quality and intelligibility. However, in order to find the true speech quality and intelligibility of a speech signal, expensive and time consuming listening tests are required. Therefore speech quality and intelligibility are instead estimated using the perceptual evaluation of speech quality (PESQ) [16] and short-time objective intelligibility measure (STOI) [32], respectively. STOI is a relative recent addition to the distortions measures used for measuring the performance of SE algorithms. However, it has been chosen as studies have shown that it is highly correlated with intelligibility of noisy speech and time-frequency (TF) weighted speech signals [17, 32]. PESQ has been chosen as it is a well known industry standard [16]. Both of the distortion measures are what is referred to as full reference algorithms, meaning they require an original clean speech signal for comparison, in order to evaluate the degraded speech signal.

4.5.1 Short-Time Objective Intelligibility (STOI) Measure

STOI is an objective intelligibility measure designed to replace subjective listening tests, when evaluating the effect on speech intelligibility by various SE methods, as subjective listening tests are costly and time consuming. Specifically STOI is intended to measure any degradations or modifications to clean/noisy speech signals brought on by a speech coder or noise reduction schemes, where the speech signal is processed by using some type of TF varying gain function [32].

The STOI measure is calculated using the clean and processed speech, denoted by x and y, respectively. It is desired that the model covers the entire frequency range relevant to speech-intelligibility, therefore a sample-rate of 10 kHz is chosen [32]. Signals with other sample-rates are re-sampled. In addition the method operates under the assumption that the clean and processed speech signals are time-aligned. The signals are then segmented into frames with a length of 256 samples, with a 50% overlap between each frame, a Hanning-window is then applied to each frame[32]. Each frame is zero-padded up to 512 samples and the Fourier transform is applied [32], resulting in the TF-representation of the signals. The silent frames of the signal are then removed, as they do not contribute to speech intelligibility.

The frames are grouped into DFT-bins to enable frequency band analysis. 15 one-third octave bands are used [32], which means that the upper band-edge frequency is $\sqrt[3]{2}$ time larger than the lower band frequency. The TF-unit for the j^{th} one-third octave band is then calculated by:

$$X_j(m) = \sqrt{\sum_{k=k_1(j)}^{k_2(j)-1} |\hat{x}(k,m)|^2}, \tag{4.65}$$

where $\hat{x}(k,m)$ denote the k^{th} DFT-bin of the m^{th} frame of the clean speech and k_1 and k_2 denote the edges of the frequency bands rounded to the nearest DFT-bin. The TF-representation of the processed signal is denoted $Y_j(m)$ and found in a similar fashion. The TF-units are grouped into temporal envelopes which consist of $N = 30$ consecutive speech frames, corresponding to an analysis window of 384 ms [2] [32]. The signal-to-distortion ratio (SDR), which is defined as:

$$SDR_j(n) = 10\log_{10}\left(\frac{X_j(n)^2}{(\alpha Y_j(n) - X_j(n))^2}\right), \tag{4.66}$$

where $\alpha = \left(\sum_n X_j(n)^2 / \sum_n Y_j(n)^2\right)^{1/2}$ is a factor used to normalize $Y_j(m)$ such that the energy of the processed signal match that of the clean signal [32]. In order to give the SDR a lower bound, $\alpha Y_j(n)$ is then clipped. This clipped and normalized TF-unit is defined as:

$$Y' = \max\left(\min\left(\alpha Y, X + 10^{-\beta/20}X\right)X - 10^{-\beta/20}X\right), \tag{4.67}$$

where β denote the lower bound for SDR. For notational convenience the indices for the frames and one-third octave bands are omitted in Equation 4.67. By taking the clean and modified processed TF-units and finding an estimate of the linear correlation coefficient between the two signals, an intermediate intelligibility measure $d_j(m)$ is obtained [32]:

$$d_j(m) = \frac{\sum_n \left(X_j(n) - \frac{1}{N}\sum_l X_j(l)\right)\left(Y'_j(n) - \frac{1}{N}\sum_l Y'_j(l)\right)}{\sqrt{\sum_n \left(X_j(n) - \frac{1}{N}\sum_l X_j(l)\right)^2 \sum_n \left(Y'_j(n) - \frac{1}{N}\sum_l Y'_j(l)\right)^2}}, \tag{4.68}$$

where $n \in \mathcal{M}$ and $\mathcal{M} = \{(m-N+1), (m-N+2), \ldots, m-1, m\}$, meaning $d_j(m)$ requires N consecutive TF-units. The final intelligibility measure d is calculated by averaging over all bands and frames [32]:

$$d = \frac{1}{JM}\sum_{j,m} d_j(m), \tag{4.69}$$

where J and M represents the number of one-third octave bands and the total number of frames, respectively. As STOI uses a correlation coefficient a value between -1 and 1 can be expected [2], where 1 is the highest integrability score possible.

[2] A consequence of this is that the STOI measure can only be calculated if a speech signal contains at least 30 speech frames

4.5.2 Perceptual Evaluation of Speech Quality (PESQ)

PESQ has originally been developed as a robust measure for speech quality evaluation for producing consistent results across various speech codecs and/or noise conditions. PESQ attempts to score the quality of the speech signal based on human perception, assigning the signal a value in the range 0.5 to 4.5 [16]. Today PESQ is widely used in the field of speech enhancement, in fact it has been chosen by the International Telecommunication Union Telecommunication Standardization Sector (ITU-T) as recommendation P.862. As mentioned, PESQ is robust towards changing noise and processing types. This is particularly true when the SNR of the speech signal is high or medium. For lower SNR values, PESQ becomes less reliable [11]. An overview of the PESQ measure can be seen in Figure 4.6. The reference and degraded signals first undergo pre-processing in the form of level-equalization and filtering with an impulse response of a standard telephone model. In order to correct any time delays between the two signals, they then go through a time alignment process. Next the loudness spectra of the two signals is computed using an auditory transform which models perceived loudness. Then the difference between the loudness spectra is computed, which is denoted as the disturbance. Finally, the PESQ score is computed by averaging the disturbance in time and frequency [16]. In the following, the blocks comprising PESQ are expanded upon.

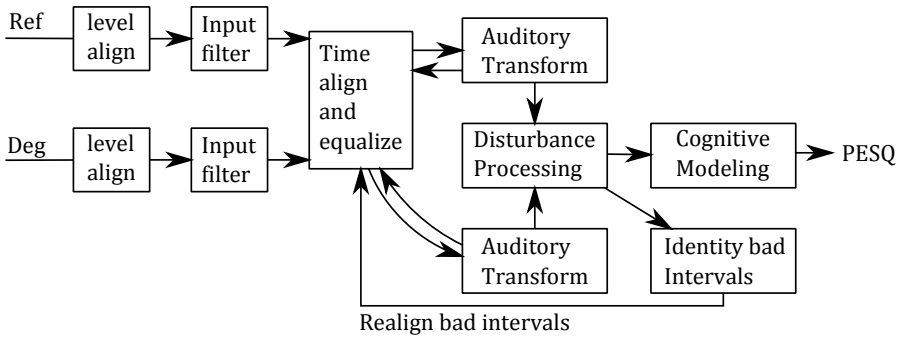

Figure 4.6: Block diagram of the PESQ model.

4.5.2.1 Level Align and Input Filter

The model begins by level aligning both signals to a standard listening level. The speech signals are band-pass-filtered and the root mean square values are used to compute gains for the original and the degraded signals. The signals are then filtered (using FFT) with an input filter designed to model the impulse response of a standard telephone handset.

4.5.2.2 Time Alignment

A crude delay estimation can be performed using cross-correlation of the envelopes for the original and the degraded signals, when working under the assumption that the delay is piecewise constant [16]. Normalized energy measures for the frames are used to compute

the signal envelopes. These crude estimations are then used to separate the signals into a number of subsections or utterances. Then the time alignment of the reference and degraded signals is improved, first by using a crude envelope based delay estimation of the utterances and afterwards applying Hamming windowing using a frame length of 64ms. These windows are then cross-correlated and the sample index providing maximum correlation is taken to be the delay estimate of each frame [16]. The confidence of the alignment for each frame is then computed as the maximum correlation raised to the power 0.125 [16].

4.5.2.3 Auditory Transform

The signals are then processed through an auditory transform which models perceived loudness. This involves equalising for linear filtering in the system and for gain variation. The transform consists of the following steps:

- Bark spectrum
- Frequency equalization
- Equalisation of gain variation
- Loudness mapping

These steps are expanded upon in the following.

Bark Spectrum
The purpose of this part is to calculate the bark spectrum (the Bark frequency scale similar to the Mel frequency scale is based on the concept of sound perception, though the scale is not as widely used as the Mel scale). Initially an estimate of the power spectrum is found using FFT. Windowing is carried out with the Hamming function using a frame length of 32ms and a 50 % overlap between frames[16]. The power spectrum is then grouped into 42 bins that are equally spaced on a modified bark scale. 49 bands are used for signals sampled at 16kHz [16].

Frequency Equalization
Working under the assumption of a constant frequency response, the transfer function is estimated as the ratio between mean bark spectra of reference and degraded signal. The reference signal is then equalized to degraded signal, though the equalization is limited to ±20 dB[16].

Equalisation of Gain Variation
In order to identify gain variations between frames, the ratio between the audible power of the reference and the degraded signal in each frame is used. The ratios are then filtered using a first order lowpass filter, $H(z) = 0.8 + 0.2z^{-1}$ [16]. The filter output is then bounded to the

range $[3 \times 10^{-4}, 5]$, and finally the degraded signal is equalized to the reference signal using the processed ratios [16].

Loudness Mapping

The bark spectrum is then mapped to the sone loudness scale (a linear scale unit for how loud a sound is perceived):

$$S(b) = S_l \left(\frac{P_0(b)}{0.5} \right)^{\gamma} \left[\left(0.5 + 0.5 \frac{B'_x(b)}{P_0(b)} \right)^{\gamma} - 1 \right], \tag{4.70}$$

where S_l is a loudness scaling factor, $P_0(b)$ is the hearing threshold for bark b and $B'_x(b)$ is the frequency compensated bark spectrum. γ is a power exponent [16].

4.5.2.4 Disturbance Processing and Cognitive Modelling

The PESQ score is computed by combining the average disturbance value and asymmetrical disturbance value [16]. The difference in the loudness spectra between the reference signal $S_n(b)$ and the degraded signal $\overline{S}_n(b)$ is denoted as the raw disturbance density and it is computed as follows:

$$r_n(b) = S_n(b) - \overline{S}_n(b), \tag{4.71}$$

where, n is the frame number. The PESQ method do not square the difference, as there is a difference between positive and negative values of the disturbance density. A positive difference value signifies that a spectral component has been added, while a negative difference value means that a component has been omitted[16]. However, as added components tend to be easier perceived than omitted components, the impact on signal quality differs [16]. A weighting scheme is applied, where omitted components are not penalized as much as added components. An updated disturbance density $D_n(b)$ can be computed as

$$D_n(b) = \begin{cases} r_n(b) - m_n(b) & \text{if } r_n(b) > m_n(b) \\ 0 & \text{if } |r_n(b)| \leq m_n(b) \\ r_n(b) + m_n(b) & \text{if } r_n(b) < -m_n(b) \end{cases}, \tag{4.72}$$

where $m_n(b)$ is defined as $m_n(b) = 0.25 \min[S_n(b), \overline{S}_n(b)]$ [16]. An estimation of the asymmetric effect of the differences can be found by multiplying disturbance density $D_n(b)$ by an asymmetry factor $AF_n(b)$ [16]. The asymmetrical disturbance density DA_n is then defined as:

$$DA_n = AF_n D_n(b) \quad 1 \leq b \leq 42. \tag{4.73}$$

The frame disturbances D_n and DA_n are found by summing the disturbance density and asymmetric density across frequency, using different norms for the disturbance density and asymmetric density, as shown in [16]. In order to avoid incorrect time delays causing preditions of large distortions over a small number of frames, the signal goes through a check that

locates any bad intervals [16]. The check is a threshold value that the frame disturbances of consecutive frames must not be above. Afterwards any bad interval is realigned and the frame disturbances are recomputed, now denoted as D''_n and DA''_n [16]. Finally the disturbance measures of the k^{th} frame are averaged in time twice, the first averaging is defined as:

$$\mathbf{D}'''_k = \left(\frac{1}{20} \sum_{n=(k-1)20}^{20k-1} \left(\mathbf{D}''_n\right)^6 \right)^{1/6}, \tag{4.74}$$

$$\mathbf{DA}'''_k = \left(\frac{1}{20} \sum_{n=(k-1)20}^{20k-1} \left(\mathbf{DA}''_n\right)^6 \right)^{1/6}, \tag{4.75}$$

where the averaging is done over intervals of 20 frames, using 50% overlapping without rectangular windowing [16]. Next a 2-norm is used to average the speech frames and compute the average disturbance value d_{sym} and the average asymmetrical disturbance value d_{asym}, given by:

$$d_{sym} = \left(\frac{\sum_k (\mathbf{D}'''_k \mathbf{t}_k)^2}{\sum_k (\mathbf{t}_k)^2} \right)^{1/2}, \tag{4.76}$$

$$d_{asym} = \left(\frac{\sum_k (\mathbf{DA}'''_k \mathbf{t}_k)^2}{\sum_k (\mathbf{t}_k)^2} \right)^{1/2}, \tag{4.77}$$

where t_k are the weights applied to the frame disturbance values. The value of these weights depend on the length of the signal [16]. Finally both the symmetrical and asymmetrical disturbance values are jointed together as a linear combination, resulting in the final PESQ score:

$$PESQ = 4.5 - 0.1 d_{sym} - 0.0309 d_{asym}. \tag{4.78}$$

As previously mentioned the range of PESQ score is 0.5 to 4.5 [16].

Speech Enhancement using ETSI AFE 5

The advanced frontend (AFE) defined by ETSI [7] is a standard for feature extraction in noise robust automatic speech recognition (ASR) as described in Section 3.1, where noise reduction is carried out in the pre-processing stages. These noise reduction stages of the ETSI AFE provide better ASR performance than if replaced with state-of-the-art SE methods for human receivers [14]. Therefore this chapter investigates the SE performance in terms of human auditory perception, i.e. speech intelligibility and quality, of the pre-processing stages from the ETSI AFE using speech data from the Aurora-2 database [26]. This performance is compared to the SE methods considered in this thesis designed for human receivers: The iterative Wiener filtering (IWF) algorithm [16], the audible noise suppression (ANS) algorithm [16] and the short-time spectral amplitude (STSA) estimator based on the weighted euclidean (WE) distortion measure [16]. The intelligibility and quality of the enhanced speech signals are estimated by the use of the STOI and PESQ measures described in Section 4.5.1 and 4.5.2, respectively.

Appendix A shows the settings for the feature extraction process, the Aurora-2 database and the SE algorithms, which have been used to produce the results presented in this chapter. Furthermore, an overview of the Matlab implementations of the SE methods for human listeners used are provided by Appendix B.

5.1 Extracting Denoised Speech Signals from ETSI AFE

The ETSI AFE algorithm carries out noise reduction in the pre-processing stages of the noisy input speech signals [7]. In this section the extraction of denoised signals from the pre-processing stages of the ETSI AFE algorithm is considered. It is required that the denoised signal is a time-domain signal and therefore only the first two blocks (*noise reduction* and *waveform processing)* of the ETSI AFE algorithm, which produce time-domain signals, are considered. This is, however, not the case for the subsequent blocks. Because time-domain signals are required, it has been chosen to let the extraction take place at three different

available locations in the ETSI AFE algorithm. As described in Section 3.1.1.1, the *noise reduction* block consists of a two-stage Wiener filter. The first extraction of a denoised speech signal $\hat{y}_{\text{wf1}}(n)$ takes place at the output of the first-stage Wiener filter, as shown in Figure 5.2. The second and third extraction of the denoised speech signals $\hat{y}_{\text{wf2}}(n)$ and $\hat{y}_{\text{wfp}}(n)$ take place at the output of the *noise reduction* block and the output of the *waveform processing* block, respectively, as shown in Figure 5.1.

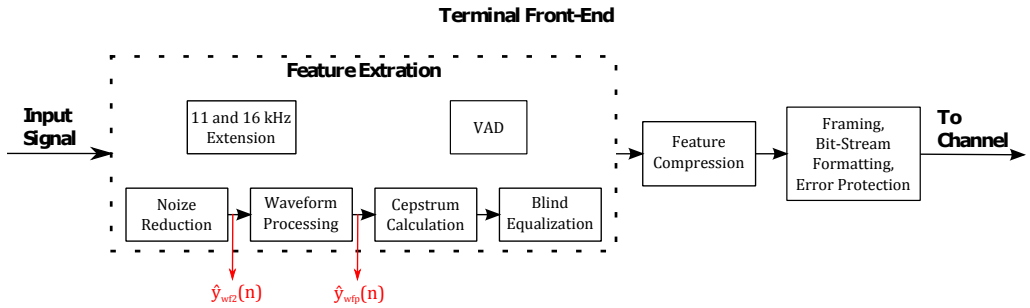

Figure 5.1: Block diagram of the terminal side of the ETSI AFE algorithm. The extraction of the denoised speech signals $\hat{y}_{\text{wf2}}(n)$ and $\hat{y}_{\text{wfp}}(n)$ takes place at the output of the *noise reduction* block and at the output of the *waveform processing* block as indicated by the red color.

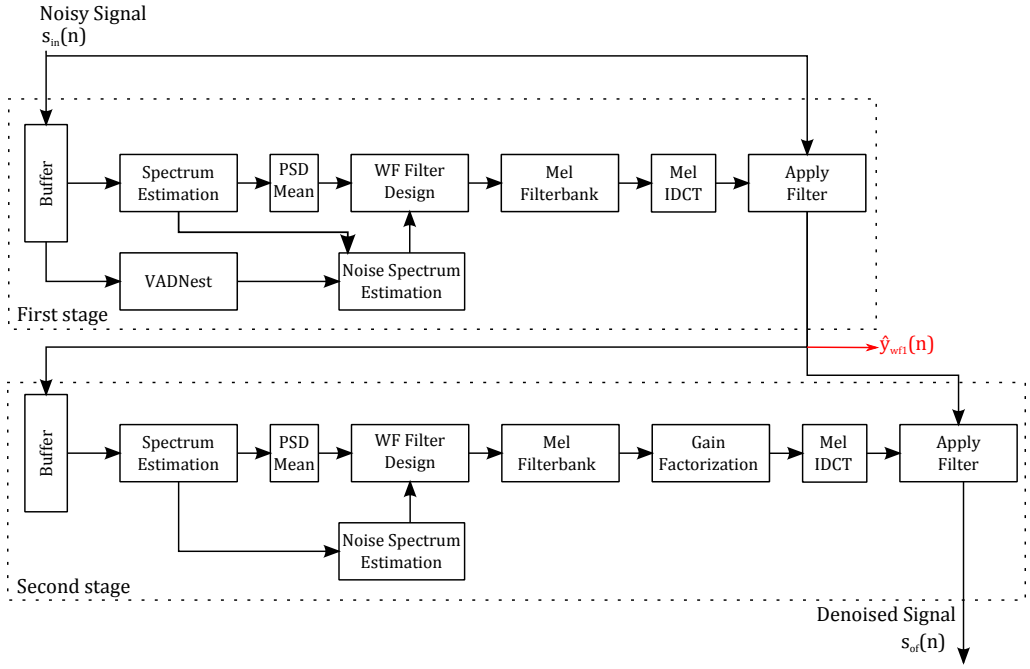

Figure 5.2: Block diagram of the *noise reduction* block of the ETSI AFE algorithm. The extraction of the denoised speech signal $\hat{y}_{\text{wf1}}(n)$ takes place at the output of the first-stage Wiener filter as indicated by the red color.

In Figure 5.3 a block diagram of the *noise reduction* block of the ETSI AFE algorithm is shown with the associated buffers.

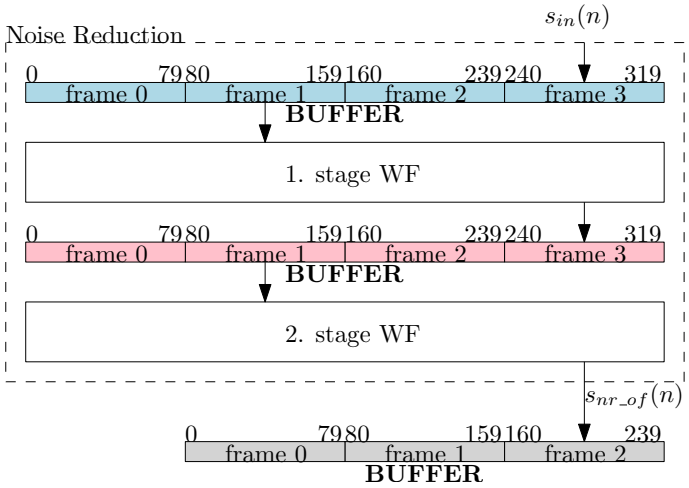

Figure 5.3: Block diagram of the *noise reduction* block of the ETSI AFE algorithm and its associated buffers.

As shown in Figure 5.3, each of the two stages in the *noise reduction* block operates with a 4-frame (frame 0 to frame 3) buffer, where each frame is defined as 80 samples. These two buffers are represented by a blue and pink colour, respectively. For each new input frame, the 2 buffers are shifted by one frame, so the new input frame becomes frame 3 of the first buffer and frame 1 of the first buffer is denoised, which becomes frame 3 of the second buffer. The frame 1 of the second buffer is denoised and is the output of the *noise reduction* block. This means that there is a latency of 2 frames at each stage of the *noise reduction* block. Therefore, when extracting the denoised speech signal at the output of the 1. stage Wiener filter, at least 2 frames are lost (2 frames + the remaining samples not filling up a frame). At the output of the 2$^{\text{nd}}$ stage Wiener filter at least 4 frames are lost (4 frames + the remaining samples not filling up a frame). Furthermore, the output of the *noise reduction* block is stored in a 240-sample buffer, which is represented by a gray colour in Figure 5.3. The subsequent *waveform processing* block is only processed when this buffer is full. This means that at least 6 frames are lost at the output of the *waveform processing* block (6 frames + the remaining samples not filling up a frame). However, it has been chosen to not recover this lost data, because with the test speech signals used in this thesis these are typically silent region frames.

5.2 Comparison of Speech Quality Measurements

In this subsection the speech quality is estimated for the speech signals belonging to the three test sets A, B and C from the Aurora-2 database when processed by the pre-processing stages of the ETSI AFE algorithm. The speech quality is evaluated by the use of the perceptual evaluation of speech quality (PESQ) measure described in Section 4.5.2, which estimates the quality of speech signals as perceived by humans. PESQ assigns speech signals values in the range 0.5 to 4.5, where a PESQ value of 4.5 means that the signal has no distortion and the lower the PESQ value becomes, the more distorted the signal is. Furthermore, the PESQ scores for the pre-processing stages of the ETSI AFE algorithm are compared to the PESQ scores calculated for state-of-the-art SE methods.

The speech signals have been extracted at the pre-processing stages of the ETSI AFE algorithm as presented in Section 5.1. Table 5.1 and 5.2 show the PESQ results for noisy and denoised speech signals of the Aurora-2 database averaged for SNR level and noise condition, respectively. The speech signals have been denoised by the use of the pre-processing stages of the ETSI AFE algorithm and the SE methods: Audible noise suppression (ANS) [16], iterative Wiener filter (IWF) [16] and short-time spectral amplitude (STSA) estimator based on the weighted euclidean (WE) distortion measure [16]. Afterwards, the improvements of each algorithm are considered and compared.

In Table 5.1 the PESQ results averaged for SNRs are shown for the speech data from test set A, B and C of the Aurora-2 database. It can be observed that in general as the SNR level decreases, the average PESQ measure given by each column also decreases. Even when the clean signals have been processed, a decrease in the average PESQ measure is observed, providing average PESQ measures below 4.5 as seen in the second row of Table 5.1.

SNR	**Noisy Speech**	**ETSI AFE**			**ANS**	**IWF**	**STSA WE**
		1st Stage WF	**2nd Stage WF**	**Waveform processing**			
Clean	4.5000	4.3532	4.3389	3.6945	4.2761	4.2994	4.3445
20 dB	2.8013	3.1588	3.1714	3.0465	2.9916	2.9090	3.1884
15 dB	2.4978	2.8262	2.8400	2.7723	2.6393	2.5332	3.0196
10 dB	2.1934	2.4830	2.4975	2.4658	2.2621	2.1463	2.5579
5 dB	1.8997	2.1142	2.1223	2.1102	1.8177	1.7085	2.2018
0 dB	1.6247	1.7256	1.7156	1.7120	1.2850	1.2294	1.8098
-5 dB	1.3580	1.3714	1.3388	1.3373	0.7557	0.7965	1.3815

Table 5.1: PESQ scores averaged for SNRs of noisy speech from test set A, B and C of the Aurora-2 database and noise reduced speech.

At SNR levels 5 dB to 20 dB, the largest improvement is observed extracted at the output of the 2nd stage Wiener filter when compared to the other pre-processing stages of the ETSI AFE

algorithm. However, at −5 dB and 0 dB SNR, the largest improvement provided by the preprocessing stages of the ETSI AFE, is given by the output of the 1st stage Wiener filter. In the application of speech recognition, the *waveform processing* block is beneficial to include in the ETSI AFE algorithm, as it improves the recognition performance by increasing the overall SNR level [27]. But as seen in Table 5.1, the average PESQ measure is reduced at all SNR levels when the speech signals at the output of the 2nd stage Wiener filter have been processed by the *waveform processing* block. Especially for clean speech signals and the speech signals at the highest tested SNR levels, 15 dB and 20 dB, significant reductions in average PESQ score occur. The *waveform processing* block is designed to increase the SNR level of the input signal by amplifying and attenuating high- and low-energy segments, respectively [27]. The PESQ scores obtained at the output of the *waveform processing* block appear to suggest that the low-energy segments of the speech signal are inadvertently suppressed in the absent of noise or at low noise levels.

At SNR levels −5 dB to 20 dB, the ANS and IWF algorithms provide significantly lower average PESQ results than the other algorithms. The IWF provides the worse PESQ scores, which can be explained by the fact that the IWF algorithm is run for a fixed number of iterations. This is not necessarily optimal for all the tested speech signals and might therefore introduce more errors than the other algorithms. The STSA WE algorithm and the 2nd stage Wiener filter of the ETSI AFE algorithm provide similar average PESQ scores at 20 dB SNR, but as the SNR level decreases the STSA WE algorithm provides larger improvement in PESQ score than the other algorithms. A gap appear between the STSA WE algorithm and the preprocessing stages of the ETSI AFE at SNR levels below 20 dB. This raises suspicion by the authors that the ETSI AFE preprocessing stages are less aggressive than the STSA WE algorithm, which is investigated further in Section 5.4.

Noise Condition	**Noisy Speech**	**ETSI AFE**			**ANS**	**IWF**	**STSA WE**
		1st Stage WF	**2nd Stage WF**	**Waveform processing**			
Subway	2.0147	2.2313	2.2210	2.1711	1.8981	1.8851	2.3611
Babble	2.1542	2.3185	2.3080	2.2602	2.0081	1.9154	2.3369
Car	2.0598	2.3304	2.3569	2.3078	2.1047	2.0557	2.4962
Exhibition	1.9800	2.2799	2.2950	2.2435	2.0310	1.9406	2.2666
Restaurant	2.1601	2.3136	2.3030	2.2548	1.9814	1.8820	2.2683
Street	2.0278	2.2630	2.2804	2.2307	2.0204	1.9455	2.3568
Airport	2.1823	2.3617	2.3598	2.3106	2.0811	1.9819	2.3804
Train-Station	2.1108	2.3435	2.3636	2.3145	2.0928	2.0189	2.4619
Subway (MIRS)	2.0277	2.2154	2.1865	2.1642	1.7447	1.7002	2.2821
Street (MIRS)	2.0025	2.2429	2.2553	2.2333	1.8978	1.8101	2.2770
Average	2.0720	2.2900	2.2930	2.2491	1.9860	1.9135	2.3487

Table 5.2: PESQ scores averaged for noise conditions of noisy speech from test set A, B and C of the Aurora-2 database and noise reduced speech.

The PESQ scores averaged for noise conditions are presented in Table 5.2. The SE algorithms designed for human listeners (ANS, IWF and STSA WE) provide the largest average PESQ scores at the car noise condition. This can be explained by the fact that this is a stationary noise condition. The restaurant noise condition, however, provide among the lowest average PESQ scores, when only considering the noise conditions of test set A and B for the ANS, the IWF and the STSA WE algorithms. This can be explained by the fact that restaurant noise contains non-stationary segments. This behaviour is, however, less apparent for the pre-processing stages of the ETSI AFE algorithm. The average PESQ scores for test set C (subway (MIRS) and street (MIRS)) with additional frequency weighting are similar to the corresponding results without spectral modifications when denoising using the pre-processing stages of the ETSI AFE algorithm. however, when denoising using of the SE algorithms designed for human listeners (ANS, IWF and STSA WE), the average PESQ scores for the test set C are significantly lower than the corresponding results without spectral modifications. The IWF algorithm provides the poorest PESQ scores for each noise condition. As described in Section 4.4, the IWF algorithm estimate a non-adaptive noise power spectrum for all the speech frames of the speech signal. This is in contrast to the method used by the pre-processing stages of the ETSI AFE algorithm, the ANS algorithm and the STSA WE algorithm, which are all using adaptive estimation of the noise power spectrum. This suggest that the significant poorer PESQ results provided by the IWF algorithm is a consequence of using a non-adaptive estimated noise power spectrum.

It should, however, be noted that when the speech signals have been processed by the noise reduction algorithms, samples are inadvertently lost. The number of samples lost is depends on the noise reduction algorithm. This might have an impact on the PESQ results presented in Table 5.1 and 5.2.

5.3 Comparison of Speech Intelligibility Measurements

In this subsection the speech intelligibility is estimated for the speech signals belonging to the test sets A, B and C from the Aurora-2 database, when processed by the pre-processing stages of the ETSI AFE algorithm and the SE algorithms designed for human receivers (ANS, IWF and STSA WE). The speech intelligibility is estimated by the use of the short-time objective intelligibility (STOI) measure described in Subsection 4.5.1, which is highly correlated with intelligibility of noisy speech and time-frequency weighted noisy speech (e.g. noise reduced speech).

The STOI measure is incalculable for speech signals containing less than 30 speech frames [32]. Consequently, the speech signals of the Aurora-2 database where less than 30 speech frames are located by STOI, are excluded from the analysis in this thesis involving the STOI measure. Excluding these speech signals results in an approximately 10 % reduction of the available test data. The PESQ measure is not limited by the number of speech frames available in the speech signals, which means all available test data is used when computing PESQ. Therefore the exclusion of speech signals is only carried out when computing STOI.

SNR	**Noisy Speech**	**ETSI AFE**			**ANS**	**IWF**	**STSA WE**
		1st Stage WF	**2nd Stage WF**	**Waveform processing**			
Clean	1.0000	0.9995	0.9995	0.9796	0.9998	0.9999	0.9992
20 dB	0.9769	0.9723	0.9716	0.9546	0.9746	0.9743	0.9659
15 dB	0.9459	0.9436	0.9423	0.9293	0.9422	0.9408	0.9315
10 dB	0.8904	0.8938	0.8923	0.8841	0.8800	0.8791	0.8732
5 dB	0.8037	0.8144	0.8140	0.8099	0.7725	0.7764	0.7808
0 dB	0.6900	0.7031	0.7041	0.7021	0.6155	0.6296	0.6590
-5 dB	0.5673	0.5689	0.5619	0.5604	0.4295	0.4616	0.5244

Table 5.3: STOI scores averaged for SNR levels for noisy speech from test set A, B and C of the Aurora-2 database and noise reduced speech.

In Table 5.3 the STOI measures averaged for SNRs are shown for speech data from test set A, B and C of the Aurora-2 database. It can be observed that the pre-processing stages of the ETSI AFE algorithm provide no significant improvement or degradation of the average STOI measure with respect to the noisy speech at any of the tested SNR levels. Except at the output of the *waveform processing* block, where a small reduction in average STOI measure is observed at the highest tested SNR levels compared to the other pre-processing stages of the ETSI AFE algorithm. A similar observation has been obtained for the average PESQ scores, as described in Section 5.2, which again suggests that the low-energy segments of the speech signals are suppressed in the absent of noise or at low noise levels. At SNR levels -5 to 15 dB the 1st and 2nd stage Wiener filters of the ETSI AFE algorithm produce larger average STOI scores than the SE algorithms designed for human receivers (ANS, IWF and STSA WE). The average STOI

scores for the ANS, the IWF and the STSA WE algorithms are decreased with respect to the STOI scores for the noisy signals at all SNR levels. Though the STOI scores are quite similar for these algorithms. It is, however, expected that the ANS improves in average STOI at the lowest tested SNR levels, as [16] refer to observations of improvement in intelligibility scores using the ANS algorithm at SNR level -5 dB. But the results obtained with the speech signals used in this thesis show the poorest results at SNR level -5 dB compared to all other algorithms tested.

In Table 5.4 the STOI results averaged for noise conditions are shown for the speech data from test set A, B and C of the Aurora-2 database. It can be observed that there is no significant improvement of the average STOI measure provided by the pre-processing stages of the ETSI AFE algorithm with respect to the STOI scores for the noisy speech at any noise condition. The average STOI scores for the ANS, the IWF and the STSA WE algorithms decrease with respect to the STOI scores for the noisy speech at all noise conditions.

Noise Condition	**Noisy Speech**	**ETSI AFE**			**ANS**	**IWF**	**STSA WE**
		1st Stage WF	**2nd Stage WF**	**Waveform processing**			
Subway	0.8044	0.7952	0.7915	0.7830	0.7520	0.7656	0.7829
Babble	0.8135	0.8144	0.8129	0.8071	0.7690	0.7790	0.7836
Car	0.8039	0.8240	0.8263	0.8194	0.7696	0.7919	0.7950
Exhibition	0.8214	0.8311	0.8310	0.8191	0.7849	0.7985	0.7917
Restaurant	0.8280	0.8242	0.8212	0.8120	0.7768	0.7810	0.7906
Street	0.8056	0.8134	0.8134	0.8059	0.7577	0.7759	0.7840
Airport	0.8319	0.8366	0.8357	0.8278	0.7910	0.7998	0.8037
Train-Station	0.8200	0.8319	0.8323	0.8238	0.7821	0.7956	0.8013
Subway (MIRS)	0.8046	0.7962	0.7905	0.7836	0.7591	0.7463	0.7842
Street (MIRS)	0.8045	0.8137	0.8124	0.8065	0.7638	0.7718	0.7842
Average	0.8138	0.8181	0.8167	0.8088	0.7706	0.7805	0.7901

Table 5.4: STOI scores averaged for noise conditions of noisy speech from test set A, B and C of the Aurora-2 database and noise reduced speech.

Ideally, we would like SE algorithms to improve both speech quality and speech intelligibility. In practice, however, most SE algorithms only improve the quality of speech [16]. This can be seen in the PESQ and STOI scores when processing the speech data with the pre-processing stages of the ETSI AFE. In some cases improvement in speech quality is accompanied by a decrease in speech intelligibility [16]. This is observed in the PESQ and STOI scores when the speech signals are processed by the ANS, the IWF and the STSA WE algorithms. This behaviour can be explained by the fact that more intelligibility is sacrificed for human receivers as humans are better trained at recognising speech in noisy conditions, than machines.

It should also be noted that the STOI results presented in this section might be effected by the fact that samples are lost when the speech signals are processed by the noise reduction

algorithms and the number of samples lost depends on the noise reduction algorithm used.

5.4 Comparisons of Spectrograms using ETSI AFE vs. STSA WE

In Section 5.2 it has been shown that the SE algorithm STSA WE produces higher average PESQ scores than the pre-processing stages of the ETSI AFE algorithm, the ANS algorithm and the IWF algorithm when processing the noisy speech signals from test set A, B and C of the Aurora-2 database. In this subsection the ETSI AFE pre-processing is compared to the STSA WE algorithm with the goal of providing explanations to the significant better PESQ performance produced by the STSA WE algorithm. As the average PESQ score is slightly better at the output of the *noise reduction* block, i.e. at the 2^{nd} stage Wiener filter, than at the other preprocessing stages of the ETSI AFE algorithm, it has been chosen to compare speech signals from the output of the *noise reduction* block in the ETSI AFE to speech signals processed by the STSA WE algorithm.

The comparison is carried out by choosing a speech signal representative of the Aurora-2 database and plotting the time waveforms and spectrograms, when the signal is clean, when adding noise to the clean signal and when the noisy speech signal has been processed by the *noise reduction* block of the ETSI AFE algorithm and the STSA WE algorithm, separately. It has been chosen to use the female utterance of the digits 3082 from test set A of the Aurora-2 database, where subway noise at 5 dB SNR is added. The SNR at 5 dB has been chosen, as it has been observed in Section 5.2 that the difference in average PESQ scores produced by the STSA WE algorithm and the preprocessing stages of the ETSI AFE algorithm increases as the SNR level decreases. The difference in the spectrograms for the denoised speech signal processed by the STSA WE algorithm and the *noise reduction* block of the ETSI AFE algorithm, might therefore appear more visible at this SNR level. In Figure 5.4a the time waveforms are shown and in Figure 5.4b the corresponding spectrograms are shown. The spectrograms are computed by the use of a Hamming window in order to avoid the sidelobe effect introduced when using a rectangular window [16]. Furthermore a 50% overlap is used between adjacent windows and the window length corresponds to 20 ms, which is commonly used in speech processing applications [16].

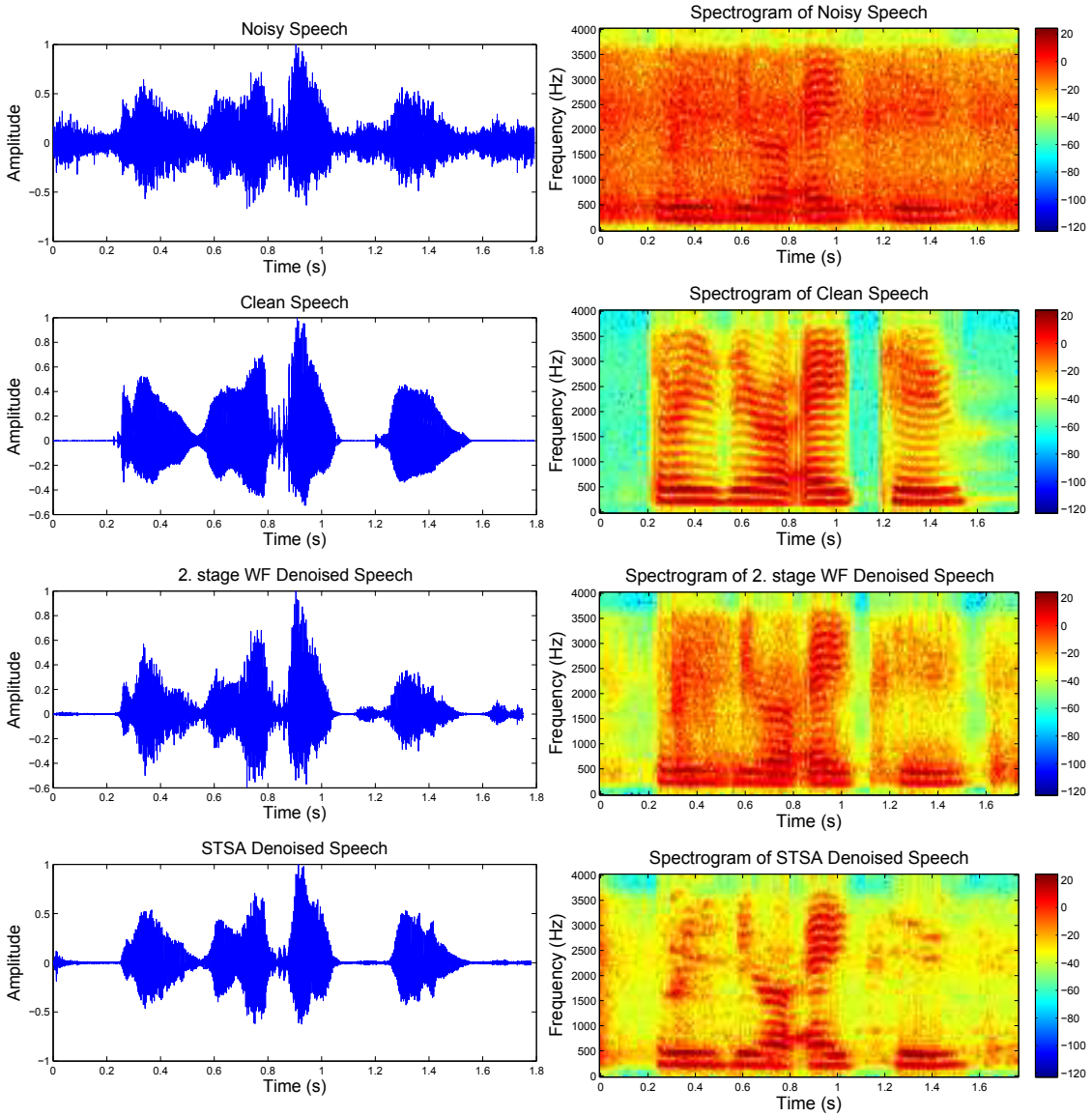

(a) Time waveforms of the female utterance of the digits 3082 from test set A of the Aurora-2 database.

(b) Spectrograms of the female utterance of the digits 3082 from test set A of the Aurora-2 database.

Figure 5.4: Time waveforms and spectrograms of the female utterance of the digits 3082 from test set A of the Aurora-2 database for the speech signal with additive subway noise, the clean speech signal, the noisy speech signal processed by the *noise reduction* block of the ETSI AFE algorithm and the noisy speech signal processed by the STSA WE algorithm.

Both the spectrogram of the 2nd stage Wiener filter denoised speech and the spectrogram of the STSA WE denoised speech shows significant noise reduction. However, the STSA WE algorithm is more aggressive than the *noise reduction* block of the ETSI AFE algorithm. This difference in aggressiveness is observed in the time interval 0.2 s to 1 s and in the frequency interval 1000

Hz to 3500 Hz in Figure 5.4b. This behaviour has been observed for multiple tested speech signals of the Aurora-2 database. We deduce from this observation that the difference in SE performance can be explained by the aggressiveness of the algorithms.

5.5 Adjustment of Aggressiveness

In Section 5.4 the ETSI AFE algorithm and the STSA WE SE algorithms have been compared by spectrograms of speech signals from the Aurora-2 database. The results showed that the algorithms differ in their aggressiveness of applying noise reduction. In this subsection it is considered to investigate the impact on the word recognition accuracy using the ETSI AFE algorithm with test set A, B and C from the Aurora-2 database, the average PESQ score and the average STOI score of the time-domain signal at the output of the *waveform processing* block, when increasing the aggressiveness of the ETSI AFE algorithm. A time-domain signal is required to compute the PESQ and STOI scores and it have been chosen to compute the STOI and PESQ scores from the time-domain signals at the output of the *waveform processing* block as it is desired to extract the time-domain signals from within the ETSI AFE algorithm as late as possible to get a fair impression of the word accuracy vs. PESQ and word accuracy vs. STOI relationships.

The aggressiveness of the ETSI AFE is adjusted in the *gain factorization* block of the 2^{nd} stage Wiener filter, which is described in Subsection 3.1.1.1. The *gain factorization* block varies the level of aggression from 10 % (during speech frames) to 80 % (during pure noise frames). The level of aggression applied by the Wiener filter is therefore higher during pure noise frames [7]. The aggression during the speech frames is increased and the impact on the word accuracy vs. the average PESQ scores and the word accuracy vs. the average STOI scores are considered.

In Figure 5.5 the word accuracy and the PESQ score averaged across SNRs -5-20 dB for speech signals from test set A, B and C of the aurora-2 database are plotted as a function of the aggressiveness of the speech frames, which has been varied between 10 % and 70 % with an interval of 10 %. As expected, the word accuracy decreases and the average PESQ measure increases as the aggressiveness applied to the speech frames increases. The increase of PESQ measure is very small and still below the PESQ measure obtained using the STSA WE algorithm, but it supports the concept of improving ETSI AFE for SE by introducing more aggressive noise reduction.

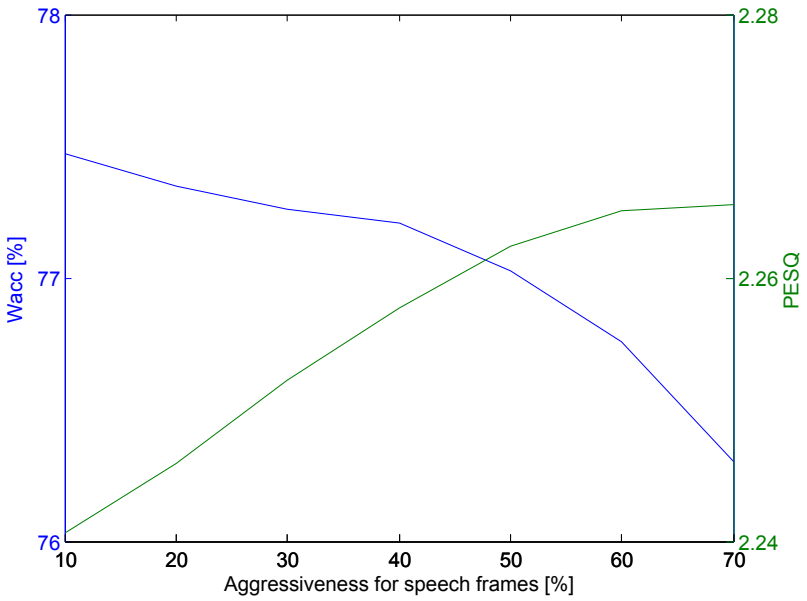

Figure 5.5: The word recognition accuracy in percentage averaged across SNRs -5-20 dB for the speech data from test set A, B and C of the Aurora-2 database and the corresponding average PESQ score averaged across SNRs -5-20 dB from the output of the *waveform processing* block as a function of the aggressiveness of the noise reduction during speech frames of the 2nd stage Wiener filter in the ETSI AFE algorithm.

In Figure 5.6 the word accuracy and the STOI score averaged across SNRs -5-20 dB for speech signals from test set A, B and C of the aurora-2 database are plotted as a function of the aggressiveness of the noise reduction during speech frames. Speech signals with less than 30 speech frames at the output of the *waveform processing* block are excluded from the STOI and word accuracy results shown in Figure 5.6. It can be observed that as the aggressiveness increases, there is small decrease of both the word accuracy and the average STOI score. Consequently, introducing improved speech quality for the speech signals processed by the ETSI AFE algorithm, has the cost of reducing speech intelligibility. This can be explained by the fact that increasing the aggressiveness and reducing the level of background noise causes speech distortion, which has an impact on speech intelligibility.

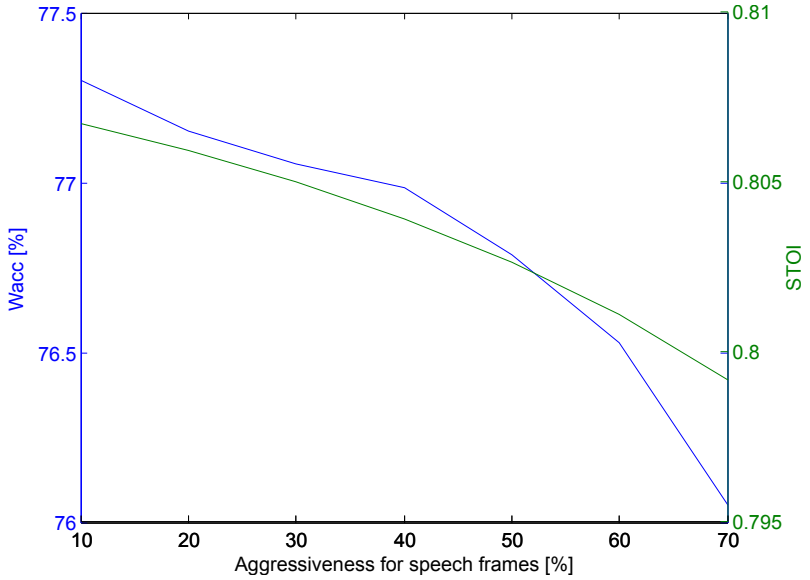

Figure 5.6: The word recognition accuracy in percentage averaged across SNRs -5-20 dB for the speech data from test set A, B and C of the Aurora-2 database and the corresponding average STOI score averaged across SNRs -5-20 dB from the output of the *waveform processing* block as a function of the aggressiveness of the noise reduction during speech frames of the 2nd stage Wiener filter in the ETSI AFE algorithm.

5.6 Discussion

In this chapter the SE performances of the noise reduction stages within the ETSI AFE have been explored. Comparison of the speech quality as measured by PESQ for the noise reduction stages of the ETSI AFE algorithm to the ANS, the IWF and the STSA WE algorithm, has produced the following observations. The 1st and 2nd stage Wiener filters contribute to improved PESQ scores with respect to noisy speech data, although the contribution of the 1st stage Wiener filter far exceed that of the 2nd stage. Unexpectedly, the ETSI AFE stages significantly outperform the IWF and ANS, particularly at the lower SNR levels. This is unanticipated as IWF and ANS have been designed for human listeners using characteristics of speech production and auditory perception, respectively. The only exception to this is the *waveform processing* block which significantly degrades speech quality as measured by PESQ at high SNRs. This can be explained by the low energy segments of the speech signal being suppressed in the absent of noise or at low noise levels. However, in terms of PESQ the ETSI AFE stages are outperformed by the STSA WE algorithm at all SNR levels. The difference is less noticeable at high SNRs, but becomes more substantial at lower SNRs. In examining the corresponding human speech intelligibility as estimated by STOI, the noise reduction stages of ETSI AFE maintain the intelligibility of the noisy speech signals. In fact ETSI AFE manages to slightly improve the STOI measure at times. Similarly to the PESQ performance measurements, the *waveform processing* block is an exception degrading the STOI score at high SNRs. Unlike the PESQ measurements, the ETSI

AFE stages tends to outperform each of the ANS, the IWF and the STSA WE algorithms, which degrade the STOI score at all SNRs with respect to the noisy speech. It is not unusual for SE algorithms designed for human receivers to sacrifice speech intelligibility for improvement of speech quality [16]. This seems to be the case for the ANS, the IWF and the STSA WE algorithms in terms of PESQ and STOI scores. The authors did not hear anything that contradicted this when listening to a small number of speech signals enhanced by the different algorithms considered in this chapter at different SNRs. Human listeners are exceptional at recognizing speech and speech intelligibility does not typically become an issue unless the speech signal is severely degraded. Thus improving speech quality is often considered more important than improving speech intelligibility. The ETSI AFE stages preserve the speech intelligibility and associated with that they show a less aggressive noise reduction performance than the STSA WE algorithm. Machine recognisers are not nearly as proficient as humans at recognizing speech, thus it suggests that it is more important to preserve minor details that can help the recognisers to transcribe the speech correctly. Increasing the noise reduction aggressiveness of the ETSI AFE has caused both the recogniser performance and the STOI measurements of the denoised speech signal to decrease. However, the PESQ measurements increases along with the aggressiveness. These relationships are of significant interest, as they indicate that some correlation between the measures exists, although it is too early to tell if it is limited to ETSI AFE.

ASR using Speech Enhancement Pre-processing Methods 6

The overall objective of this chapter is to study if that the ETSI AFE algorithm feature extraction standard designed for ASR provide higher ASR performance than when utilizing speech enhancement algorithms designed for human receivers to pre-process the noisy speech data for ASR as reported by [14]. The ASR results presented in this chapter have been generated by the use of the speech data from the Aurora-2 database [26]. The SE algorithms designed for human listeners considered in the thesis are used: The audible noise suppression (ANS) algorithm [16], the iterative Wiener filtering (IWF) algorithm [16] and the short-time spectral amplitude (STSA) estimator using the weighted euclidean (WE) distortion measure [16].

First, the ASR results using the ETSI AFE feature extraction standard are provided and the contribution of the stages composing this feature extraction algorithm are evaluated. Then the ASR performance using SE algorithms designed for human listeners for pre-processing of the noisy speech data is investigated and compared to the ETSI AFE algorithm designed for speech recognition. In Chapter 5 it has been found that the STSA WE algorithm differed from the ETSI AFE algorithm by the amount of aggressiveness applied by the denoising process, where the ETSI AFE algorithm is less aggressive. In this chapter the aggressiveness of a SE algorithm designed for human listener is reduced with the expectation of observing an improvement in the ASR performance. Finally, the ASR performance of the ETSI AFE algorithm and the STSA WE algorithm is compared by removing the silence frames of the speech signals using reference VAD labels, such that only the performance at the speech regions are compared. This is done to investigate the contribution of the errors provided by the noisy-only regions of the speech signals.

In this chapter recognisers are used with acoustic models trained with clean speech signals and acoustic models trained with multi-condition (clean and noisy) speech signals, which

is referred to as *clean* training mode and *multi-condition* training mode, respectively. In Appendix A the settings are shown for the feature extraction process, the recognition process, the Aurora-2 database and the SE algorithms, which have been used to produce the results presented in this chapter. Furthermore, an overview of the Matlab implementations of the SE methods for human listeners used are provided by Appendix B.

6.1 ASR Results

In this subsection the ASR performance is evaluated in terms of word accuracy when the noisy speech signals from test set A, B and C of the Aurora-2 database are preprocessed by a SE algorithm either designed for ASR or human listeners. Performance is evaluated in terms of word accuracy as it takes into account the three error types experienced in speech recognition, which are called substitutions, deletions and insertions as described in Section 3.3.

The ETSI AFE algorithm is the feature extraction standard considered for speech recognition in this thesis, which carries out noise reduction in the preprocessing stages on noisy input speech data [7]. The contribution of the blocks processing the input speech data within the ETSI AFE are investigated within this subsection in terms of ASR performance. This is carried out by extracting denoised time-domain speech signals at selected locations in the ETSI AFE algorithm and using the basic ETSI MFCC-based front end (FE) [6] for feature extraction, which generates MFCCs without noise reduction and subsequent blind equalization done by ETSI AFE. Finally speech recognition is performed for all the speech data extracted at the selected locations within the ETSI AFE algorithm. Because it is required that the selected signals of the ETSI AFE algorithm are time-domain signals before being processed by the basic FE algorithm, the extraction takes place as described in Section 5.1 (see Figure 5.1 and 5.2).

The ASR results obtained, when pre-processing the noisy input speech data by SE algorithms designed for human listeners followed by feature extraction by the basic ETSI MFCC-based front end, are compared to the ASR results obtained when performing feature extraction by the ETSI AFE algorithm. The state-of-the-art SE algorithms considered in thesis are used: ANS, IWF and STSA WE.

In Table 6.1 the word accuracies averaged for SNRs are shown in percentage for the speech data from test set A, B and C of the Aurora-2 database and for different types of SE algorithm, when the training mode is *clean*. The 1^{st} stage Wiener filter gives the most contribution to the improved word accuracy performance with respect to the basic ETSI MFCC-based FE in comparison to the other preprocessing stages of the ETSI AFE algorithm. Especially at SNR levels 0 dB to 10 dB, the 1^{st} stage Wiener filter provides significant improvements. The 2^{nd} stage Wiener filter improves the average word accuracy slightly at all SNR levels, which can be explained by the fact that the 2^{nd} stage Wiener filter removes residual noise as the 1^{st} stage Wiener filter produces inaccurate noise spectrum estimates [27]. The *waveform processing*

SNR	FE	1st Stage WF	2nd Stage WF	Waveform Processing	AFE	ANS	IWF	STSA WE
Clean	99.1533	98.7900	99.2050	98.9450	99.2367	98.5233	98.5017	99.2267
20 dB	96.4383	97.9992	98.1000	97.9250	98.0642	89.5700	82.7283	95.1300
15 dB	91.3433	96.5525	96.6900	96.5875	96.6142	80.1267	72.5208	91.1508
10 dB	76.5433	91.9733	92.7942	92.6600	93.0692	64.1308	59.1542	82.5350
5 dB	49.4983	80.6408	82.1950	82.9192	84.4242	40.8808	40.7833	65.9742
0 dB	22.7058	55.7517	57.9267	59.2325	62.2867	20.0400	21.5883	41.2375
-5 dB	10.6667	25.5125	26.3167	27.3633	30.3817	10.8342	11.7775	19.0933

Table 6.1: Word recognition accuracies [%] averaged for SNRs of noisy speech from test set A, B and C of the Aurora-2 database and different types of SE algorithms in *clean* training mode.

block of the ETSI AFE algorithm improves the average word accuracy slightly at SNR levels -5 dB to 5 dB compared to the 2nd stage Wiener filter. The *waveform processing* blocks attempts to increase the overall SNR level of the input speech signals by increasing the energy of high-energy periods and decreasing it for low-energy ones. This suggests that the *waveform processing* block has less impact on the speech recognition performance when processing speech signals of high SNR levels, because in the absent of noise it might inadvertently lower the energy of the speech signals. Using the entire ETSI AFE algorithm improves the word accuracy further at all SNR levels, which can be explained by the inclusion of blind equalisation of the speech features. This improves the word accuracy by reducing distortion in the cepstral domain. It can be observed that the ANS algorithm, the IWF algorithm and the STSA WE algorithm, which are the SE algorithms designed for human listeners, show significant lower word accuracies than the ETSI AFE algorithm. The word accuracies provided by the ANS and the IWF algorithms are similar or lower than the word accuracy of the basic ETSI MFCC-based FE algorithm. The IWF shows the worst average word accuracy results at most SNR levels, which can be explained by the fact that it is the only algorithm of Table 6.1 that uses a non-adaptive noise power spectrum estimate at all speech frames, see Section 4.4. In Section 5.5 it has been revealed that a difference between SE algorithms applied to speech recognition and SE algorithms for human listeners is that the SE algorithms are more aggressive in noise reduction. Therefore the lower word accuracy results of the SE algorithms used for human listeners suggests that they are too aggressive.

In Table 6.2 the word accuracies averaged for noise types are shown, when *clean* training mode is used. The average word accuracy across all noise conditions reveals that all the subsequent stages after the 1st stage Wiener filter in the ETSI AFE algorithm contribute to improving recognition performance. It can be observed that the word accuracy is worse for the noise conditions babble and restaurant when using the ETSI AFE algorithm. However, it provides the best word accuracy results for the car noise condition. Similar behaviour can be observed for the PESQ and STOI scores after the preprocessing stages of the ETSI AFE algorithm shown in Section 5.2 and 5.3. It is suspected that it is due to that the car noise is a stationary

Noise Condition	FE	1st Stage WF	2nd Stage WF	Waveform Processing	AFE	ANS	IWF	STSA WE
Subway	62.2767	74.8383	77.0733	76.1333	79.3117	51.0133	48.9833	69.5617
Babble	51.4367	70.8517	71.6517	70.3383	74.1083	54.5167	50.1167	59.7550
Car	56.8433	80.4050	80.1717	82.5033	81.2550	53.4617	51.6750	71.0067
Exhibition	61.4317	78.4733	78.6500	80.6817	79.3267	48.4950	46.4517	65.2950
Restaurant	53.7150	70.4333	71.8500	70.7167	73.7633	54.4250	49.2883	57.8100
Street	58.3133	76.0117	76.3400	78.2900	78.3350	49.5167	46.8000	65.6683
Airport	54.7233	75.8550	77.3150	76.5283	78.9233	57.0833	52.7050	63.7133
Train-Station	54.3650	78.3017	78.9767	80.0467	79.9600	54.5967	53.2650	67.8650
Subway (MIRS)	59.9067	72.0400	73.5933	73.1217	76.1950	47.8917	43.9000	69.2033
Street (MIRS)	60.7367	73.8050	74.4150	75.9467	76.1533	46.6367	45.0100	65.5800
Average	57.3748	75.1015	76.0037	76.4307	77.7332	51.6637	48.8195	65.5458

Table 6.2: Word recognition accuracies [%] averaged for noise conditions of noisy speech from test set A, B and C of the Aurora-2 database and different types of SE algorithms in *clean* training mode.

noise condition and babble and restaurant are non-stationary noise conditions. The IWF and the ANS algorithms show similar or lower average word accuracy than the basic ETSI MFCC-based FE algorithm at all noise conditions. The IWF provides the worst word accuracy results compared to the other algorithms, but at the car noise condition the IWF performs similar to the ANS algorithm. This can be explained by the fact that the car noise is a stationary noise condition, which is more advantageous for the IWF as it uses a non-adaptive noise power spectrum estimate for all speech frames. The STSA WE provides significantly better word accuracy results than both the ANS and the IWF algorithm. The STSA WE algorithm provide the worse word accuracy results at the noise conditions babble, restaurant and airport, which can also be explained by the non-stationary segments. Furthermore the average word accuracies for test set C (subway (MIRS) and street (MIRS)) with additional frequency weighting are as expected lower for all algorithms when compared to the corresponding results without spectral modifications.

SNR	FE	1st Stage WF	2nd Stage WF	Waveform Processing	AFE	ANS	IWF	STSA WE
Clean	98.7833	97.7100	99.0333	98.6083	99.1783	97.9083	97.6350	98.6650
20 dB	97.7092	98.5033	98.5108	98.3808	98.5675	96.5600	95.0617	97.9350
15 dB	96.7575	97.6750	97.7750	97.5975	97.8650	94.9567	91.8933	97.1958
10 dB	94.3167	95.8367	95.7917	95.5667	96.0625	90.3508	85.2892	94.9833
5 dB	86.6100	89.6625	89.8758	89.4692	90.7917	79.7775	71.9917	88.1875
0 dB	59.7967	70.6158	70.8692	70.8475	74.6308	53.2033	49.1125	69.3358
-5 dB	24.8033	34.9058	36.0217	37.1400	40.7267	22.2233	22.2658	33.5225

Table 6.3: Word recognition accuracies [%] averaged for SNRs of noisy speech from test set A, B and C of the Aurora-2 database and different types of SE algorithms in *multi-condition* training mode.

In Table 6.3 the word accuracies averaged for SNRs are shown in percentage for the speech data from test set A, B and C of the Aurora-2 database and for different types of SE algorithms, when using a *multi-condition* trained recogniser. The word accuracies are better for all algorithms at all SNR levels compared to the *clean* training mode. Especially at the lower SNR levels, -5 dB and 0 dB, significant improvement can be observed. These results confirm the advantage of training using the noise characteristics as part of the word models.

Noise Condition	**FE**	**1st Stage WF**	**2nd Stage WF**	**Waveform Processing**	**AFE**	**ANS**	**IWF**	**STSA WE**
Subway	79.0750	82.0433	81.7417	81.2717	84.2433	70.5367	68.8283	82.2517
Babble	78.0517	78.8650	80.0983	80.9133	80.8950	74.3750	72.2400	79.1517
Car	75.4733	86.5683	86.0617	86.8217	86.5300	75.4933	78.7700	82.2450
Exhibition	77.6467	83.9100	84.3517	84.5367	84.9233	76.8283	73.2650	82.1800
Restaurant	76.8983	78.6100	79.9583	80.8833	80.6783	72.2133	69.1233	76.0367
Street	78.5733	82.1700	82.4433	82.7150	83.6150	72.1833	68.0517	80.3350
Airport	79.4000	83.4633	83.9950	84.3767	85.0233	75.1467	73.1583	80.8383
Train-Station	75.3983	84.2583	84.4850	85.2050	84.7700	75.0333	76.1483	81.4583
Subway (MIRS)	74.0750	77.8067	77.6317	76.2933	81.8250	69.8450	61.9883	80.7333
Street (MIRS)	75.6600	79.4483	79.6450	79.3467	81.4800	71.3217	63.8333	78.1783
Average	77.0252	81.7143	82.0412	82.2363	83.3983	73.2977	70.3407	80.3408

Table 6.4: Word recognition accuracies [%] averaged across noise conditions of noisy speech from test set A, B and C of the Aurora-2 database and different types of SE algorithms in *multi-condition* training mode.

In Table 6.4 the word accuracies averaged for noise conditions, when *multi-condition* training mode is used. Even though that the noise types from test set A (subway, babble, car and exhibition) have been used for *multi-conditioned* training, the word accuracy results for the noise type of test set B (restaurant, street, airport and train) do not provide notable worse results than the noisetypes from test set A for any of the algorithms in Table 6.2. It can be observed that the word accuracies provided by the ANS algorithm, the IWF algorithm and the STSA WE algorithm are significantly improved compared to *clean* training mode. The ETSI AFE provides a smaller improvement with respect to the results using *clean* training mode, which confirms that the ETSI AFE algorithm is more noise robust for speech recognition.

6.2 Adjustment of Aggressiveness

In Section 5.5 it has been revealed that a difference between the performance of the pre-processing stages of the ETSI AFE and the STSA WE algorithm is that the STSA WE algorithm is more aggressive than the pre-processing stages of the ETSI AFE algorithm in regards to noise reduction. In Section 6.1 it has been shown that the SE algorithms designed for human listeners (ANS, IWF and STSA WE) considered in this thesis provide worse word recognition accuracies than the ETSI AFE algorithm. Therefore it is desired to investigate the ASR performance when decreasing the aggressiveness of the STSA WE algorithm. The aggressiveness can be decreased

by changing the power exponent p of the STSA WE algorithm. As described in Subsection 4.3.1, large and positive values of p provide small attenuation, whereas large and negative values of p provide larger attenuations. The ASR results of the STSA WE algorithm presented in Section 6.1 have been obtained by the use of the power exponent $p = -1$. This means that in order to decrease the aggressiveness in terms of noise reduction, the value of p has to be increased.

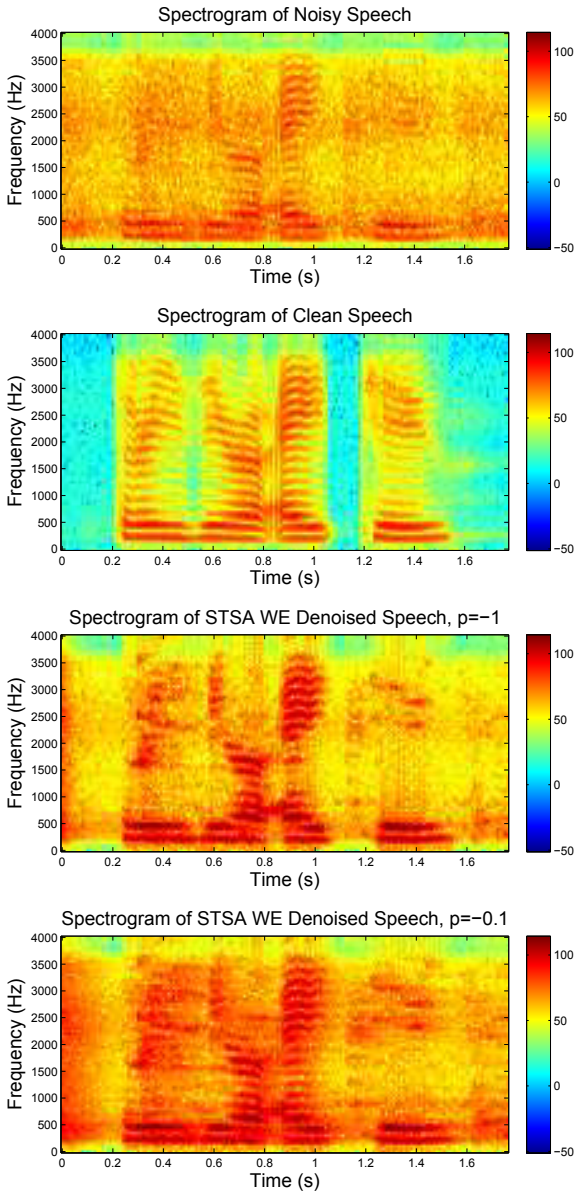

Figure 6.1: Spectrograms of the female utterance of the digits 3082 from test set A of the Aurora-2 database for the speech signal with additive subway noise, the clean speech signal, the noisy speech signal processed by the STSA WE algorithm for $p = -1$ and $p = -0.1$.

In Figure 6.1 an example is provided of how the aggressiveness of the STSA WE algorithm is reduced in terms of noise reduction by increasing the value of the power exponent p. It has been chosen to use the female utterance of the digits 3082 from test set A of the Aurora-2

database, where subway noise at 5 dB SNR is added. Spectrograms are showed for the clean signal, the noisy signal and the noisy signal processed by the STSA WE algorithm for $p = -1$ and $p = -0.1$. The spectrograms are computed by the use of a Hamming window in order to avoid sidelobes. An overlap of 50% is used between adjacent windows and a window length corresponding to 20 ms, as is commonly used in speech processing applications [16]. The spectrogram for the noisy speech signal processed by the STSA WE algorithm for $p = -0.1$ shows less aggressiveness at the time interval 0.2 s to 1 s and in the frequency interval 500 Hz to 3500 Hz, than the spectrogram for the noisy speech signal processed by the STSA WE algorithm for $p = -1$. Similar behaviour has been observed for multiple tested speech signals of the Aurora-2 database. Therefore it has been chosen to generate ASR results with variations of the power exponent p of the STSA WE algorithm, where it is expected to observe improvement in terms of word accuracy when p is increased thus lowering the aggressiveness. It is only the *clean* training mode that is considered, as the difference between the ETSI AFE algorithm and the STSA WE algorithm is less pronounced in *multi-conditioned* training as this does not depend as much on the denoising process as shown in Section 6.1.

SNR	**FE**	**AFE**	**STSA WE p=-1**	**STSA WE p=-0.3**	**STSA WE p=-0.1**
Clean	99.1533	99.2367	99.2267	99.2133	99.2133
20 dB	96.4383	98.0642	95.1300	96.7167	96.9592
15 dB	91.3433	96.6142	91.1508	93.5825	94.0367
10 dB	76.5433	93.0692	82.5350	85.8950	86.2808
5 dB	49.4983	84.4242	65.9742	69.9733	70.2542
0 dB	22.7058	62.2867	41.2375	44.9000	44.0825
-5 dB	10.6667	30.3817	19.0933	19.3608	18.3750

Table 6.5: Word recognition accuracies [%] averaged for SNRs of noisy speech from test set A, B and C of the Aurora-2 database and different types of SE algorithms in *clean* training mode. Word accuracy results are shown for the STSA WE algorithm, when its power exponent p is varied.

It Table 6.5 the word accuracy results averaged for SNRs are shown for the basic ETSI MFCC-based FE algorithm, the ETSI AFE algorithm and the STSA algorithm with $p = -1$, $p = -0.3$ and $p = -0.1$. Noisy speech signals from test set A, B and C of the Aurora-2 database have been used. It can be observed that increasing the power exponent p from -1 to -0.3 increases the word accuracy results at all tested SNR levels, from -5 dB to 20 dB. Furthermore the average word accuracies increases slightly at SNR levels 5 dB to 20 dB when the power exponent p is increased from -0.3 to -0.1. However, the optimal value of p seems to be SNR dependent, where a high value of p appears beneficial for high SNRs, while at low SNRs a smaller value of p is useful. In Table 6.6 the corresponding word accuracy results averaged for noise conditions are shown. Improvement of average word accuracy can be observed at most noise types when

increasing the value of the power exponent p of the STSA WE algorithm, except for the babble and restaurant noise types which can be explained by the fact that they contain non-stationary noise components. Even though improvement in word accuracy can be observed for most noise type averages in Table 6.6 for the STSA WE algorithm when the power exponent p is increased, the ETSI AFE algorithm is still significant better. Testing power exponents $p > 0$ revealed no further improvement of the average word accuracies.

Noise Condition	**FE**	**AFE**	**STSA WE p=-1**	**STSA WE p=-0.3**	**STSA WE p=-0.1**
Subway	62.2767	79.3117	69.5617	71.6050	71.0683
Babble	51.4367	74.1083	59.7550	58.6167	58.3550
Car	56.8433	81.2550	71.0067	75.0817	75.2617
Exhibition	61.4317	79.3267	65.2950	68.5217	69.1367
Restaurant	53.7150	73.7633	57.8100	57.4033	57.8233
Street	58.3133	78.3350	65.6683	68.7767	69.4800
Airport	54.7233	78.9233	63.7133	64.0283	64.0833
Train-Station	54.3650	79.9600	67.8650	70.2000	70.4650
Subway (MIRS)	59.9067	76.1950	69.2033	73.1250	71.6400
Street (MIRS)	60.7367	76.1533	65.5800	70.1867	70.5117
Average	57.3748	77.7332	65.5458	67.7545	67.7825

Table 6.6: Word recognition accuracies [%] averaged for noise conditions of noisy speech from test set A, B and C of the Aurora-2 database and different types of SE algorithms in *clean* training mode. Word accuracy results are shown for the STSA WE algorithm, when its power exponent p is varied.

6.3 Frame Dropping by the use of Reference VAD Labels

The ETSI AFE algorithm includes a VAD algorithm, which is used to mark each 10 ms frame in a speech signal as either speech or non-speech. As described in Subsection 3.1.1.1, this decision is based on an energy criterion which is a fixed threshold. This information can optionally be used for frame dropping at the recogniser [33]. This can considerably reduce insertion errors in any pauses between the spoken words, particularly in noisy utterances.

In this section the ETSI AFE and the STSA WE algorithms are compared in terms of word recognition accuracy when frame dropping is applied. This is applied, since it can provide insight into if it is the silence regions that causes the significant lower word accuracy results for the STSA WE algorithm during *clean* training as shown in Section 6.1.

Frame dropping is applied by the use of frame-by-frame reference VAD labels for both the training set and test set A, B and C of the Aurora-2 database, which have been generated from forced-alignment speech recognition experiments and is used as a "ground truth" [34, 35]. In these reference VAD labels, '0' and '1' denote the silence and speech frames, respectively. In

Section 6.2 it has been observed that increasing the power exponent p from -1 to -0.1 in the STSA WE algorithm, reduces the aggressiveness and increases the average word recognition accuracies. Therefore it has been chosen to apply frame dropping with the reference VAD labels using the STSA WE algorithm with both the $p = -0.3$ and $p = -0.1$, to see if the word accuracy improves with respect to $p = -1$.

In Table 6.7 the word accuracies in percentage are shown averaged across for SNRs of the speech data from test set A, B and C of the Aurora-2 database. The results are shown for the ETSI AFE algorithm and the STSA WE algorithm for $p = -0.3$ and $p = -0.1$ with and without frame dropping. The word accuracy results for the basic ETSI MFCC-based FE algorithm and the STSA WE algorithm for $p = -1$ without frame dropping are included too as references. It can be observed that the ETSI AFE algorithm only experience a small increase in word accuracy results at SNR levels -5 dB to 15 dB when applying frame dropping. Applying frame dropping for the STSA WE algorithm at $p = -0.3$ and $p = -0.1$, however, provides a larger increase in average word accuracy at the SNR levels -5 dB to 15 dB. Therefore a lot of errors introduced by the STSA WE algorithm occur in the noise-only regions. But the AFE is still better, when considering only the speech regions.

SNR	**FE**	**AFE**	**AFE VAD**	**STSA WE p=-1**	**STSA WE p=-0.3**	**STSA WE p=-0.3 VAD**	**STSA WE p=-0.1**	**STSA WE p=-0.1 VAD**
Clean	99.1533	99.2367	99.1583	99.2267	99.2133	99.2233	99.2133	99.2233
20 dB	96.4383	98.0642	98.0550	95.1300	96.7167	96.9283	96.9592	97.5400
15 dB	91.3433	96.6142	96.8175	91.1508	93.5825	94.5100	94.0367	95.3017
10 dB	76.5433	93.0692	93.3042	82.5350	85.8950	88.6525	86.2808	89.2883
5 dB	49.4983	84.4242	84.9717	65.9742	69.9733	76.1142	70.2542	76.5850
0 dB	22.7058	62.2867	63.2933	41.2375	44.9000	54.8400	44.0825	54.7817
-5 dB	10.6667	30.3817	32.0992	19.0933	19.3608	28.6600	18.3750	28.6492

Table 6.7: Word recognition accuracies [%] averaged for SNRs of noisy speech from test set A, B and C of the Aurora-2 database and different types of SE algorithms in *clean* training mode. Additionally, word accuracy results are shown for the 1st stage Wiener filter algorithm, the AFE algorithm and the STSA WE algorithm, when silence frames have been removed by the use of the reference VAD labels.

In Table 6.8 the word accuracy results are shown averaged for noise conditions corresponding to Table 6.7. There it can be observed that at the noise conditions babble and restaurant, which contain non-stationary segments, the STSA WE algorithm provides large improvement with frame dropping by the use of the reference VAD labels for both $p = -0.3$ and $p = -0.1$. At these noise conditions the improvement is significantly smaller for the ETSI AFE algorithm with frame dropping by the use of the reference VAD labels. However, at the more stationary noise condition, car, the STSA WE experience a significant smaller improvement in word

accuracy than for the non-stationary noise conditions for both $p = -0.3$ and $p = -0.1$ with frame dropping using reference VAD labels. These observations therefore suggest that it is more challenging to improve word accuracy at the non-stationary noise conditions using the STSA WE algorithm, where more errors occur in the noise-only regions of the speech signals.

Noise Condition	**FE**	**AFE**	**AFE VAD**	**STSA WE p=-1**	**STSA WE p=-0.3**	**STSA WE p=-0.3 VAD**	**STSA WE p=-0.1**	**STSA WE p=-0.1 VAD**
Subway	62.2767	79.3117	79.2600	69.5617	71.6050	75.7883	71.0683	75.8450
Babble	51.4367	74.1083	77.6750	59.7550	58.6167	68.5683	58.3550	69.1200
Car	56.8433	81.2550	79.4350	71.0067	75.0817	77.9933	75.2617	77.8400
Exhibition	61.4317	79.3267	79.2867	65.2950	68.5217	71.5350	69.1367	72.3133
Restaurant	53.7150	73.7633	78.2833	57.8100	57.4033	68.0900	57.8233	68.8450
Street	58.3133	78.3350	78.2150	65.6683	68.7767	72.8683	69.4800	73.4533
Airport	54.7233	78.9233	80.9917	63.7133	64.0283	72.2383	64.0833	72.7250
Train-Station	54.3650	79.9600	80.3550	67.8650	70.2000	76.1283	70.4650	76.1467
Subway (MIRS)	59.9067	76.1950	75.8317	69.2033	73.1250	75.4017	71.6400	75.4700
Street (MIRS)	60.7367	76.1533	75.9583	65.5800	70.1867	72.6983	70.5117	73.5317
Average	57.3748	77.7332	78.5292	65.5458	67.7545	73.1310	67.7825	73.5290

Table 6.8: Word recognition accuracies [%] averaged for noise conditions of noisy speech from test set A, B and C of the Aurora-2 database and noise reduced speech in *clean* training mode. Additionally, word accuracy results are shown for the 1st stage Wiener filter algorithm, the AFE algorithm and the STSA WE algorithm, when silence frames have been removed by the use of the reference VAD labels.

6.4 Discussion

In this chapter it has been verified that the recognition performance of the ETSI AFE feature extraction algorithm is superior to the recognition performance achieved by using SE algorithms for feature pre-processing, as reported by [14]. Exploring the recognition performance of the ANS, IWF and STSA WE SE algorithms compared to the ETSI AFE algorithm, the following observations have been made. The recognition performance evaluated in terms of word accuracy, is significantly larger for the ETSI AFE algorithm than when applying the ANS, IWF and STSA WE algorithms using a recogniser trained with clean speech data. Comparing the recognition performance of STSA WE to the ANS and IWF algorithms, it is clear that STSA WE performs far better as a feature pre-processing method. Both ANS and IWF show poor results, though the ANS algorithm outperforms the IWF algorithm at medium to high SNRs. Proceeding with the recogniser trained with multi-condition speech data, i.e. clean and noisy speech data, the performances of the ANS, IWF and STSA WE algorithms have been significantly increased. However, recognition performance is also improved for the ETSI AFE algorithm, consequently it remains superior. The performance increase for the ANS, IWF and STSA WE algorithms tends to be larger than the increase

experienced by the ETSI AFE algorithm. This difference can most likely be explained by the ETSI AFE being more robust towards noisy speech data as observed during *clean* training mode. The recognition performance of the STSA WE has been increased by adjusting its power exponent p, which has an influence on the aggressiveness of the applied noise reduction. The most significant increase occurs for reduced aggressiveness at medium SNRs. However, the recognition performance can suffer at low SNRs, if the aggressiveness is reduced too much. The difference of recognition performance between STSA WE and ETSI AFE is further explored by introducing frame dropping using reference VAD labels i.e. dropping the silence frames from the speech signals. Frame dropping increases recognition performance of the STSA WE algorithm regardless of the aggressiveness applied. However, the STSA WE algorithm is still outperformed by the ETSI AFE algorithm even though frame dropping only slightly increases the recognition performance of ETSI AFE. This means that the STSA WE algorithm is more affected by recognition errors in the noise-only regions at low SNRs. This suggest that in order to improve the recognition performance of the STSA WE, it might be reasonable to improve its VAD and noise power spectrum estimation, to allow for better handling of the noise-only regions.

Correlation of ASR and Speech Enhancement Performance Measures

7

In this chapter the correlation between selected ASR performance measures and selected SE performance measures is investigated. In [39] it has been investigated if it is possible to create an estimator of the performance of a speech recognition system using the PESQ measure for various noise reduction algorithms, with positive results. This chapter investigates if such a predictor can be created for the ETSI AFE algorithm using either STOI or PESQ.

It takes a larger computational load to perform speech recognition than computing STOI and PESQ scores for speech signals. Therefore an estimator can be used to enable more rapid configuration during the development phases of ASR systems. It is mostly aimed at development phases as STOI and PESQ both require an original noise free reference signal.

First, the correlation coefficients utilized are presented. These are then used to investigate the feasibility of using denoised signals to estimate the final ASR performance using the ETSI AFE. The denoised signals are extracted after the *waveform processing* block in the ETSI AFE algorithm as shown in Figure 5.1. Next the correlation between the ASR performance measures and SE performance measures of the ETSI AFE is explored, where it is attempted to design an estimator of ASR performance using SE performance measures representing the difference between a denoised speech signal and its original clean version, see Figure 7.1. Finally the correlation between ASR performance measures and STOI/PESQ for the different feature extraction algorithms at fixed SNR levels is explored.

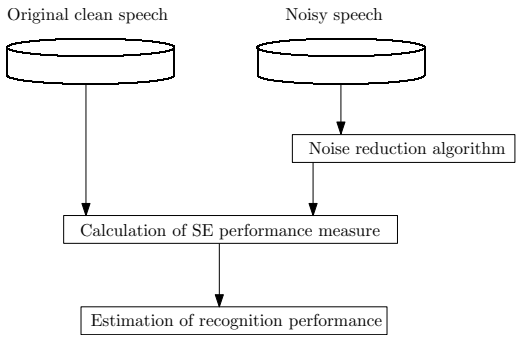

Figure 7.1: Concept of proposed estimator of recognition performance using STOI or PESQ scores.

The noisy speech signals used in this chapter originate from test set A, B and C of the Aurora-2 database. When STOI scores are computed, speech signals with less than 30 speech frames are excluded. It should be noted that speech signals where less than 30 speech frames are located after using any of the feature extraction algorithms considered in this thesis, are excluded. All available test data is used when working with PESQ.

The STOI and PESQ measures are calculated using the denoised speech signals extracted after the *waveform processing* block in the ETSI AFE algorithm. This has been chosen despite the fact that the ETSI AFE algorithm further processes the MFCC in the *blind equalization* stage, as the speech signal would have to be reconstructed from the MFCCs. See Figure 3.2. Given the potential estimation errors of the speech signals reconstructed from MFCCs, this has been rejected.

The basic ETSI FE is used for feature extraction when dealing with speech signals that are already enhanced either by an SE algorithm for human listeners or by the denoising blocks in the ESTI AFE. The basis FE is used for this as it contains the same cepstral calculation blocks as the ESTI AFE without having the feature pre-enhancement blocks the ETSI AFE contains.

In this chapter recognisers are used with acoustic models trained with clean speech signals and acoustic models trained with multi-condition (clean and noisy) speech signals, which is referred to as *clean* training mode and *multi-condition* training mode, respectively. In Appendix A the settings are shown for the feature extraction process, the recognition process, the Aurora-2 database and the SE algorithms, which have been used to produce the results presented in this chapter. Furthermore, an overview of the Matlab implementations of the SE methods for human listeners used are provided by Appendix B. Due to the way the ETSI AFE implementation reports the recognition results there are a limited number of data points as the ASR measures are only meaningful when calculated over a large number of samples. Therefore a total of 70 data points is all that is available.

7.1 Correlation Coefficients

In this section the correlation coefficients utilized in this chapter are presented, specifically the Pearson correlation coefficient, the Spearman rank correlation coefficient and the Kendall Tau rank correlation coefficient. The Pearson correlation coefficient is considered as this is the basic linear and most commonly used correlation coefficient [2]. But we do not assume that the relationships considered are linear. Therefore the Spearman and Kendall correlation coefficients are additionally considered, as they measure the monotonic correlation between two dataset and are also commonly used [2]. The value of the correlation coefficients are within the range [-1, 1], where the magnitude of the coefficient indicates the strength of the correlation. This mean if the correlation coefficient is 0 there is no correlation and if it is 1 there is perfect correlation, while the sign indicates if the correlation is positive or negative [2]. A description of the Pearson, the Spearman and the Kendall correlation coefficients are given in the following subsections.

7.1.1 Pearson Correlation Coefficient

The Pearson correlation coefficient is a measure of the linear correlation between two data sets. Two datasets of raw scores, $\mathbf{x} = [x_1 x_2 \cdots x_N]^{\mathrm{T}}$ and $\mathbf{y} = [y_1 y_2 \cdots y_N]^{\mathrm{T}}$, are considered and are linear transformed into standardizes z-scores, z_{x_i} and z_{y_i} for $i = 1, ..., N$. Each member i of the set of raw scores $\mathbf{x}$ is linear transformed by the use of the following equation:

$$z_{x_i} = \frac{x_i - \bar{x}}{s_x}, \tag{7.1}$$

where $\bar{x}$ is the mean and s_x is the standard deviation of $\mathbf{x}$ given by:

$$\bar{x} = \frac{1}{N}\sum_{i=1}^{N} x_i, \tag{7.2}$$

$$s_x = \sqrt{\frac{1}{N-1}\sum_{i=1}^{N}(x_i - \bar{x})^2}. \tag{7.3}$$

The z-score representing a raw score can be interpreted as the number of standard deviations the raw score is above or below the mean of the distribution. The mean of a complete set of z-scores is zero and both the standard deviation and the variance have a value of 1 [24]. The Pearson correlation coefficient for the two datasets $\mathbf{x}$ and $\mathbf{y}$ is then given by:

$$r_{xy} = \frac{1}{N-1}\sum_{i=1}^{N} z_{x_i} z_{y_i}. \tag{7.4}$$

This correlation coefficient is basically the average of the dot product of the z-scores of $\mathbf{x}$ and $\mathbf{y}$. r_{xy} can be interpreted as a measure of how similar z_{x_i} is to z_{y_i} on average. If there is a perfect positive correlation between $\mathbf{x}$ and $\mathbf{y}$, then $z_{y_i} = z_{x_i}$ for $i = 1, ..., N$, so the correlation is

$$r_{xy} = \frac{1}{N-1}\sum_{i=1}^{N} z_{x_i} z_{y_i} = \frac{1}{N-1}\sum_{i=1}^{N} z_{x_i}^2 = 1. \tag{7.5}$$

If there is a perfect negative correlation, $z_{y_i} = -z_{x_i}$ for $i = 1, ..., N$, then $r_{xy} = -1$ [24]. Equation 7.4 can also be reformulated as the covariance between **x** and **y**, normalized by the product of the standard deviations of **x** and **y**:

$$r_{xy} = \frac{\sum_{i=1}^{N}(x_i - \bar{x})(y_i - \bar{y})}{\sqrt{\sum_{i=1}^{N}(x_i - \bar{x})^2}\sqrt{\sum_{i=1}^{N}(y_i - \bar{y})^2}}. \tag{7.6}$$

This equation can be thought of as an expression of a ratio of how much **x** and **y** vary together compared to how much **x** and **y** vary separately [2]. In summary, the Pearson correlation coefficient is a numerical measure of the degree to which **x** and **y** are linearly related [24].

7.1.2 Spearman Rank Correlation Coefficient

The Spearman rank correlation coefficient is obtained by the use of the Pearson correlation coefficient. Spearman assess the monotonic relationship function between two datasets $\mathbf{x} = [x_1 x_2 \cdots x_N]^{\mathrm{T}}$ and $\mathbf{y} = [y_1 y_2 \cdots y_N]^{\mathrm{T}}$, where a function is said to be monotonic if it is either entirely increasing or decreasing [24].

The raw data is converted into ranking variables. The Spearman correlation coefficient is obtained by applying Pearson on the ranked data. Ranking variables are found by assigning rank 1 to the smallest raw value and rank N to the largest raw value. If there are tied values, all the ranking scores in a group of ties are given the mean of the ranks they would have received had there been no ties. For example, if four scores are tied for the 10^{th} place after the nine largest scores have been ranked, each receives the rank 11.5 (mean of 10, 11, 12 and 13). The next largest score receives a rank of 14 [24].

There exists a simplified expression for computing the Spearman rank correlation coefficient, which takes advantage of the characteristics of ranks. This assumes that no ties exists, therefore the mean and the variance of a set of N ranks are given by $(N+1)/2$ and $N(N+1)/12$, respectively [24]. Substituting these expressions into the Pearson correlation coefficient formula, given by Equation 7.6, yields the following expression of the Spearman rank correlation coefficient [24]:

$$r_s = 1 - \frac{6\sum_{i=1}^{N} d_i^2}{N(N^2-1)}, \tag{7.7}$$

where d_i is the difference between ranks for the i^{th} case. Equation 7.7 only applies if there are no tied ranks as the variance gets reduced when ties are present.

Finally an example of the computation of the Spearman rank correlation coefficient is provided. In Table 7.1 raw data for **x** and **y** are presented with their corresponding rankings and the squared difference between the rankings d_i^2 for the i^{th} case.

x	Rank of x	y	Rank of y	d^2
59	7	89	10	9
55	5	46	6	1
58	6	41	5	1
50	4	22	3	1
8	1	13	2	1
69	8	30	4	16
94	10	69	8	4
33	3	73	9	36
90	9	64	7	4
32	2	1	1	1

Table 7.1: Example of ranking the dataset **x** and **y**.

The Spearman rank correlation coefficient for the data of Table 7.1 is given by:

$$r_s = 1 - \frac{6\sum_{i=1}^{N} d_i^2}{N(N^2-1)} \tag{7.8}$$

$$= 1 - \frac{6 \cdot 74}{10 \cdot 99} \tag{7.9}$$

$$= 0.55 \tag{7.10}$$

7.1.3 Kendall Tau Rank Correlation Coefficient

The Kendall tau rank correlation coefficient also measures the relationship between two datasets **x** and **y** based on their ranks, but with a different approach than Spearman. Kendall depends on the number of agreements and disagreements in rank order when pair of items are considered [24]. It is possible to consider a total of $\frac{1}{2}N(N-1)$ number of pairs. Two observations (x_i, y_i) and (x_j, y_j) are concordant if they are in the same order with respect to each other, i.e

- $x_i < x_j$ and $y_i < y_j$, or if
- $x_i > x_j$ and $y_i > y_j$.

The two observations are discordant if they are in reverse order with respect to each other, i.e.

- $x_i < x_j$ and $y_i > y_j$, or if
- $x_i > x_j$ and $y_i < y_j$.

The two observations are tied if $x_i = x_j$ and/or $y_i = y_j$ [24]. The Kendall tau rank coefficient is the difference between the probability of concordant pairs and the probability of discordant

pairs:

$$\tau = \frac{\text{(number of concordant pairs)} - \text{(number of discordant pairs)}}{\frac{1}{2}N(N-1)}, \tag{7.11}$$

where N is the number of observations in each data set and the denominator is the total number of pairs. Equation 7.11 is only valid when there are no tied ranks [24].

7.2 Impact of Blind Equalization on Correlation Between STOI/PESQ Scores and ASR Results

This section investigates the correlation between the STOI/PESQ scores of denoised speech signals and the corresponding ASR measures obtained using the ETSI AFE feature extraction algorithm. The denoised signals are extracted after the *waveform processing* block of the ETSI AFE algorithm as shown in Figure 5.1. But the ETSI AFE algorithm includes an additional *blind equalization* block operating in the cepstral domain in order for the ASR system to be robust against channel variations as described in Section 3.1. In order for the correlation results obtained using the ETSI AFE algorithm to be comparable to other algorithms, the impact of the *blind equalization* block on the correlation results has to be ignored. If the impact is negligible, then the comparison is fair. The impact of the *blind equalization* block is then evaluated by comparing correlation coefficients when ASR results are obtained for feature extraction with and without blind equalization. ASR results without blind equalization are obtained by applying the basic ETSI MFCC-based FE on the denoised speech signals extracted after the *waveform processing* block in the ETSI AFE algorithm (denoted by WFP-FE). It should be noted that the contribution of the *blind equalization* block on ASR performance can be seen in Section 6.1 by comparing the performance of the extracted waveform processing speech signals to the AFE.

Table 7.2 shows the Pearson, Spearman and Kendall correlation coefficients between the word accuracies (using the feature extraction methods (AFE and WFP-FE) in ASR) and the corresponding STOI/PESQ scores for the denoised speech signals. Furthermore, correlation coefficients are calculated over all data i.e. combining the data for feature extraction with and without blind equalization. Both *clean* and *multi-condition* training modes are considered. It has been chosen to consider only the word accuracy of the available ASR performance measures, as it accounts for all kinds of errors appearing in ASR unlike word correct and the fact that each error is weighted equally unlike the sentence correct performance measure.

Clean Training Mode	**Correlation Coefficient**		
SE performance measure/ Feature extraction method	**Pearson**	**Spearman**	**Kendall**
STOI/AFE	0.9723	0.9830	0.8897
STOI/WFP-FE	0.9711	0.9820	0.8809
STOI/Combined	0.9683	0.9819	0.8860
PESQ/AFE	0.8597	0.9883	0.9096
PESQ/WFP-FE	0.8558	0.9855	0.8992
PESQ/Combined	0.8574	0.9871	0.9055

Multi-condition Training Mode	**Correlation Coefficient**		
SE performance measure/ Feature extraction method	**Pearson**	**Spearman**	**Kendall**
STOI/AFE	0.9481	0.9841	0.8928
STOI/WFP-FE	0.9541	0.9761	0.8826
STOI/Combined	0.9489	0.9806	0.8877
PESQ/AFE	0.8144	0.9882	0.9060
PESQ/WFP-FE	0.8155	0.9790	0.8964
PESQ/Combined	0.8196	0.9863	0.9093

Table 7.2: Pearson, Spearman and Kendall correlation coefficients between the PESQ/STOI measures and the word accuracy ASR results in *clean* and *multi-condition* training mode for speech data from test set A, B and C of the Aurora-2 database.

In Table 7.2 it can be seen that there is a strong positive correlation between the SE performance measures (STOI/PESQ) and the word accuracy results for the feature extraction methods considered (AFE and WFP-FE), as all correlation scores provided are above 0.8.

The correlation scores for the AFE and WFP-FE algorithms are similar for each type of correlation coefficient and for both *clean* and *multi-conditioned* training. However, the correlation scores for AFE tend to be larger than the scores for WFP-FE. Furthermore it can be observed that the correlation coefficients computed by combining all data generated for the feature extraction methods (ETSI AFE and WFP-FE) have similar magnitude compared to the correlation coefficients of the separate feature extraction methods. This would seem to confirm that the impact of the *blind equalization* block is negligible on the correlation results

and that using the WFP speech signals to predict the ASR performance does not present an issue.

Figure 7.2 shows scatterplots of the relationship between the word accuracy and the STOI scores averaged for SNRs and noise conditions for the feature extraction methods AFE and WFP-FE. Speech data from test set A, B and C of the Aurora-2 database is used and both *clean* and *multi-condition* training modes are considered. Figure 7.3 show the corresponding scatter plots for the PESQ scores.

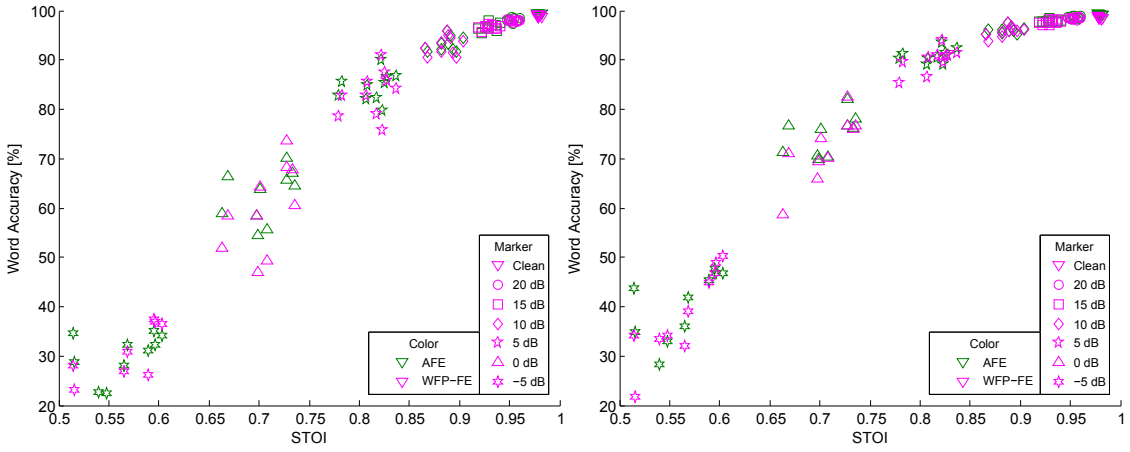

(a) Scatter plot of the STOI scores vs. the word accuracies for *clean* training mode.

(b) Scatter plot of the STOI scores vs. the word accuracies for *multi-condition* training mode.

Figure 7.2: Scatter plots of the relation between the STOI scores and the word accuracies averaged for SNRs and noise conditions for the AFE and the WFP-FE feature extraction methods using speech data from test set A, B and C of the Aurora-2 database.

For now only the relationship between AFE and and WFP-FE is evaluated, other relationships e.g. the difference in correlation between STOI and PESQ are evaluated in the subsequent sections. In the scatter plots from Figure 7.2 and 7.3 it can be seen that regardless of which training mode used and which SE performance measure is considered, the data points of the feature extraction methods WFP-FE and AFE show tendency towards a similar curve. Thus the assumption that the speech signals extracted after the *waveform processing* block in the ETSI AFE algorithm can be used for investigating the final ASR performance applying the ETSI AFE seems solid.

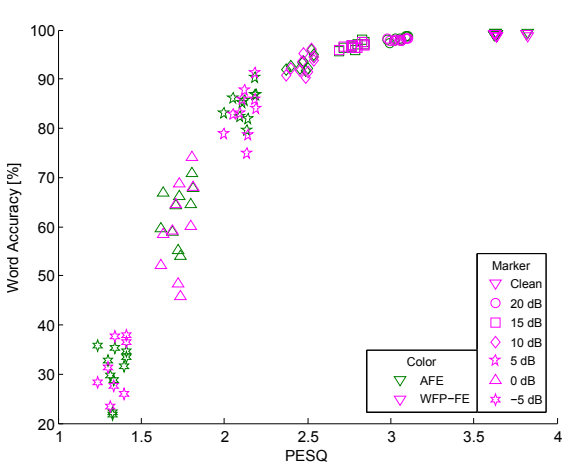

(a) Scatter plot of the PESQ scores vs. the word accuracies for *clean* training mode.

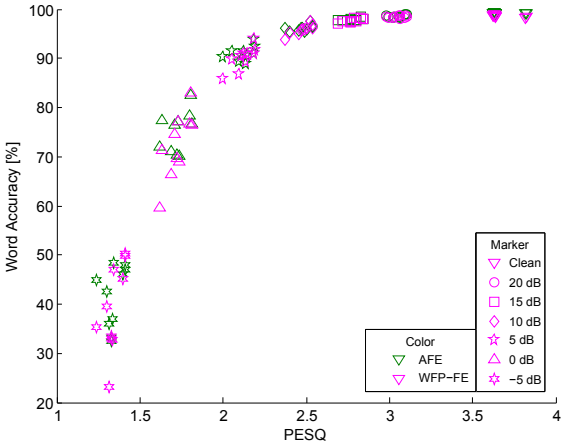

(b) Scatter plot of the PESQ scores vs. the word accuracies for *multi-condition* training mode.

Figure 7.3: Scatter plots of the relation between the PESQ scores and the word accuracies averaged for SNRs and noise conditions for the AFE and the WFP-FE feature extraction methods using speech data from test set A, B and C of the Aurora-2 database.

7.3 Correlation Between ASR and SE Performance Measures using ETSI AFE

In this section the relationships between the ASR performance applying the ETSI AFE feature extraction method and the SE performance measures are considered. The SE performance measures, STOI and PESQ, represent the difference between the denoised speech extracted at the output of the *waveform processing* block and its original clean version. Correlation scores are investigated in terms of Pearson, Spearman and Kendall for *clean* and *multi-condition* training modes. Finally an estimator of the ASR performance is created and evaluated.

7.3.1 Correlation of STOI Measure with ASR Measures

In this section the correlation between the STOI measures and the ASR results is investigated in detail. The ETSI AFE feature extraction algorithm is used to provide the ASR results. The denoised speech signals extracted after the *waveform processing* block of the ETSI AFE are used to compute the STOI scores. The speech signals containing less than 30 speech frames after denoised by any of the noise reduction algorithms considered in this thesis are excluded, as calculating STOI requires at least 30 speech frames. The relationship between the ASR results and STOI results is investigated for different noise conditions and different SNR levels. This explores the feasibility of creating an estimator for the ASR performance when applying the ETSI AFE feature extraction method, based on the STOI score of denoised speech signal. The

estimator considered should apply at any SNR level within the tested range from -5 dB to ∞ dB (clean signal). In order to measure the correlation between the performance measures for different noise conditions, the Pearson correlation coefficient is used, as Kendall or Spearman coefficient do not allow for meaningful analysis of the different noise conditions as there is only one data point for each SNR level. This results in a monotonic but necessarily linear function, therefore computing Kendall and Spearman correlation coefficients for a single noise condition results in a coefficient of 1.

In Table 7.3 and 7.4, the Pearson correlation coefficients between the STOI measures and ASR results at different noise conditions are shown for *clean* and *multi-condition* training modes, respectively. The ASR performance measures used are word accuracy, word correct and sentence correct. Furthermore Figure 7.4 shows scatter plots of the relationship between average STOI measures with respect to noise conditions at different SNR levels and ASR results using ETSI AFE for *clean* and *multi-condition* training modes. Speech data from test set A, B and C of the Aurora-2 database has been used.

	ASR MEASURES		
Noise Condition	**Word Accuracy**	**Word Correct**	**Sentence Correct**
Subway	0.9750	0.9696	0.9976
Babble	0.9900	0.9825	0.9907
Car	0.9561	0.9538	0.9900
Exhibition	0.9816	0.9790	0.9954
Restaurant	0.9937	0.9859	0.9801
Street	0.9765	0.9729	0.9970
Airport	0.9833	0.9762	0.9932
Train-Station	0.9751	0.9654	0.9959
Subway (MIRS)	0.9795	0.9750	0.9967
Street (MIRS)	0.9839	0.9813	0.9957
All Noise Conditions	0.9723	0.9689	0.9848

Table 7.3: Pearson correlation coefficients between the STOI scores and ASR performance measures for different noise conditions using ETSI AFE for speech data from test set A, B and C of the Aurora-2 database in *clean* training mode.

	ASR MEASURES		
Noise Condition	**Word Accuracy**	**Word Correct**	**Sentence Correct**
Subway	0.9491	0.9418	0.9916
Babble	0.9612	0.9464	0.9931
Car	0.9280	0.9255	0.9709
Exhibition	0.9627	0.9600	0.9897
Restaurant	0.9719	0.9581	0.9953
Street	0.9490	0.9437	0.9894
Airport	0.9610	0.9446	0.9919
Train-Station	0.9636	0.9456	0.9902
Subway (MIRS)	0.9460	0.9426	0.9861
Street (MIRS)	0.9564	0.9529	0.9898
All Noise Conditions	0.9481	0.9410	0.9834

Table 7.4: Pearson correlation coefficients between the STOI scores and ASR performance measures for different noise conditions using ETSI AFE for speech data from test set A, B and C of the Aurora-2 database in *multi-condition* training mode.

In Table 7.3 and 7.4 it can be observed that there exists a strong positive linear correlation between STOI and ASR results, as all Pearson correlation coefficients are above 0.92. It should be noted that the sentence correct performance measure provides the highest Pearson correlation coefficients for both *clean* and *multi-condition* training mode. It should be noted that the sentences excluded in order to enable comparison to STOI primarily consist of one word. Observing the sentence correct scores before and after excluded speech data reveal that a drop occur when sentences are excluded. This may have an impact on the correlation scores for sentence correct scores too.

In both *clean* and *multi-condition* training mode it can be observed that the Pearson correlation coefficient is lower at the car noise condition than at the other noise conditions, while the noise conditions restaurant and babble containing non-stationary segments provide among the largest correlations. However, it has also been observed that the word accuracy scores are significantly larger at the lower SNR levels for the car noise condition with respect to the restaurant and babble noise conditions. This turns out to give a more linear relationship at the non-stationary noise conditions, which can be inspected in Figure 7.4a.

Considering all noise conditions, the Pearson correlation coefficients in Table 7.3 and 7.4 are lower for all ASR measures in *multi-condition* training mode with respect to *clean* training mode. This can be explained by the fact that the ASR performance increases particularly at

lower SNR levels for the *multi-condition* training mode, which has been observed in Chapter 5. This increase in performance occurs only for the ASR performance measures as it is the training mode of the recognizer that is changed thus the STOI measure remain unchanged. This results in a less linear relation as seen in Figure 7.4 (b), (d) and (f). It is conceivable that high Pearson correlation scores are obtained in the *clean* training mode because both the ASR and the STOI measures are very dependent on the denoising process. But in the *multi-condition* training mode the ASR measures are less dependent on the denoising process.

Kendall Correlation Coefficient	**ASR MEASURES**		
Training Mode	**Word Accuracy**	**Word Correct**	**Sentence Correct**
Clean	0.8576	0.9366	0.8147
Multi-condition	0.8668	0.9213	0.8626

Spearman Correlation Coefficient	**ASR MEASURES**		
Training Mode	**Word Accuracy**	**Word Correct**	**Sentence Correct**
Clean	0.9760	0.9931	0.9597
Multi-condition	0.9771	0.9888	0.9754

Table 7.5: Spearman and Kendall correlation coefficients between the STOI scores and ASR performance measures using ETSI AFE for speech data from test set A, B and C of the Aurora-2 database in *clean* and *multi-condition* training mode.

In Table 7.5 the Spearman and Kendall correlation coefficients are shown computed across all noise conditions. These are all above 0.81 and indicate a strong monotonic relationship between the STOI scores and the ASR performance measures. For both Kendall and Spearman there is less difference between the correlation coefficients for word accuracy and word correct in *clean* training mode with respect to *multi-condition* training mode than it has been observed for the Pearson correlation coefficients. In addition, it should be noted that word correct shows the highest monotonic relationship in both Kendall and Spearman.

In Figure 7.4 the high correlation between the STOI measures and the ASR results are observable, as tendency within each scatterplot toward a curve is provided. Furthermore it can be observed that data is clustered with respect to SNR level at all scatter plots, where there are larger distance between the data points in clusters at low SNR levels than those at higher SNR levels. In Figure 7.4 (a), (b), (c) and (d) it can be observed that most noise conditions maintain roughly the same relative positioning with respect to each other in the clusters of SNR levels -

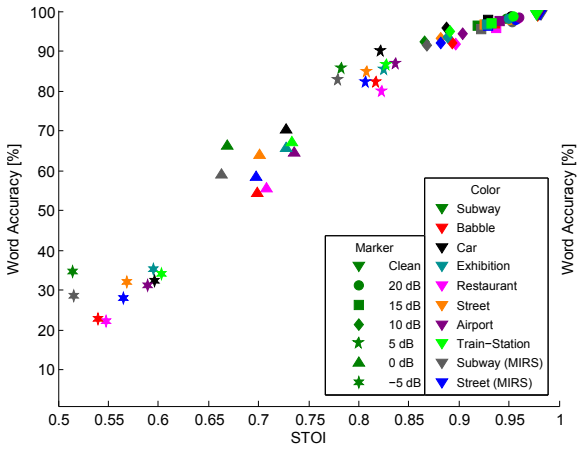

(a) Scatter plot of the STOI scores vs. the word accuracy in *multi-condition* training mode.

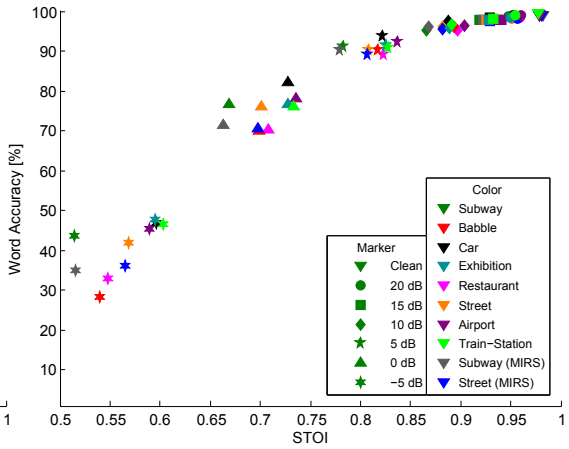

(b) Scatter plot of the STOI scores vs. the word accuracy in *multi-condition* training mode.

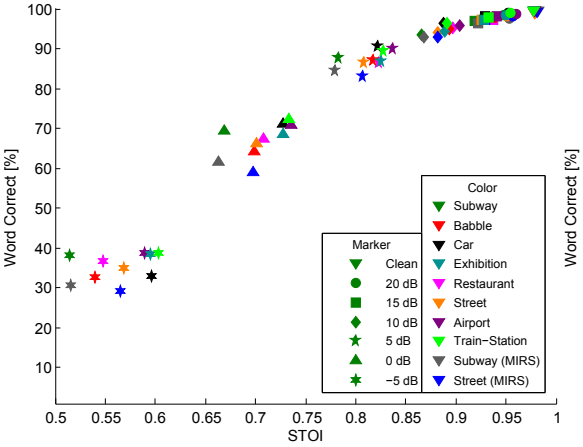

(c) Scatter plot of the STOI scores vs. the word correct in *clean* training mode.

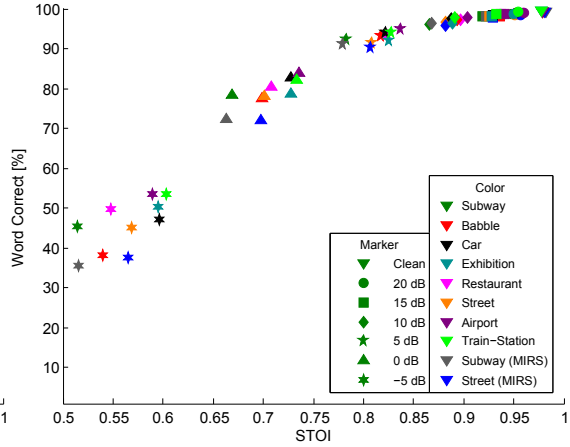

(d) Scatter plot of the STOI scores vs. the word correct in *multi-condition* training mode.

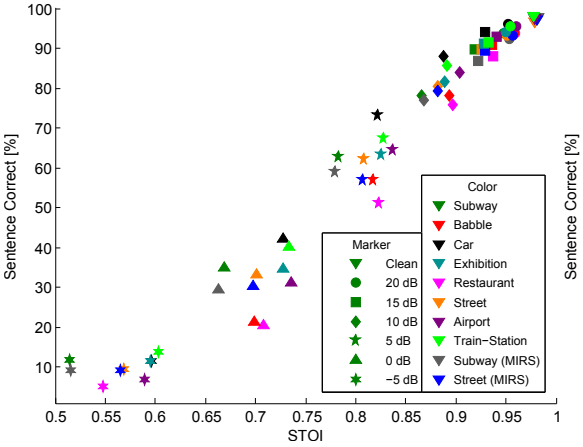

(e) Scatter plot of the STOI scores vs. sentence correct in *clean* training mode.

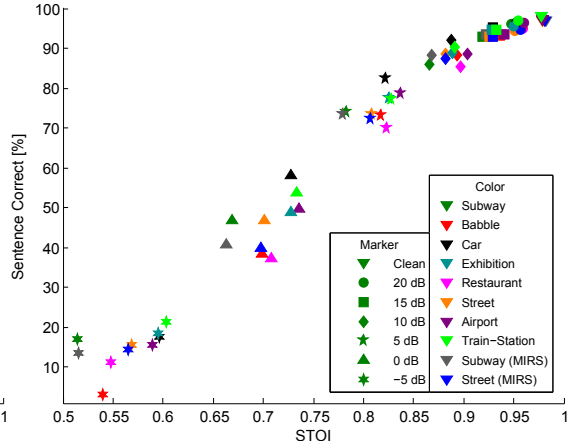

(f) Scatter plot of the STOI scores vs. sentence correct in *multi-condition* training mode.

Figure 7.4: Scatter plots of the relation between the STOI scores and the ASR performance measures for the ETSI AFE using speech data from test set A, B and C of the Aurora-2 database. Each sample represent the averaged STOI and ASR performance for a noise condition at a given SNR level.

5dB to 10 dB. The other noise conditions do remain in small clusters regardless of the SNR level though. The subway and subway (MIRS) noise conditions maintain positioning regardless of training mode and ASR measure.

7.3.2 Correlation of PESQ Measure with ASR Measures

This section investigates the feasibility of creating an estimator of the ASR performance when applying the ETSI AFE feature extraction algorithm, based on the PESQ score of the denoised signals. This is investigated by considering correlation between PESQ scores and the ASR results. The denoised speech signals extracted after the *waveform processing* block of the ETSI AFE are used to compute the PESQ scores.

In Table 7.6 and 7.7 the Pearson correlation coefficients between the average PESQ measures and ASR results are presented for *clean* and *multi-condition* training modes, respectively. Only the Pearson correlation coefficients are presented for the different noise conditions for the same reason as described in Subsection 7.3.1.

	ASR MEASURES		
Noise Condition	**Word Accuracy**	**Word Correct**	**Sentence Correct**
Subway	0.8662	0.8566	0.9384
Babble	0.8881	0.8705	0.9427
Car	0.8330	0.8295	0.9005
Exhibition	0.8705	0.8651	0.9319
Restaurant	0.8937	0.8689	0.9543
Street	0.8741	0.8673	0.9373
Airport	0.8689	0.8520	0.9302
Train-Station	0.8654	0.8481	0.9290
Subway (MIRS)	0.8361	0.8254	0.9124
Street (MIRS)	0.8572	0.8529	0.9218
All Noise Conditions	0.8597	0.8509	0.9238

Table 7.6: Pearson correlation coefficients between the PESQ scores and ASR performance measures for different noise conditions using ETSI AFE for speech data from test set A, B and C of the Aurora-2 database in *clean* training mode.

	ASR MEASURES		
Noise Condition	**Word Accuracy**	**Word Correct**	**Sentence Correct**
Subway	0.8225	0.8119	0.8992
Babble	0.8361	0.8200	0.9051
Car	0.7936	0.7905	0.8562
Exhibition	0.8360	0.8321	0.8916
Restaurant	0.8407	0.8152	0.9141
Street	0.8302	0.8227	0.8996
Airport	0.8267	0.7982	0.8916
Train-Station	0.8439	0.8158	0.8970
Subway (MIRS)	0.7723	0.7671	0.8510
Street (MIRS)	0.8081	0.8027	0.8789
All Noise Conditions	0.8144	0.8025	0.8848

Table 7.7: Pearson correlation coefficients between the PESQ scores and ASR performance measures for different noise conditions using ETSI AFE for speech data from test set A, B and C of the Aurora-2 database in *multi-condition* training mode.

In Table 7.6 and 7.7 it can be observed that there is a strong linear correlation between the PESQ scores and ASR performance measures, as they fall in the range between 0.80 and 0.93. But it indicates a lower linear correlation between PESQ scores and ASR performance measures at all noise conditions compared to the correlation scores for STOI and ASR performance measures.

In Table 7.8 the Spearman and Kendall correlation coefficients between PESQ scores and ASR performance are shown using all noise conditions. All the Kendall and Spearman correlation coefficients are above 0.79, which indicate a strong monotonic relationship between the PESQ scores and the ASR performance measures using the ETSI AFE algorithm. The correlation scores are similar to those obtained for the STOI scores in Subsection 7.3.1. So both STOI and PESQ show strong monotonic relationships to the ASR performance measures, but STOI is more linearly dependent on the ASR measures than PESQ.

Kendall Correlation Coefficient	**ASR MEASURES**		
Training Mode	**Word Accuracy**	**Word Correct**	**Sentence Correct**
Clean	0.8283	0.9187	0.7980
Multi-condition	0.8571	0.9150	0.8550

Spearman Correlation Coefficient	**ASR MEASURES**		
Training Mode	**Word Accuracy**	**Word Correct**	**Sentence Correct**
Clean	0.9706	0.9895	0.9549
Multi-condition	0.9746	0.9876	0.9735

Table 7.8: Spearman and Kendall correlation coefficients between the PESQ scores and ASR performance measures using ETSI AFE for speech data from test set A, B and C of the Aurora-2 database in *clean* and *multi-condition* training mode.

In Figure 7.5 scatter plots of the relationship between average PESQ measures with respect to noise conditions at different SNR levels and ASR results using ETSI AFE for *clean* and *multi-condition* training modes. Speech data from test set A, B and C of the Aurora-2 database has been used.

When observing the scatter plots in Figure 7.5 it is clear that high correlation is present. However, unlike the scatter plots in Figure 7.4 showing the relationship between STOI and ASR measures, they appear less linearly related. The data points are clustered with respect to SNR level, where the clusters are relatively tight even at low SNRs compared to the observations made for the STOI scatter plots in Figure 7.4. Particularly in the PESQ measure axis, the difference is small. At the clusters of lower SNRs the dependence seems linear, but as SNR increases a curvature appear. Observing the entire SNR clusters of the scatter plots, a logistic dependency seems to appear.

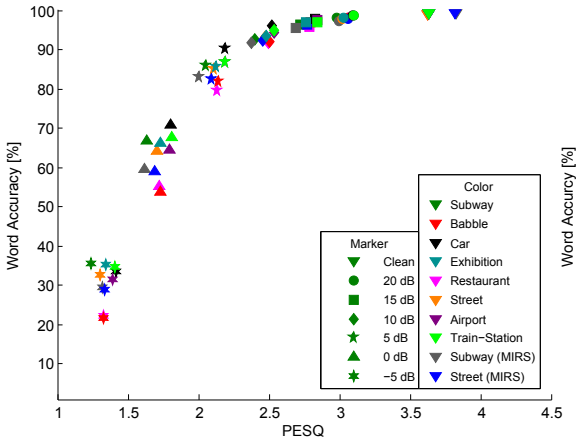

(a) Scatter plot of the PESQ scores vs. word accuracy in *clean* training mode.

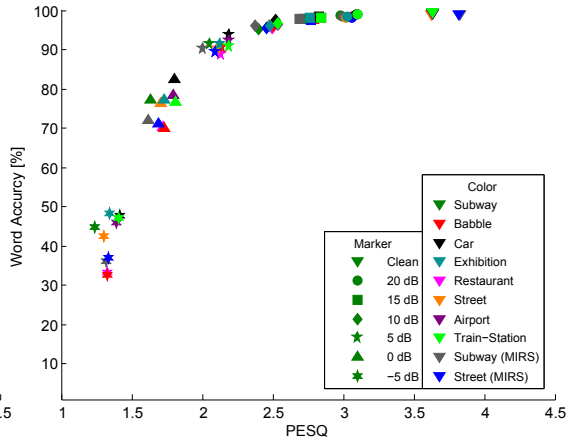

(b) Scatter plot of the PESQ scores vs. word accuracy in *multi-condition* training mode.

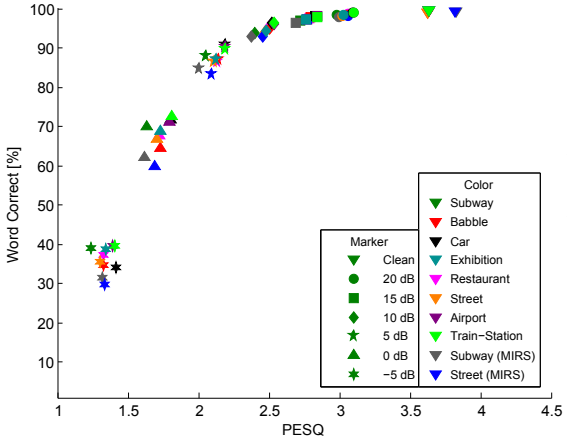

(c) Scatter plot of the PESQ scores vs. word correct in *clean* training mode.

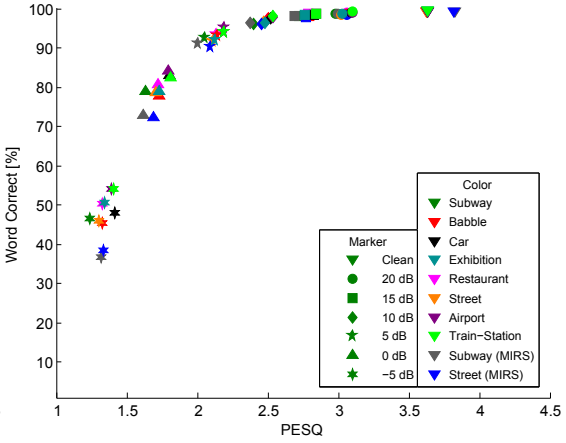

(d) Scatter plot of the PESQ scores vs. word correct in *multi-condition* training mode.

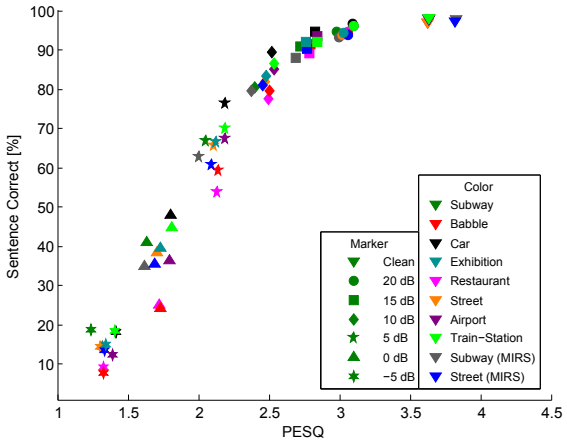

(e) Scatter plot of the PESQ scores vs. sentence correct in *clean* training mode

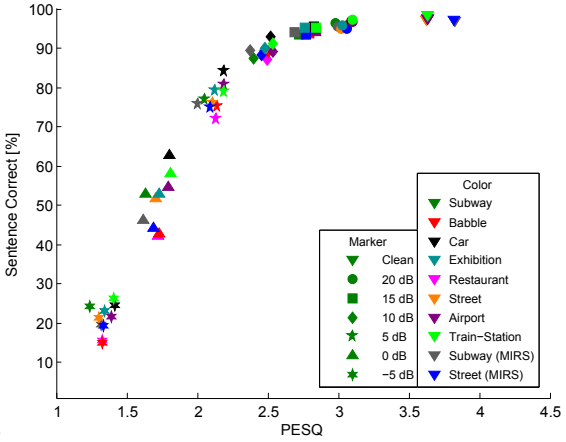

(f) Scatter plot of the PESQ scores vs. sentence correct in *multi-condition* training mode

Figure 7.5: Scatter plots of the relation between the PESQ scores and the ASR performance measures for the ETSI AFE using speech data from test set A, B and C of the Aurora-2 database. Each sample represent the averaged PESQ and ASR performance for a noise condition at a given SNR level.

7.3.3 Estimation of the ETSI AFE Recognition Performance

In Subsection 7.3.1 and 7.3.2 it has been observed that a strong monotonic relationship exist between STOI/PESQ and the ASR performance measures when applying the ETSI AFE feature extraction algorithm. The denoised speech signals extracted after the *waveform processing* block of the ETSI AFE algorithm have been used to compute PESQ and STOI.

Therefore this section investigates if these strong correlations allow for a decent estimator of the ASR performance based on the STOI or PESQ score of the denoised speech signals, when the ETSI AFE feature extraction algorithm is used. It has been chosen to consider word accuracy of the available ASR performance measures, as it accounts for all kind of errors appearing in ASR.

It has been chosen to model the estimator as a logistic function:

$$\hat{y} = \frac{100}{1 + e^{-b(x-c)}}, \tag{7.12}$$

where b and c are constants to be determined by datafitting, x represents the PESQ/STOI score and y is the word accuracy to be estimated. This is inspired by the estimator used in [40] which is used for estimating the word accuracy results based on PESQ scores. The general form of the logistic estimator is given by:

$$\hat{y} = \frac{a}{1 + e^{-b(x-c)}}. \tag{7.13}$$

This has been chosen as the basis for the model due to a number of factors. First it ensures a monotonic estimator, which a polynomial model for instance do not necessarily ensure. Due to high monotonic correlation found previously this was viewed an important criteria for an estimator. In addition a monotonic relationship is very useful feature for an estimation as it avoids any ambiguity. It can also be observed in the scatter plots of Figure 7.4 and 7.5 representing the relationship between STOI/PESQ scores and ASR measures that logistic dependencies appear. Finally, given that the logistic model in Equation 7.3.3 performed well in [40], it has been an obvious choice to use this model.

It has been chosen to fix the a parameter in Equation 7.3.3 of the model applied to $a = 100$. Although, this obviously degrades the quality of the resulting curve fitting, setting a to 100 ensures that an estimator can not estimate a performance above the limit of the ASR measures. It has been chosen to use test set A from the Aurora-2 database to build the estimator and validate the performance using test set B and C.

Regression is performed using the Matlab application 'Curve Fitting Toolbox' using a nonlinear least squares method that is made robust by applying the least absolute residuals, which minimizes the influence of outliers by only using the absolute value of the residuals rather than the squared value [20]. The applied nonlinear least squares algorithm uses a 95 % trust region to iteratively adjust the coefficients.

Figure 7.6 shows the relationship between the STOI/PESQ scores of test set A from Aurora-2 and the word accuracy results averaged for noise conditions at different SNR levels. The word accuracy results have been obtained for *multi-condition* training mode. Additionally, the corresponding fitted curves are shown.

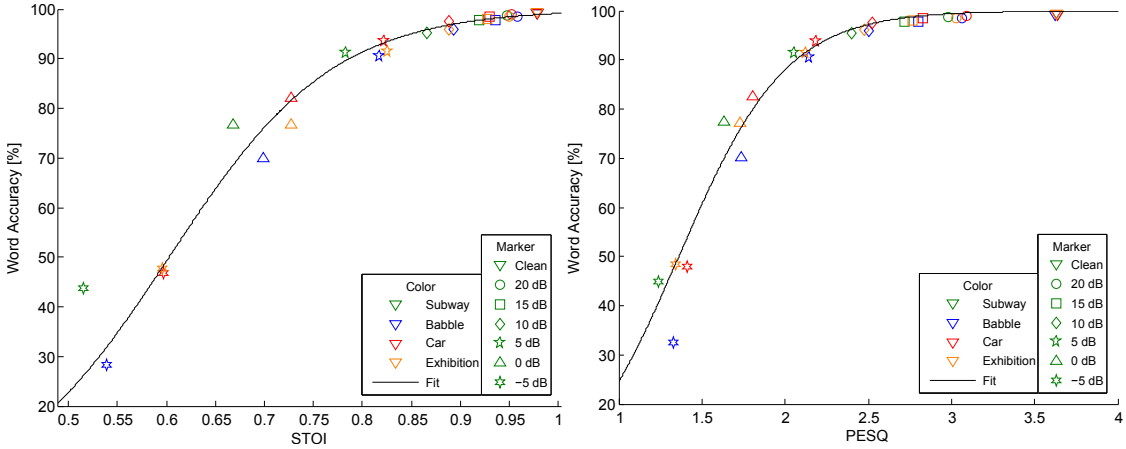

(a) Estimator fitted for word accuracy and STOI performance

(b) Estimator fitted for word accuracy and PESQ performance

Figure 7.6: The estimators of the relation between the SE performance measures and word accuracy scores for the ETSI AFE using speech data from test set A of the Aurora-2 database. Each sample represent the averaged word accuracy and SE performance for test set A at a given noise condition and SNR level using *multi-condition* training mode.

In Figure 7.6 it can be seen that the fit of word accuracy estimation by the use of PESQ increases more rapidly than the fit for the estimation using STOI. This is line with the observation in Subsection 7.3.1 and 7.3.2, where STOI provides a larger linear correlation score than PESQ. Both estimators have closer fit to car noise than to the noise conditions of subway and exhibition. For both estimators it can be seen that the distance between the fit and the outliers increase at the lower SNR levels.

In order to objectively measure the goodness of the fit and validate the fit the following three measures is used. The sum of squares error (SSE), the coefficient of determination R^2 and the root mean squared error (RMSE). These measures are briefly explained in the following.

The SSE is used to measure the total deviation of the estimated values to the true values. In order for the fit to estimate accurately the value of SSE needs to be close to 0, as this means the random error component of the model is small [36]. The SSE is found by:

$$SSE = \sum_{i=1}^{n} (y_i - \hat{y}_i)^2, \tag{7.14}$$

where n is the number of measurements, y_i is the true value and $\hat{y}_i$ is the value estimated using

Equation 7.12.

The coefficient of determination R^2 measures the proportion of variability of the fit that can be explained. The explained variance thus describes how well the estimator represents the data being modelled. It is defined as [36]:

$$R^2 = 1 - \frac{\sum_{i=1}^{n} (y_i - \hat{y}_i)^2}{\sum_{i=1}^{n} (y_i - \bar{y})^2}, \tag{7.15}$$

where $\bar{y}_i$ is the mean of the true values. The value of R^2 lies in the range 0 to 1, where a R^2 score of 0.8645 means that 86.45% of total variation of the data around the mean is explained by the fit. Thus the closer to 1 the score is, the better [29].

The RMSE is an estimate of the standard deviation of the estimation error and is defined by:

$$RMSE = \sqrt{MSE} = \sqrt{\frac{SSE}{\upsilon}} = \sqrt{\frac{\sum_{i=1}^{n} (y_i - \hat{y}_i)^2}{\upsilon}}, \tag{7.16}$$

where υ is defined as $\upsilon = n - m$ for the fitting and $\upsilon = n$ in the validation, where m is the number of fitted coefficients.

In Table 7.9 the measures of goodness of fit and goodness of validation for the estimators of word accuracy with STOI/PESQ. Both *clean* and *multi-condition* training modes are considered. Additionally, the estimator coefficients are shown. The goodness of the fit is reported using SSE, R^2 and RMSE measures. The goodness of validation is presented using SSE and RMSE. Furthermore the validation data is evaluated by the proportion of data inside a prediction bound of 95 %, because it is commonly used in regression analysis as observed in [36]. Test set A from the Aurora-2 database has been used to create the estimators and test set B and C are used for validation.

Word Accuracy	**Coefficients**		**Goodness of fit**			**Goodness of validation**		
SE performance measure/ ASR Training Mode	**b**	**c**	**SSE**	**R^2**	**RMSE**	**SSE**	**RMSE**	**Inside 95 % prediction bound [%]**
STOI/Clean Mode	11.79	0.6472	70.58	0.9955	1.648	641.333	3.90766	76.19
STOI/Multi-condition Mode	11.92	0.6027	50	0.9955	1.387	313.577	2.73242	80.95
PESQ/Clean Mode	2.995	1.54	64.04	0.9959	1.569	492.977	3.42601	78.57
PESQ/Multi-condition Mode	3.111	1.361	44.41	0.9957	1.307	629.926	3.87276	78.57

Table 7.9: Estimator coefficients and fitting measures for the estimators using test set A from the Aurora-2 database. Validation measures are shown from the performance of the estimator with test sets B and C. The measures are presented for the estimators designed for STOI and PESQ using both *clean* and *multi-condition* training mode

Comparing the measures of the goodness of the fit for STOI in Table 7.9 for *clean* and *multi-condition* training modes, it can be observed that the two training modes have the same R^2. But the *multi-condition* training mode have the lowest RMSE score of the two. This difference in RMSE is also observed when validating the estimator. In fact the estimator using STOI with *multi-condition* training mode have the highest percentage inside the prediction bounds and the lowest RMSE score by a considerable amount.

When comparing the measures for goodness of the fit for the estimators build for PESQ, the behaviour is the same as for the STOI estimators, i.e. the estimator for *multi-condition* training mode outperforms the one for *clean* training mode. The R^2 score for the estimator using PESQ for for *multi-condition* training mode is slightly lower than the score for *clean* training mode and the RMSE is also significantly lower. However, when validating the estimators, they have the same percentage of data points inside the prediction bound, while the RMSE for the *clean* training mode estimator is significantly lower. Concerning the validation, it is interesting to note how that for STOI it is the *multi-condition* training mode estimator the performs best, while for PESQ it is the estimator for *clean* training mode.

In Figure 7.7 the estimators of word accuracy during *multi-condition* training mode using STOI and PESQ is plotted along with the 95 % prediction boundaries of the estimators. The validation data from test B and C in Aurora-2 are included in the plots.

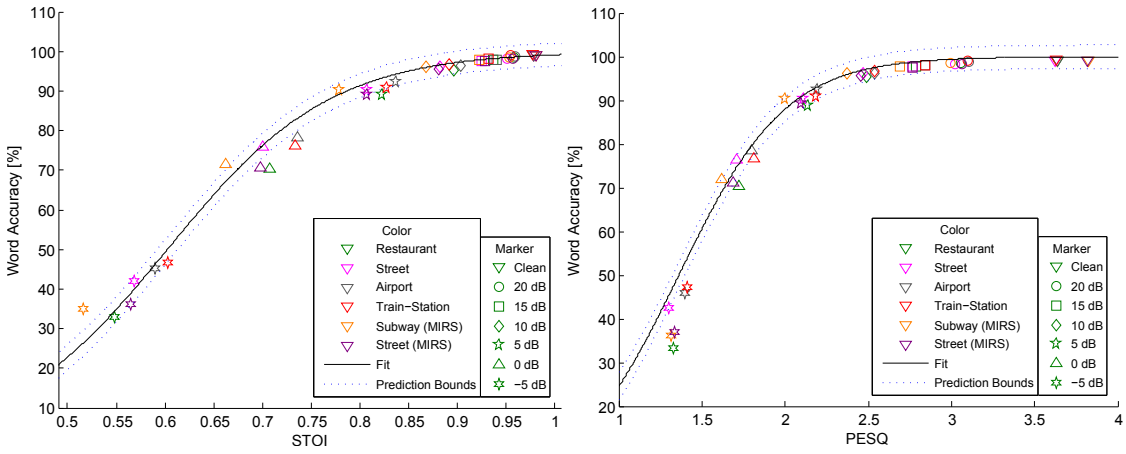

(a) Estimator fitted for word accuracy and STOI performance.

(b) Estimator fitted for word accuracy and PESQ performance.

Figure 7.7: The estimators of the relation between the SE performance measures and word accuracy scores for the ETSI AFE and the validation speech data from test set B and C of the Aurora-2 database. Each sample represent the averaged word accuracy and SE performance for test set B and C at a given noise condition and SNR level using *multi-condition* training mode.

From Figure 7.7 it can be seen that it is primarily at −5 dB and 0 dB that the data points fall outside the estimator prediction boundaries. This is particular noticeable for PESQ estimator at −5 dB where almost all of the data point lie the outside prediction band. This seems reasonable behaviour as these speech signal have a lower word accuracy performance consequently the word accuracy span of the prediction band also decreases. In addition, it has also been observed that the differences in denoising different noise conditions also become more pronounced at the lower SNR levels.

7.4 Correlation Across Feature Extraction Algorithms

This section looks into the correlation between STOI/PESQ scores and ASR scores across different feature extraction algorithms for speech signals at fixed SNR levels. The intention is to investigate the possibility of estimating the ASR performance for any denoising algorithm using its STOI or PESQ scores. Predicting the performance of any algorithms without having to spend the resources on the time consuming ASR processes, would allow for a more rapid configuration and development phase. It has be chosen to only use the word accuracy measurement to represent the ASR score in this section too. Word accuracy is chosen as it accounts for all types of ASR errors and the word errors are weighted equally.

The feature extraction algorithms have in common that they are all MFCC based. The following algorithms are used for investigating the correlations in this section: ETSI AFE, WFP-FE, ANS, IWF and STSA WE. The basic ETSI MFCC-based FE algorithm is used to perform feature extraction after the speech signals have been processed by either ANS, IWF and STSA WE. In addition, the STOI, PESQ and word accuracy performance measures for the raw noisy speech signals processed by the basic FE algorithm are also included.

In Section 5.5 the relationship between STOI/PESQ and word accuracy has been investigated when adjusting the aggressiveness of the ETSI AFE feature extraction algorithm. The denoised speech extracted after the *waveform processing* block has been used for this investigation. Based on the relationships shown in Figure 5.5 and 5.6 it is expected that a negative correlation should exists between PESQ and ASR performance across algorithms with fixed SNR. Furthermore it is expected to observed a positive correlation between STOI and ASR performance.

The Pearson, Spearman and Kendall correlation coefficients calculated across all algorithms (i.e. ETSI AFE, WFP-FE, ANS, IWF, STSA WE and the raw noisy speech) between the word accuracies and the PESQ/STOI scores for different SNR levels are shown in Table 7.10 and 7.11. Both *clean* and *multi-condition* training modes are considered.

ASR MODE: Clean	**Correlation Coefficient**		
SNR	**Pearson**	**Spearman**	**Kendall**
Clean	0.0120	-0.2366	-0.1974
20 dB	-0.7312	-0.7606	-0.6253
15 dB	-0.7589	-0.5634	-0.3752
10 dB	-0.3460	-0.2465	-0.2189
5 dB	0.3218	0.4930	0.3439
0 dB	0.5142	0.5423	0.4377
-5 dB	0.2661	0.1972	0.0938

ASR MODE: Multi	**Correlation Coefficient**		
SNR	**Pearson**	**Spearman**	**Kendall**
Clean	-0.3271	-0.3872	-0.2961
20 dB	-0.7994	-0.7183	-0.5628
15 dB	-0.5563	-0.3592	-0.2501
10 dB	0.1622	0.0000	0.0000
5 dB	0.4506	0.5352	0.3439
0 dB	0.6148	0.5423	0.4377
-5 dB	0.3683	0.2042	0.0938

Table 7.10: Pearson, Spearman and Kendall correlation coefficients between the STOI scores and word accuracy ASR results across raw noisy speech (using basic FE), AFE, WFP-FE, ANS, IWF and STSA WE at different SNR levels. The speech data used comes from test set A, B and C of the Aurora-2 database. The recogniser is applied for both *clean* and *multi-condition* training mode.

In Table 7.10 unexpected correlation scores for STOI can be observed over the SNR levels considering the results from Section 5.5, as no clear trend is discernible. For both *clean* and *multi-condition* training mode, a negative correlation exists at the high SNR levels, the magnitude of the correlation at 20 dB is particular high, while at the lower SNR levels the correlation turns positive.

ASR MODE: Clean	**Correlation Coefficient**		
SNR	**Pearson**	**Spearman**	**Kendall**
Clean	0.0547	0.0287	0.0331
20 dB	0.4007	0.6514	0.4690
15 dB	0.4860	0.8677	0.7561
10 dB	0.6460	0.7535	0.5315
5 dB	0.8482	0.7465	0.5315
0 dB	0.6573	0.6690	0.5002
-5 dB	-0.1101	-0.0599	-0.0938

ASR MODE: Multi	**Correlation Coefficient**		
SNR	**Pearson**	**Spearman**	**Kendall**
Clean	-0.3050	-0.1721	-0.0987
20 dB	0.7679	0.6561	0.4883
15 dB	0.7092	0.7535	0.5940
10 dB	0.6939	0.7549	0.6616
5 dB	0.7777	0.8536	0.7089
0 dB	0.6295	0.6479	0.4690
-5 dB	0.0424	0.1761	0.0938

Table 7.11: Pearson, Spearman and Kendall correlation coefficients between the PESQ scores and word accuracy ASR results for raw noisy speech (using basic FE), AFE, WFP-FE, ANS, IWF and STSA WE at different SNR levels. The speech data used comes from test set A, B and C of the Aurora-2 database. The recogniser is applied for both *clean* and *multi-condition* training mode.

Table 7.11 shows for both *clean* and *multi-condition* training mode that the correlation across the SNR levels are more stable than what has been observed in Table 7.10. Though there are a few weak negative correlations, they are mainly positive. The magnitude of the correlation is particularly lower at the *clean* training mode and -5 dB SNR, where the few negative correlations appear. The monotonic correlations is particular high at 5 dB to 15 dB for *clean* and *multi-condition* training mode, respectively.

In Figure 7.8 and 7.9 scatter plots for the relationship between STOI/PESQ scores and word accuracy are shown for the aforementioned feature extraction algorithms. Different noise types

are applied at 20 dB and 0 dB SNR. The plots are provided for *multi-condition* training only as the magnitudes of the correlations for *multi-condition* training mode tends to be larger than those for *clean* training mode.

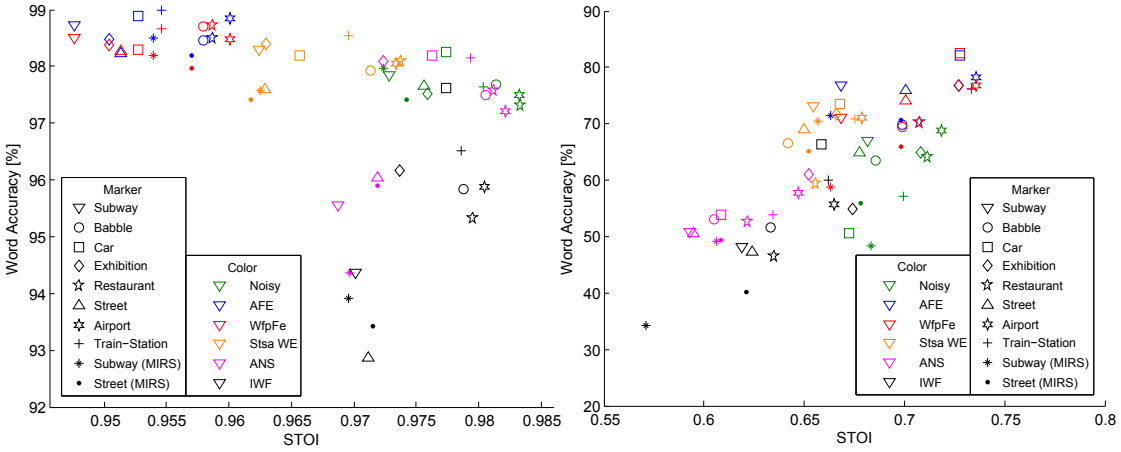

(a) Scatter plot of the STOI scores vs. the word accuracies at 20 dB SNR for different pre-processing methods.

(b) Scatter plot of the STOI scores vs. the word accuracies at 0 dB SNR for different pre-processing methods.

Figure 7.8: Scatter plots of the relation between the STOI scores and the word accuracy ASR results for the raw noisy speech (using basic FE), AFE, WFP-FE, ANS, IWF and STSA WE using speech data from test set A, B and C of the Aurora-2 database. Each sample represent the averaged STOI and word accuracy performance for a noise condition at the given SNR level using *multi-condition* training mode.

In Figure 7.8a and 7.9a it can be observed that the data points seems to have a tendency to fall on the same curve when disregarding the data points from ANS and IWF for 20 dB SNR. But these scatter plots share a common issue as well. The range of their axes are very small, which could increase the chances of a measurement error for the estimator. This is resolved somewhat in Figure 7.8b and 7.9b as the range of word accuracy axis have increased greatly. The range for the STOI and PESQ measurements have also increased, but it remains limited. One thing that can be observed in all the scatter plots in Figure 7.8 and 7.9 is that the measurements for the ANS and IWF algorithm tend to cluster together. This may indicate some common denominator shared by the two algorithms that differentiate them from the others.

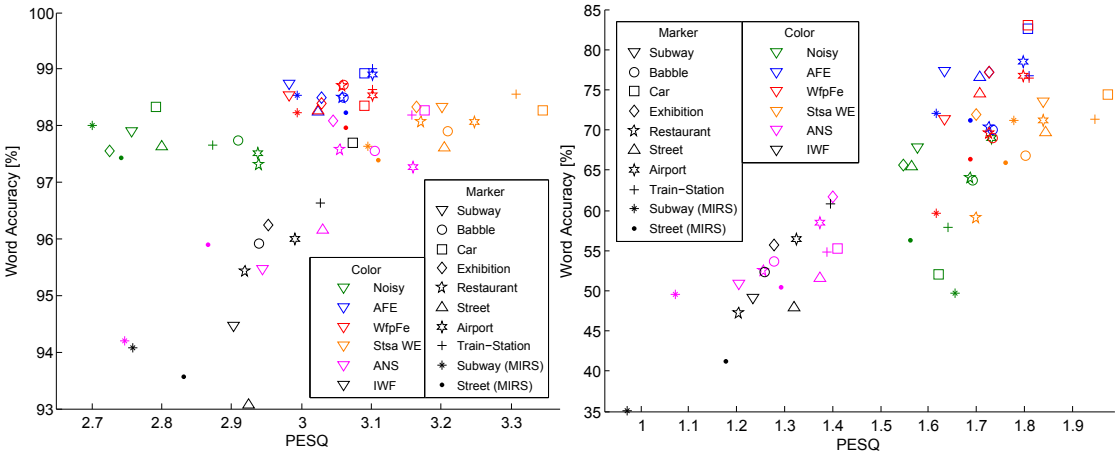

(a) Scatter plot of the PESQ scores vs. the word accuracies at 20 dB SNR for different pre-processing methods.

(b) Scatter plot of the PESQ scores vs. the word accuracies at 0 dB SNR for different pre-processing methods.

Figure 7.9: Scatter plots of the relation between the PESQ scores and the word accuracy ASR results for the raw noisy speech (using basic FE), AFE, WFP-FE, ANS, IWF and STSA WE using speech data from test set A, B and C of the Aurora-2 database. Each sample represent the averaged PESQ and word accuracy performance for a noise condition at the given SNR level using *multi-condition* training mode.

Based on the observed correlations between STOI/PESQ and the word accuracy across the feature extraction algorithms considered, it has been decided to not design any performance estimators for these relationship as the correlation between the ASR and SE performance do not seem to support this.

7.5 Discussion

In this chapter the linear and monotonic correlation coefficients between ASR performance measures and SE performance measures have been calculated by applying the ETSI AFE feature extraction algorithm. Comparison of the correlation coefficients calculated between the SE performance measures of the speech signals processed by the *waveform processing* block and the recognition performance of both the ETSI AFE and WFP-FE algorithms, show slight differences. Meaning the impact of *blind equalization* block on correlation is negligible. This is advantageous as it means that the ETSI AFE can be compared to other algorithms using its final recognition performance. The recognition performance and SE performance of the ETSI AFE showed high linear and monotonic correlations. The linear correlation has been found to be higher for recognisers trained with clean speech signal, than if trained with multi-condition speech data. This drop in correlation can most likely be explained by *multi-conditioned* recognisers being less dependent on the denoising processes, however, the

monotonic correlation remains strong for the *multi-condition* training mode. Scatterplots used in conjunction with correlation coefficients revealed that while the STOI measure has a higher linear correlation than the PESQ measure, both measures follow logistic-like curves. Estimators have been created inspired by a logistic model presented in [39]. The estimators have been fitted to a limited data set, where the fitted estimators provide the smallest RMSEs when considering a *multi-condition* training mode of ASR. Based on the validation data, the estimator using STOI to predict the word accuracy of a *multi-condition* recogniser performs the best. Although [39] present estimators of ASR performance using PESQ, the authors of this thesis are not aware of any studies using STOI to predict the ASR performance of feature-extraction algorithms. Based on the work of this theis, STOI seems to be a viable option for predicting ASR performance using ETSI AFE. Discouraging results have been obtained when comparing calculated correlations across different feature-extraction algorithms for fixed SNRs. Based on the aggressiveness testing in terms of noise reduction from Section 5.5, it has been anticipated that STOI and PESQ have positive and negative correlations, respectively. It is possible that they do not behave as expected from the aggressiveness testing, because the algorithms take fundamentally different approaches to the denoising process. As it can be observed that some of the algorithms cluster together in the scatterplots, it is possible that different results might be obtained if using algorithms all based on similar principles.

Conclusion 8

This thesis investigates the relationship and differences between a noise reduction algorithm from the field of automatic speech recognition (ASR) and algorithms from the field of speech enhancement (SE) for human receivers. Estimators of recognition performance are created for the European telecommunication standards institute (ETSI) advanced frontend (AFE) feature extraction algorithm using the distortion measures for speech quality and intelligibility. The perceptual evaluation of speech quality distortion measure estimates speech quality and the short-time objective intelligibility (STOI) distortion measure estimates speech intelligibility.

Given the performance difference between ETSI AFE and state-of-the-arts SE algorithm in recognition performance, it is of interest to know if the ETSI AFE perform decently in a speech enhancement context [14]. Unexpectedly the ETSI AFE preprocessing stages outperform the state-of-the-art SE methods audible noise suppression (ANS) and the iterative Wiener filtering (IWF) algorithms designed for human listeners in both PESQ and STOI. However, the ETSI AFE does not outperform the remaining state-of-the-art method, the short-time spectral amplitude (STSA) estimator based on the weighted euclidean (WE) distortion measure, in terms of speech quality as estimated by PESQ. It should be noted that SE performance measures used are only estimates and listening tests need to be carried out to confirm these results. In improving the PESQ scores for the SE algorithms designed for human listeners inadvertently degrade their STOI scores, however, the ETSI AFE preprocessing stages avoids this degradation. The results concerning recognition performance of ANS, IWF and STSA WE as feature preprocessing methods agree with the observations made by [14] concerning the inferior recognition performance of the SE algorithms for human listeners compared to the ETSI AFE algorithm.

The use of a *multi-conditioned* recognizer (i.e. acoustic model build using clean and noisy speech signals) can to some extent compensate for the lack of robustness in ASR performance using the ANS, IWF and STSA WE algorithms as feature preprocessing methods. The STSA WE algorithm provides more recognition errors in the noise-only regions of the speech signal as explored by the use of reference voice activity detection (VAD) labels. The ASR performance could be enhanced further by improving the behaviour of the STSA WE implementation during

noise-only regions. This is demonstrated by frame dropping experiments, where the noise-only regions of the speech signal is removed using reference VAD labels, where significant increases in ASR performance has been observed for the STSA WE algorithm when operating exclusively with speech-only regions. The primary observed difference between the algorithms from the field of ASR and SE for human listeners is the aggressiveness of the noise reduction applied. In the spectrogram analysis it has been observed that the ETSI AFE preprocessing stages preserves more of the noisy speech signals than the STSA WE algorithm. It is suspected by the authors that this difference in aggressiveness exists as human listeners are superior to machines in recognising speech and thus require less information to perform recognition successfully. In addition the SE algorithms for human listeners are expected to operate at lower signal-to-noise ratios, as human intelligibility is usually not an issue in the expected operating range of ASR system. Attempts at influencing the aggressiveness of the ETSI AFE and STSA WE algorithms only produced minor improvements in performance in their rivalling field. This would make the design of an algorithm to be used in both fields challenging as it would require a large adjustable range of aggressiveness.

The correlation between the ASR performance across feature extraction algorithms and SE performance of the corresponding preprocessing stages at fixed SNRs, failed to produce satisfactory high correlations to justify designing any estimators. However, an estimator has been designed for the word accuracy performance of the ETSI AFE algorithm. This is based on the strong correlation between the ASR performance of the ETSI AFE and the SE performance of the speech signals extracted before feature computation. From the observed relationships and [40], a logistic model has been chosen for the estimators. The most accurate estimator of the word accuracy performance of the ETSI AFE, proved to be the one designed for STOI using a recogniser trained with *multi-conditioned* speech data. As potential future work we propose investigating the performance of a STOI based estimator of word accuracy for other feature extraction methods. In addition the performance of ANS and IWF when frame dropping with reference VAD is applied should be investigated.

References

[1] C. Bishop. *Pattern Recognition and Machine Learning*. Springer, 2006.

[2] P. Y. Chen and P. M. Popovich. *Correlation*. SAGE Publications, Inc., 2002.

[3] Deller, Jr., J. R. and Hansen, J. H. L. and Proakis, J. G. *Discrete-Time Processing of Speech Signals*. Wiley-IEEE Press, 1999.

[4] Encyclopaedia Britannica. Tympanic Membrane. `http://global.britannica.com/EBchecked/topic/611539/tympanic-membrane`, 1997.

[5] Y. Ephraim and D. Malah. Speech Enhancement Using a Minimum-mean Square Error Short-time Spectral Amplitude Estimator. *Acoustics, Speech and Signal Processing, IEEE Transactions on*, 32(6):1109–1121, Dec 1984.

[6] ETSI Standard ES 201 108. Speech Processing, Transmission and Quality Aspects (STQ); Distributed Speech Recognition; Front-end Feature Extraction Algorithm; Compression Algorithms. ETSI Standard, ETSI, Apr 2000.

[7] ETSI Standard ES 202 050. Speech Processing, Transmission and Quality Aspects (STQ); Distributed Speech Recognition; Extended Front-end Feature Extraction Algorithm; Compression Algorithms. ETSI Standard, ETSI, Jan 2007.

[8] S. A. Gelfand. *Hearing - An Introduction to Psychological and Physiological Acoustics*. Marcel Dekker, 4 edition, 2004.

[9] M. Greenacre. *Correspondence Analysis in Practice*. Chapman and Hall/CRC , 2 edition, 2007.

[10] J. Hansen. *Analysis and Compensation of Stressed and Noisy Speech with Application to Robust Automatic Recognition*. PhD thesis, Georgia Institute of Technology, 1988.

[11] Hendriks, R. C. and Gerkmann, T and Jensen, J. *DFT-Domain Based Single-Microphone Noise Reduction for Speech Enhancement: A Survey of the State-of-the-Art*. Morgan & Claypool, 2013.

[12] G. Hirsch and D. Pearce. Applying the Advanced ETSI Frontend to the Aurora-2 Task. Technical report, 2006.

[13] D. M. Howard and J. Angus. *Acoustics and Phychoacoustics*. Elsevier, 3 edition, 2006.

[14] J. Jensen and Z.-H. Tan. Minimum Mean-Square Error Estimation of Mel-Frequency Cepstral Features - A Theoretically Consistent Approach. *Audio, Speech, and Language Processing, IEEE/ACM Transactions on*, 23(1):186–197, Jan 2015.

[15] J.S. Lim and A.V. Oppenheim. All-Pole Modeling of Degraded Speech. *Acoustics, Speech and Signal Processing, IEEE Transactions on*, 26(3):197–210, Jun 1978.

[16] P. C. Loizou. *Speech Enhancement: Theory and Practice*. CRC Press, 2007.

[17] P. C. Loizou. *Speech Enhancement: Theory and Practice*. CRC Press, 2 edition, 2013.

[18] P.C. Loizou. Speech Enhancement Based on Perceptually Motivated Bayesian Estimators of the Magnitude Spectrum. *Speech and Audio Processing, IEEE Transactions on*, 13(5): 857–869, Sep 2005.

[19] V. K. Madisetti. *The Digital Signal Processing Handbook - Digital Signal Processing Fundamentals*. CRC Press, 2 edition, 2010.

[20] *Curve Fitting Toolbox*^{TM} *User's Guide*. The MathWorks, Inc, 2015.

[21] A. R. Møller. *Hearing - Its Physiology and Pathphysiology*. Academic Press, 2000.

[22] B. C. J. Moore. *Cochlear Hearing Loss: Physiological, Psychological and Technical Issues*. John Wiley & Sons, 2007.

[23] B. C. J. Moore. *An Introduction to the Psychology of Hearing*. Emerald, 5 edition, 2008.

[24] J. L. Myers and A. D. Well. *Research Design and Statistical Analysis*. L. Erlbaum, 2 edition, 2003.

[25] D. O'Shaughnessy. *Speech Communication: Human and Machine*. Addison Wesley, 1987.

[26] D. Pearce, H. Hirsch, and Ericsson Eurolab Deutschland Gmbh. The Aurora Experimental Framework for the Performance Evaluation of Speech Recognition Systems under Noisy Conditions. In *ISCA ITRW ASR2000*, pages 29–32, 2000.

[27] A. Peinado and J. Segura. *Speech Recognition Over Digital Channels: Robustness and Standards*. Wiley, 2006.

[28] Quatieri, T. F. *Discrete-Time Speech Signal Processing: Principles and Practice*. Prentice Hall PTR, 2002.

[29] A. Sen and M. Srivastava. *Regression Analysis - Theory, Methods, and Applications*. Springer-Verlag, 1990.

[30] S. Sigurdsson, K. B. Petersen, and T. Lehn-Schiøler. Mel Frequency Cepstral Coefficients: An Evaluation of Robustness of mp3 Encoded Music. *Seventh International Conference on Music Information Retrieval (ISMIR)*, 2006.

[31] S. S. Stevens, J. Volkmann, and E. B. Newman. A Scale for the Measurement of the Psychological Magnitude Pitch. *The Journal of the Acoustical Society of America*, 8(3):185–190, 1937.

[32] C. H. Taal, R. C. Hendriks, R. Heusdens, and J. Jensen. A Short-Time Objective Intelligibility Measure for Time-Frequency Weighted Noisy Speech. In *Acoustics Speech and Signal Processing (ICASSP), 2010 IEEE International Conference on*, pages 4214–4217. IEEE, 2010.

[33] Z.-H. Tan and B. Lindberg. *Automatic Speech Recognition on Mobile Devices and over Communication Networks*. Springer, 2008.

[34] Z.-H. Tan and B. Lindberg. Low-complexity Variable Frame Rate Analysis for Speech Recognition and Voice Activity Detection. *IEEE Journal of Selected Topics in Signal Processing*, 4(5):798–807, Sep 2010.

[35] Tan, Z.-H. Noise-robust Voice Activity Detection (rVAD) - Source Code, Reference VAD for Aurora 2. `http://kom.aau.dk/~zt/online/rVAD/`, Dec 2014.

[36] M. D. Ugarte, A. F. Militino, and A. T. Arnholt. *Probability and Statistics with R*. Chapman and Hall/CRC, 2008.

[37] T. Virtanen, R. Singh, and B. Raj. *Techniques for Noise Robustness in Automatic Speech Recognition*. John Wiley & Sons, 2012.

[38] M. Woelfel and J. McDonough. *Distant Speech Recognition*. John Wiley & Sons, 2009.

[39] T. Yamada and N. Kitawaki. A PESQ-based Performance Prediction Method for Noisy Speech Recognition. *Proc. International Congress on Acoustics*, 2:1695–1698, Apr 2004.

[40] T. Yamada, M. Kumakura, and N. Kitawaki. Performance Estimation of Speech Recognition System Under Noise Conditions Using Objective Quality Measures and Artificial Voice. *Audio, Speech, and Language Processing, IEEE Transactions on*, 14(6): 2006–2013, Nov 2006.

[41] S. Young, G. Evermann, M. Gales, T. Hain, D. Kershaw, X. Liu, G. Moore, J. Odell, D. Ollason, D. Povey, V. Valtchev, and P. Woodland. *The HTK Book (for HTK Version 3.4)*. Cambridge University Engineering Department, 2009.

Settings A

In this appendix the standard settings for the SE and ASR algorithms used in this thesis are shown. In Table A.1 the standard settings are shown for the SE algorithms STSA WE, the IWF and the ANS designed for human listeners. In Table A.2 the conditions are shown for the feature extraction and recognition processes. Finally an overview of the Aurora-2 database is given in Table A.3.

Algorithm	**Standard Settings**
STSA WE	Power exponent $p = -1$
IWF	Iteration $i = 2$
ANS	Iteration $i = 2$

Table A.1: Standard setting for the SE algorithms.

Frame length	25 ms
Frame period	10 ms
Feature vector	12 MFFCs, log power combined with MFCC(0), and their Δ and $\Delta\Delta$ The cepstrum mean normalization is applied.
HMM (digits)	16 states, 3 Gaussians per state
HMM (silence)	3 states, 6 Gaussians per state
HMM (short pause)	1 state tied with the 2^{nd} state of the silence model

Table A.2: Conditions of the feature extraction and recognition processes.

Training and Test set	Speech	Noise	Channel	SNR (dB)
Clean training	8440 utterance of 110 people	None	G.712	Clean
Multi-condition training		Subway, Babble, Car, Exhibition		Clean, 20, 15, 10, 5
Test set A	4004 utterance of 104 people			Clean, 20, 15, 10, 5, 0, -5
Test set B		Restaurant, Street, Airport, Station		
Test set C	2002 utterance of 104 people	Subway, Street	MIRS	

Table A.3: Training and test set of the Aurora-2 database.

Matlab Scripts B

In this appendix an overview is given over selected Matlab scripts, all of which can be found on the CD.

Filename	Folder	Functionality
SE_Frontend.m	Matlab\ServerSide	Create preprocessed speech data using SE algorithms to be used for the basic FE.
AFE_SignalsFrontend.m	Matlab\ServerSide	Write extracted speech signal from AFE into correct folder for the basic FE.
testResultsEnhancedSpeech.m	Matlab\ServerSide	Compute STOI and PESQ, for speech signals processed using SE algorithms.
testResultsExtractedSpeech.m	Matlab\ServerSide	Compute STOI and PESQ for speech signal extracted from AFE.
testResultsNoisySpeech	Matlab\ServerSide	Compute STOI and PESQ for noisy source speech signal.

Table B.1: Selected Matlab scripts used for processing speech signals.

Filename	Folder	Functionality
SE_spectrogramAnalysis.m	Matlab\Spectrogram Analysis	Spectrogram analysis of the signals of the output of the 1st stage Wiener filter of the AFE and the STSA SE algorithm.
TestPredictor.m	Matlab	Plot scatterplot of test set A, with fit and test set B and C, with fit and prediction bounds.

Table B.2: Selected Matlab scripts used for evaluation purposes.

Filename	Folder	Functionality
audnoise.m	Matlab\ServerSide\Algorithms	Implements the audible noise suppression algorithm.
stsa_weuclid.m	Matlab\ServerSide\Algorithms	Implements the Bayesian estimator based on the weighted euclidean distortion measure.
wiener_iter.m	Matlab\ServerSide\Algorithms	Implements the basic iterative Wiener filtering algorithm.

Table B.3: Selected Matlab scripts of SE algorithms [17].